STRUCTURAL STYLES AND KINEMATICS OF DEFORMATION ON THE EDGE OF THE NEW ZEALAND PLATE BOUNDARY ZONE, MID-WAIPARA REGION, NORTH CANTERBURY.

A thesis

submitted in partial fulfilment

of the requirements for the degree

of

Doctor of Philosophy

at the

University of Canterbury

by

ANDREW NICOL

University of Canterbury

1991

FRONTISPIECE. These prominent limestone scarps dominate this view of 'The Deans', one of the most photographed landscapes in New Zealand geology. The limestones are preserved on the gently tilted (20-30^0) SE flanks of the Doctors Dome, an asymmetric fold interference structure. The geometry and structures within these resistant units, particularly the white lower-most Oligocene limestones, provide the basis for many of the conclusions reached in this thesis.

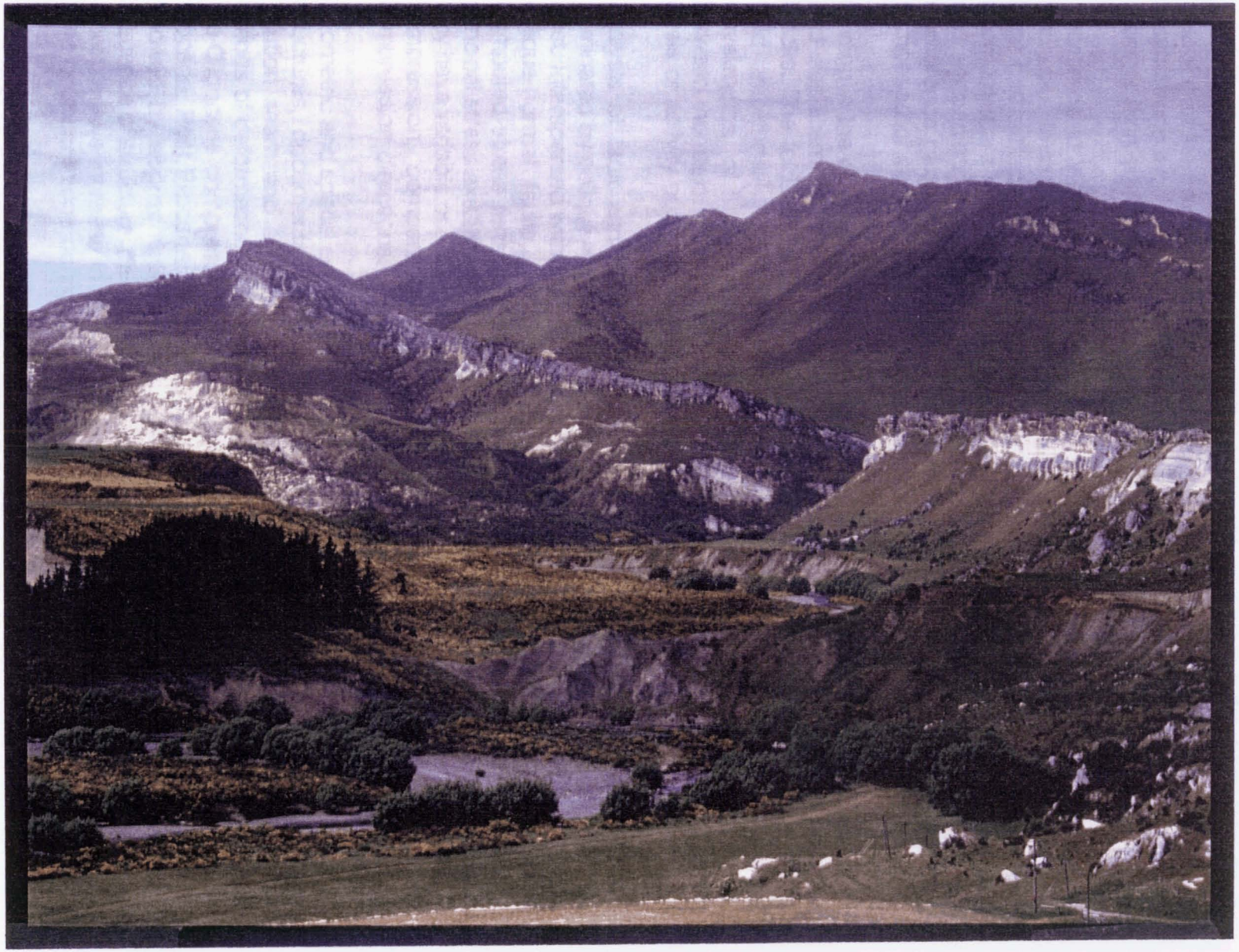

ABSTRACT

In North Canterbury, on the SE edge of the New Zealand plate boundary zone, deformation in late Cretaceous and younger cover rocks is complex. Detailed mapping of the cover sequence (which is about 1 km. thick), has revealed a pattern of synchronous faulting and folding about orthogonal E-ESE and N-NNE orientations younger than early Pleistocene.

Complex and irregular basin and dome fold interference patterns are defined by distinctive limestone marker horizons, and partial star, triangular and corrugated hose fold surface geometries (defined by structure contours) are common. These geometries are often associated with folds that vary in shape along their hinge line and secondary folds developed oblique to the main interfering fold sets. Fold interference geometries are also characterised by composite conical geometries, composed of several distinct cone segments.

Folding in the cover sequence has developed in response to: (1) fault propagation and displacement in the basement; and, (2) shortening within the fault bounded blocks. The folds related to faulting are asymmetric and parallel the major faults. Fold amplitudes of 0.5-1.6 km. are proportional to vertical fault displacements, and wavelengths of 5-20 km. are approximately equal to the strike-normal distances between the major faults. Fold interference patterns are indicative of the styles and levels of activity of the orthogonal faulting.

Analysis of fault and slickenside striation geometries suggests that faulting is dominated by oblique-reverse faults and thrusts, which verge north, south, east and west. Interspersed with the regional contractional faulting are local areas of E-ESE oblique-normal faults, inferred to be reactivated late Cretaceous structures. Computed stress tensors derived from minor fault motion data suggest that the principal stress axes most commonly plunge at shallow to moderate angles. Locally they have variable orientations but regionally these data imply a predominant NW-SE compression, comparable to local geodetic shortening and focal mechanism compression directions.

Geometric and spatial analysis of large numbers of sets of small scale, mainly brittle structures, documents the local history of deformation. Multiple joint, pressure solution seam and stylolite, macrofracture and mesofault sets record only two periods of deformation since the mid-Cenozoic. The first was a weak regional mid-late Oligocene compression; the second involving a NW-SE compression since the Pliocene. Post Pliocene deformation is characterised by initial NW-SE shortening, followed by approximate N-S and E-W shortening associated with folding. The sequence of structural development during the late Pliocene and Pleistocene implies a progressive increase in the intensity of deformation and a rapid widening of the plate boundary zone during the last 2-3 ma.

The mainly contractional deformation in North Canterbury, commonly associated with thrusting to the NW, is distinct from the major right-lateral and eastward directed thrust tectonics in Marlborough. This not only reflects a difference between inner and outer plate boundary deformation, but also the diminishing influence of subduction related tectonics.

TABLE OF CONTENTS

LIST OF FIGURES

page

LIST OF TABLES

MAP POCKET

Mid-Waipara Region geological map and cross sections.

Torlesse Bedding Map of the Doctors Dome area, with detailed observations from the Doctors Gorge and Weka Creek.

CHAPTER 1 INTRODUCTION

1.1 THESIS AIMS

New Zealand lies across an actively deforming plate boundary where earthquakes are moderately frequent. In the Canterbury region, the frequency of destructive earthquakes prior to 1850 is poorly constrained by data. To further our understanding of coseismic active deformation the "North Canterbury Active Tectonics Programme" was established, with the expressed aim of designing a new form of "Neotectonic Map".

In this framework the current project was established with the intention of documenting the styles of deformation and using these to analyse the geomorphic response to active deformation in the study area (Figures 1.1 and 2.10). Apparently simple styles of folding expressed in outcrop patterns are geometrically complex in detail. These outcrop patterns reflect strain imposed on the cover rocks by basement faulting, which had not previously been considered or investigated. It became clear that before a close examination of the active deformation could take place, a better understanding of the deformation was essential. Consequently, while active faulting and folding are noted they are not addressed in this work, rather the complex and interesting interrelationships of the structures in the cover rocks have received the full attention of the author. The objectives of this work were to build up a data base to establish the geometries and kinematics of both the macroscopic faults and folds, and a suite of small scale structures. Detailed examination of these mainly late Cenozoic structures permit the local styles of deformation and genetic

relationships of the structural elements to be characterised, which it was hoped would ultimately allow inferences to be made about regional and plate boundary tectonics. It is envisaged that this structural data, representing several million years of cumulative deformation may also have implications for the age and rates of current deformation, and contribute to the evaluation of seismic hazard in the region.

1.2 THESIS ORGANISATION

This project forms part of an ongoing and co-operative "North Canterbury Active Tectonics Programme". The programme was established in 1988 by Jarg Pettinga and Jocelyn Campbell of the Department of Geology, University of Canterbury, to document and study active deformation. The initial phases of the project have concentrated on the area between Christchurch and the Hope Fault. This thesis represents the first major project to be completed within the active tectonics programme since it was formally established, although the programme grew from, and incorporated several projects at M.Sc. and Ph.D levels on North Canterbury and the Hope Fault.

This work was undertaken in three broad phases; (1) field mapping and reconnaissance data collection, (2) detailed structural data collection at selected sites and data analysis, (3) data collation and interpretation. While the bulk of the field work was undertaken during the summers of 1988/'89 and 1989/'90 phases 1-2 and 2-3 overlapped in time. Field mapping was carried out primarily at a 1:15 000 scale, with detailed mapping at 1:1 000 to 1:5 000. During the course of the

thesis joint work was undertaken with Don Wise and Hugh Cowan (refer to acknowledgements).

The thesis has been structured so as to facilitate ease of publication. Several sections, principally chapters two to six, have been collated so that with a minimum of rewriting they can form discrete papers without recourse to material elsewhere. This has resulted in some repetition between chapters. Lengthy written descriptions of the stratigraphy, structures and the techniques used have been omitted, and where relevant reference has been made to appropriate diagrams and publications. The data not used in the manuscripts are presented in appendices. Detailed relationships between the structures and the main lithologic units are presented in the maps and cross sections (map pocket).

1.3 REGIONAL TECTONICS

In the South Island, plate boundary deformation is taking place across a 200 kilometre wide zone (Walcott, 1978; Walcott, 1987), with much of the strain concentrated along the Alpine Fault. This is emphasised by the 480 kilometre strike-separation of distinctive Permian and Mesozoic rocks across the fault (Wellman, 1953). The Alpine Fault forms a trench-trench transform (Le Pichon, 1968), connecting E directed subduction in the south and W directed subduction in the north (Figure 1.1). The initiation of this fault, primarily as a major strike slip fault, is thought to have begun during the late Oligocene (Molnar et al, 1975; Carter and Norris, 1976; Kamp, 1986), but during the last 10 ma the rate of convergence has increased (Molnar et al, 1975; Walcott, 1978 and 1984; Stock and

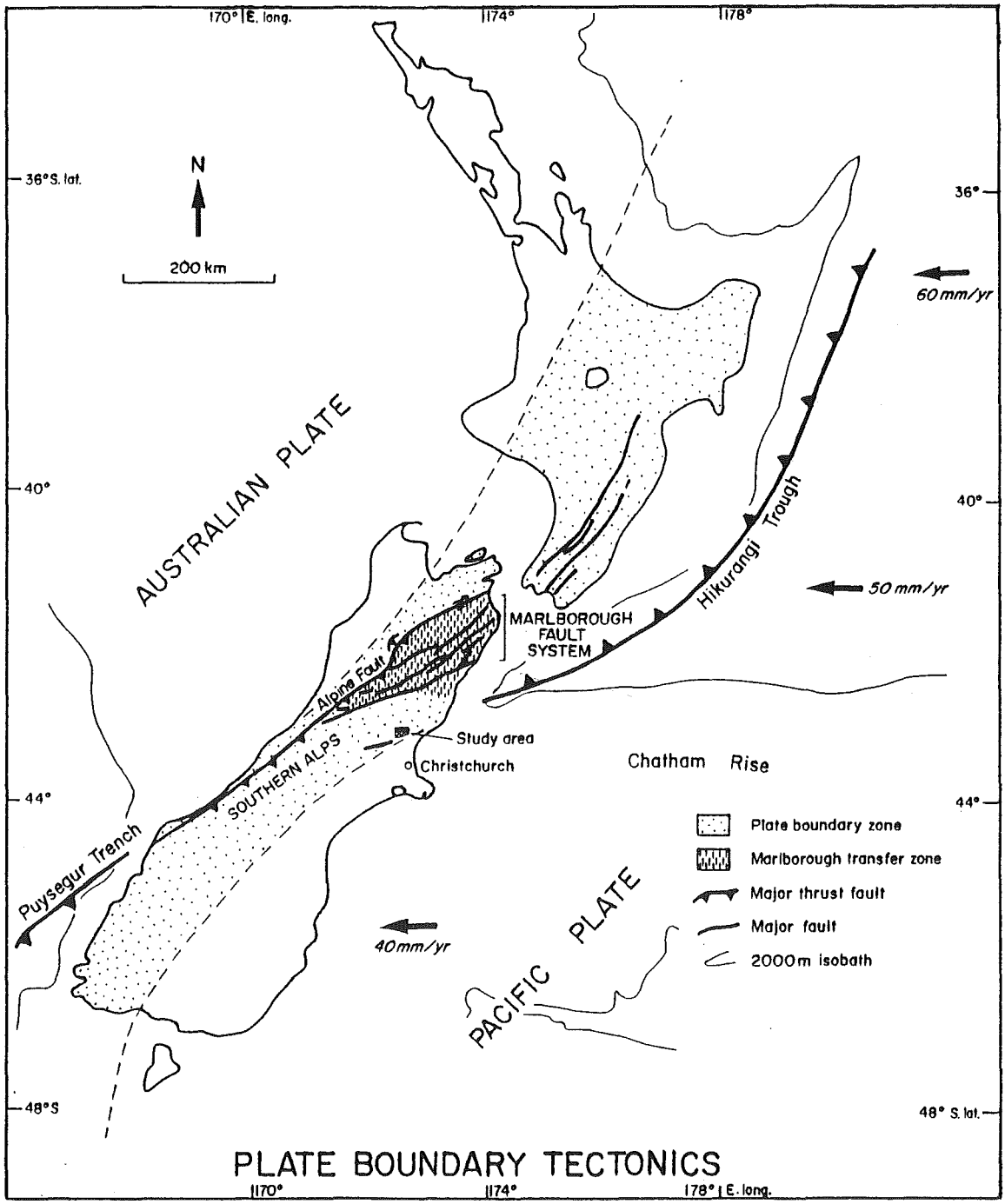

Figure 1.1. Tectonic map of the plate boundary through New Zealand. The large teeth represent areas of subduction, while the arrows show the motion of the Pacific Plate relative to the Australian Plate (Chase, 1978). The plate boundary zone limits are from Walcott (1987), where they are defined as "the outer limit of post-Miocene plate boundary zones". The Marlborough Transfer Zone defines the zone over which Alpine Fault deformation is transferred to deformation of the Hikurangi margin (Wise et al, in prep). The 2000 m isobath represents the inferred edge of the continental crust.

Molnar, 1982). The plate boundary in the South Island is presently accommodating oblique continent-continent collision of the Australian and Pacific plates.

In Marlborough, five major predominantly NE striking dext ral faults (Wairau, Awatere, Clarence, Kekerengu and Hope faults) splay from the Alpine Fault and constitute the Marlborough Fault System (Figure 1.1). The faults of this system are accompanied by several major, but less well known, secondary faults. These faults have complex interconnecting relationships with the main faults of the Marlborough System. Right lateral displacements on the faults of the Marlborough system range from 5 to 50 kilometres (Lensen, 1962; Lamb and Bibby, 1989) and current rates of activity appear to increase from N to S (Campbell, 1973; Yeats and Berryman, 1987). The Hope Fault is presently the most active member of the system, with horizontal slip rates of between 14 +/- 3 mm a^{-1} (Cowan, 1990) and 33 mm a^{-1} (Bull pers. comm., 1991). The Marlborough faults help accommodate the change from the E dipping oblique Alpine Fault to the W dipping subduction of the Hikurangi margin. Although the limits of subduction are well marked by the Hikurangi Trough (Figure 1.1), the connecting relationships of the subduction complex and the Marlborough Fault System, remain unclear. Recent work suggests that the major faults of the Marlborough system pass progressively eastward into a series of thrusts close to the Marlborough coastline (Lamb, 1988; Lamb and Bibby, 1989; Van Dissen, 1987).

The area comprising this study encompasses the mid-Waipara area of North Canterbury, which lies 50 km SE of the Hope Fault just north of the eastward projection of the Porters Pass Fault Zone (PPFZ) (Figure 1.1). The PPFZ has been inferred to represent a juvenile strike slip fault zone, which defines the SE edge of

the Marlborough Fault System (Carter and Carter, 1982; Coyle, 1988). The style of deformation in North Canterbury is quite different to that of Marlborough. The region is characterised by basement-cored elongate uplifts, bounded by local range-front thrusts, with structural relief of 1-3 km. Wide, but apparently shallow basins lie between the uplifts, the most prominent of which is the Culverden Basin. These structures appear to be mainly contractional and reflect locally the late Cenozoic development of the plate boundary in northern Canterbury. Wilson (1963) believed deformation in this part of Canterbury to be mainly Miocene and Pliocene in age, but inferences made in this study suggest that most of the structures are Pleistocene to Recent in age (0-2 Ma). Numerous Holocene fault traces and eight damaging seismic events in the region since 1850 testify to the continuing deformation.

1.4 LOCAL GEOLOGY OF THE MID-WAIPARA AREA

The study area covers approximately 400 Km^2, including the mid-Waipara and Weka Pass areas, 70 Km north of Christchurch (Figure 1.1). This area separates the southern end of the Culverden Basin from the Canterbury Plains (see Figure 2.10). The region is characterised by rolling pastoral farmlands ranging in altitude from 150-800 m, with public road access. Exposure is good along the major rivers (appendix 1A), but patchy elsewhere. The structures are defined by well indurated limestone lithologies (frontispiece) and are often reflected in the topography, with indurated Mesozoic basement forming elevated areas in the cores of folds and on the upthrown side of faults.

1.4.1 STRATIGRAPHY

The stratigraphy is summarised in figure 1.2. It comprises a late Cretaceous to early Pleistocene sequence of sedimentary cover rocks, which are separated from Mesozoic metasedimentary basement rocks by a marked regional angular unconformity. The following discussion of the stratigraphy is a brief summary of the unit lithologies, drawn from fieldwork undertaken in this study, Browne and Field (1985), and Bradshaw (1972). Where relevant to the interpretation of late Cenozoic tectonics, elements of the stratigraphy are discussed elsewhere in the thesis. Additional data pertaining to unit dimensions and exposure, and coal analyses for Broken River and Kowai Formation coals, are presented in appendices 1B and 1C, respectively.

1.4.1.1 Basement Rocks

Local basement forms part of the Torlesse Supergroup, a suite of Mesozoic quartzo-feldspathic sandstones and mudstones, which constitute basement throughout the eastern South Island and grade westwards into schist (New Zealand Geological Survey, 1972, 1:1 000 000 geological map). Torlesse rocks have been metamorphosed to zeolite and prehnite-pumpellyte facies (Bishop et al, 1985), and are complexly deformed (Bradshaw, 1972; Sporli and Lillie, 1974). In the mid-Waipara area basement is probably Jurassic (Andrews et al, 1976) or early Cretaceous (Wilson, 1984) in age. Basement lithologies are dominated by massive sandstones, and interbedded fine sandstones and mudstones, with sparse volcanics, red cherts, and slightly calcareous horizons forming occasional local

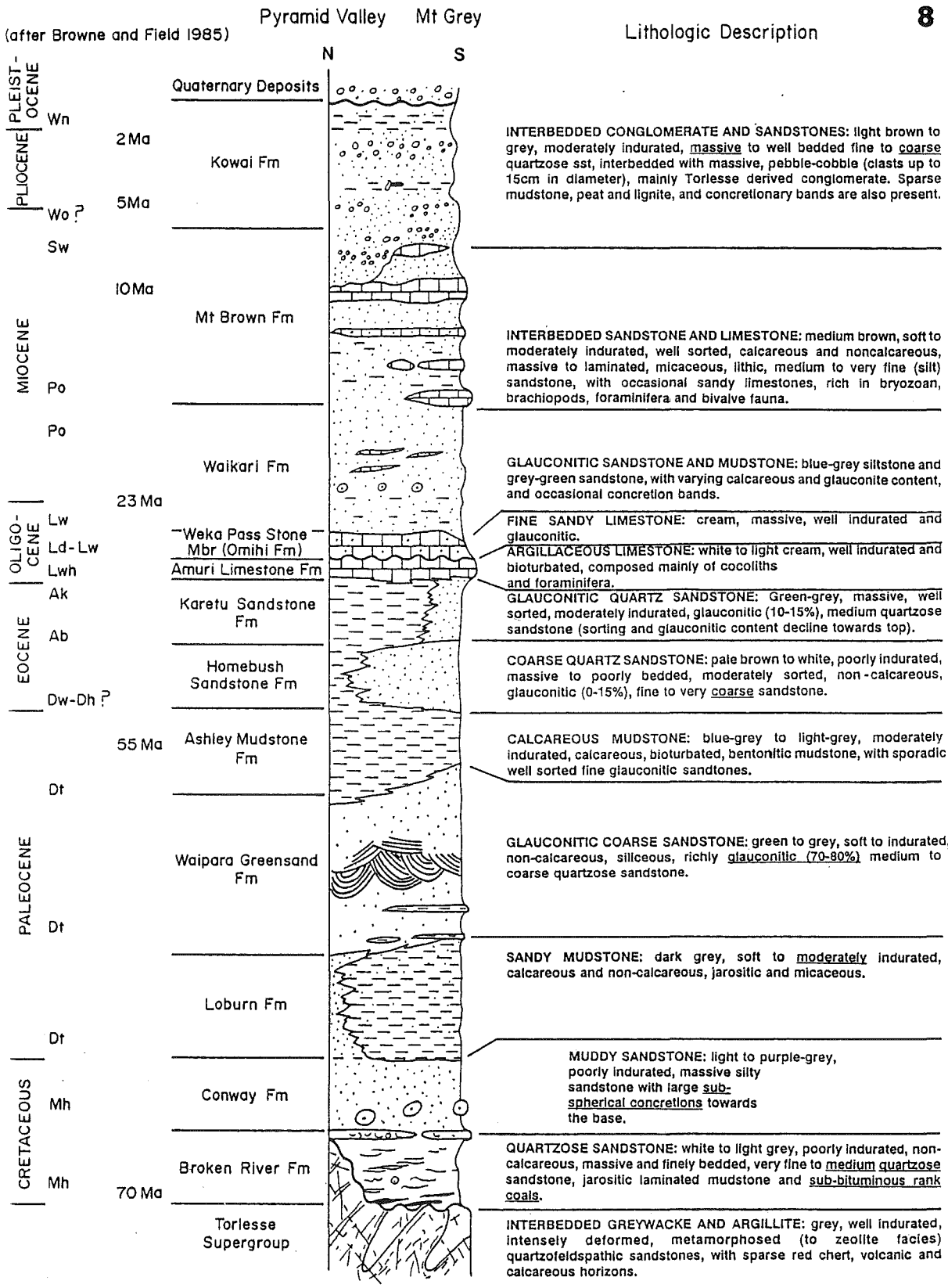

Figure 1.2. Generalised and schematic stratigraphic column representing the lithological units between Pyramid Valley and Mt Grey (see top of column). The nomenclature, age determinations and parts of the descriptions are from Browne and Field (1985), the remainder of the data is from this study. The section is not drawn to scale.

markers (see Torlesse bedding map in map pocket).

1.4.1.2 Cover Sequence

The late Cretaceous-early Pleistocene cover sequence presently averages about one kilometre in thickness and is dominated by thick poorly bedded sandstone and mudstones (Figure 1.2). The stratigraphy is well exposed along incised reaches of the Waipara River, and in numerous small streams (e.g. Weka Creek, Dungeon Creek, Birch Hollow Stream and Tommy's Creek) mainly on the flanks of the Doctors Dome (see Figure 2.1 and appendix 1A). As a consequence of the good exposure and the proximity of the area to Christchurch, the stratigraphy has received much attention (Haast, 1871; Hector, 1887; Mckay, 1887; Thomson, 1920; Wilson, 1963; Andrews, 1963; M^{c}Culloch, 1981; Browne and Field, 1985). The names and definitions of the formations have been subject to numerous changes, and interpretations of the environments of deposition have also varied. In this study all unit names, ages and some of the descriptions follow the nomenclature of Browne and Field (1985).

The sequence is dominated by glauconitic sandstones and jarositic sandy mudstones. The glauconite content ranges up to 80% within the Waipara Greensand Formation, but is more commonly between 5 and 15%. Many of the glauconitic sandstone and jarositic mudstone lithologies are similar and appear to have been mapped by Wilson (1963) as biostratigraphic units. The calcareous content of many of the units is variable.

Limestone horizons are dispersed throughout the sequence; the most prominent of these include the Ostrea shell bed (at the top of the Broken River Formation), the Amuri Limestone Formation, the Weka Pass Stone Member of the Omihi Formation and the limestone members of the Mt Brown Formation (Figure 1.2). These limestones are well indurated and form prominent marker beds (frontispiece), which facilitates recognition of the main stratigraphic units and structures, and permits the analysis of fold interference geometries.

There are two regional unconformities. One of late Cretaceous age, between cover and basement, and a second mid-Oligocene unconformity between the Oligocene limestone units. These unconformities are distinctive and have provided datums for structure contour maps (see Figures 3.3 and 3.4). Two further unconformities of local extent bound the Kowai Formation. The remaining sedimentary contacts between the main lithologic units commonly interfinger (Figure 1.2), forming lensoid sedimentary bodies and units of varying thickness (appendix 1B). With the exception of the Cretaceous formations, lateral changes in unit thicknesses appear to be mainly unrelated to the structures presently developing. These complex boundary relationships have added to the problem of unit nomenclature and definition. In this thesis only one change has been made to the definition of the lithologic units. The boundary between the Mt Brown Formation and the Kowai Formation is defined by Browne and Field (1985) as being marked by the last appearance of limestones. Here the boundary is recognised by the first appearance of conglomerate, which indicates the unroofing of basement. This does not affect the location of the contact where the contact is unconformable because conglomerates rest on limestone. However, where the contact between these units is gradational (e.g. Weka Creek) shell, conglomerate and shelly conglomerate beds are interfingered. This change in

unit definition has been made to confine the conglomerates, which mark the onset of rapid tectonics to the N and NW, to one stratigraphic unit.

1.4.2 STRUCTURE

The deformation is dominated by large range-front faults, which extend upwards from basement, dissecting and offsetting (0.1-0.6 km) the cover rocks (see main map in map pocket). The faults control the topographic grain, and are closely associated with folding in the cover, which accounts for most of the apparent strain. These faults and folds are mainly orientated E-W and N-S, which contrasts with the regional NE structural grain in North Canterbury (see Figure 2.10).

Mapping was centred on the Doctors Dome, a basement cored, boomerang-shaped fold interference structure (Figure 2.1). The shape of the 12 by 15 km dome is defined by the cover sequence (see Figure 2.1). The west flank of the dome is bounded by an almost isoclinal N-S striking syncline (MacDonald Syncline) with nearly vertical dips and about 3 km of structural relief. Here, basement rocks have been thrust over both flanks of the syncline by the Mt Arden Fault and Karetu Thrust. A SE continuation of the Karetu Thrust on the east side of the syncline produces a westward verging anticline. On the remaining three sides of the dome, bedding in the cover dips away from the basement core at relatively shallow angles ($< 30^0$) and is folded on kilometre wavelengths with non-cylindrical forms.

CHAPTER 2 SIMULTANEOUS ORTHOGONAL FAULTING

2.1 INTRODUCTION

South Island faulting is dominated by the oblique lateral Alpine Fault and the associated major lateral faults of the Marlborough Fault System (Figure 1.1). In North Canterbury, south of the Marlborough Fault System, the rates of deformation, size and continuity of the main faults diminish. These changes in part signify a change in the style of deformation southwards, from the major lateral faults of the Marlborough system to compression dominated deformation (Lensen, 1975). Compression dominated tectonics is implied by the presence of thrusts and reverse faults in North Canterbury (Gregg, 1964; Maxwell, 1964; Dibble, unpublished data) and offshore (Carter and Carter, 1982; Lewis et al, 1985).

Little is known about the details of late Cenozoic faulting within the outer part of the plate boundary zone, to the south of the Marlborough Fault System, where compressional faulting is significant. The aim of this study is to establish the style and kinematics of faulting in North Canterbury, by close examination of the regional to outcrop scale faulting characteristics in the area between Waikari and Mt Grey.

2.2 TORLESSE BASEMENT FAULTS

Although the Torlesse is widespread, the details of how it has deformed during the recent and on-going orogeny is not well documented. Late Cenozoic faults in the basement represent only the youngest part of an extensive suite of mainly Mesozoic structures. Accordingly, to avoid unduly clouding the late Cenozoic fault story, faulting of the basement and cover rocks are dealt with separately.

Basement rocks are exposed in the core of the Doctors Dome (Figure 2.1), a late Cenozoic fold interference structure, bound on the west and north side by two range-front faults. Much of the basement deformation is concentrated along these faults, with local rotation of the unconformity contact. On the shallow dipping flanks of the dome, the late Cretaceous unconformity exhibits little evidence of detachment from the basement, apparently rotating in sympathy with the cover sequence. Late Cenozoic brittle deformation in the basement appears to have accommodated similar shortening strain as folding in the cover rocks.

2.2.1 DEFORMATION IN BASEMENT

Basement is extensively deformed by multiple fold, fault, vein and joint sets. Bedding parallel small scale folding and bedding plane faulting is ubiquitous. Because of this, single beds are rarely traceable for more than five metres, even though gross bedding is generally parallel across most outcrops.

Figure 2.1. A simplified geological map of the Doctors Dome. Lower hemisphere equal area nets display poles to bedding in basement for five areas (A-E) and a cumulative plot of measured mesoscopic and calculated fold axis orientations.

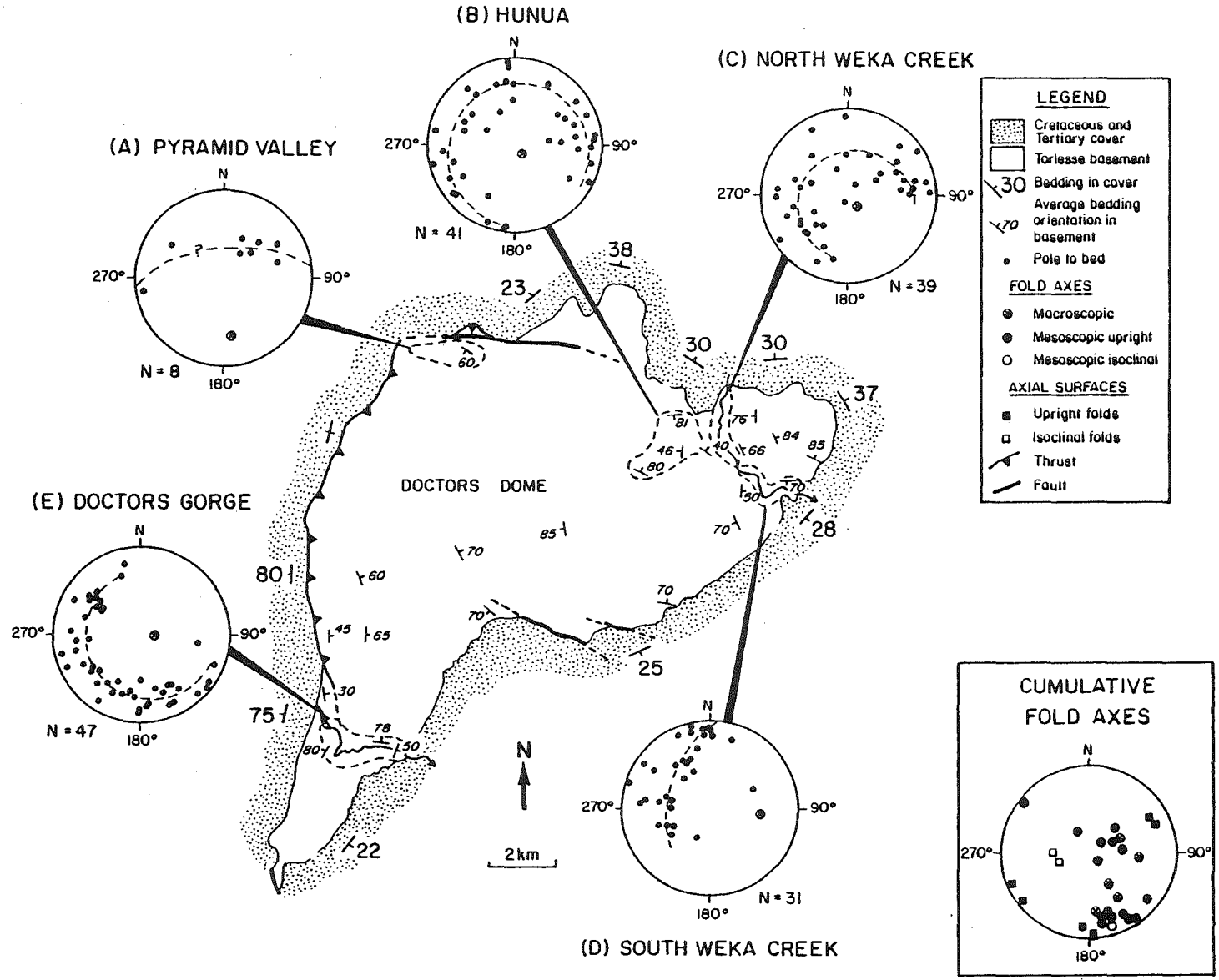

BASEMENT FOLDING

2.2.1.1 Folding

Bedding within basement commonly dips steeply, with average strikes mostly in the northwest quadrant (Figure 2.1 and Torlesse bedding maps). At least two sets of folds are present and pre-date the development of the Cretaceous unconformity, which is relatively planar and essentially undisturbed. Data from areas where numerous bedding attitudes were determined describe conical folds with steeply plunging axes and 30-70^0 apical angles (B,C and E on Figure 2.1) or cylindrical folds (A and D on Figure 2.1). Many outcrop-scale folds and the calculated axes of conical folds (Figure 2.1, lower right) are steeply plunging. A broader scale and apparently younger folding produced the general northwest strike of the basement mass. The clustering of this class of younger axes is evident in the SSE portion of the cumulative plot in figure 2.1.

2.2.1.2 Veins

Mineralised veins of laumontite, laumontite with calcite, calcite, and silica are extensively developed within sandstone horizons. A cumulative plot showing the orientations of all these vein types indicates an almost random scatter (Figure 2.2, left). However, the veins were separated in the field into two classes, non-sheared/non-brecciated veins and those marked by extensive shearing and brecciation. The poles to the undeformed group produce a broad NNE trending girdle with mostly steep dips (Figure 2.2, centre).

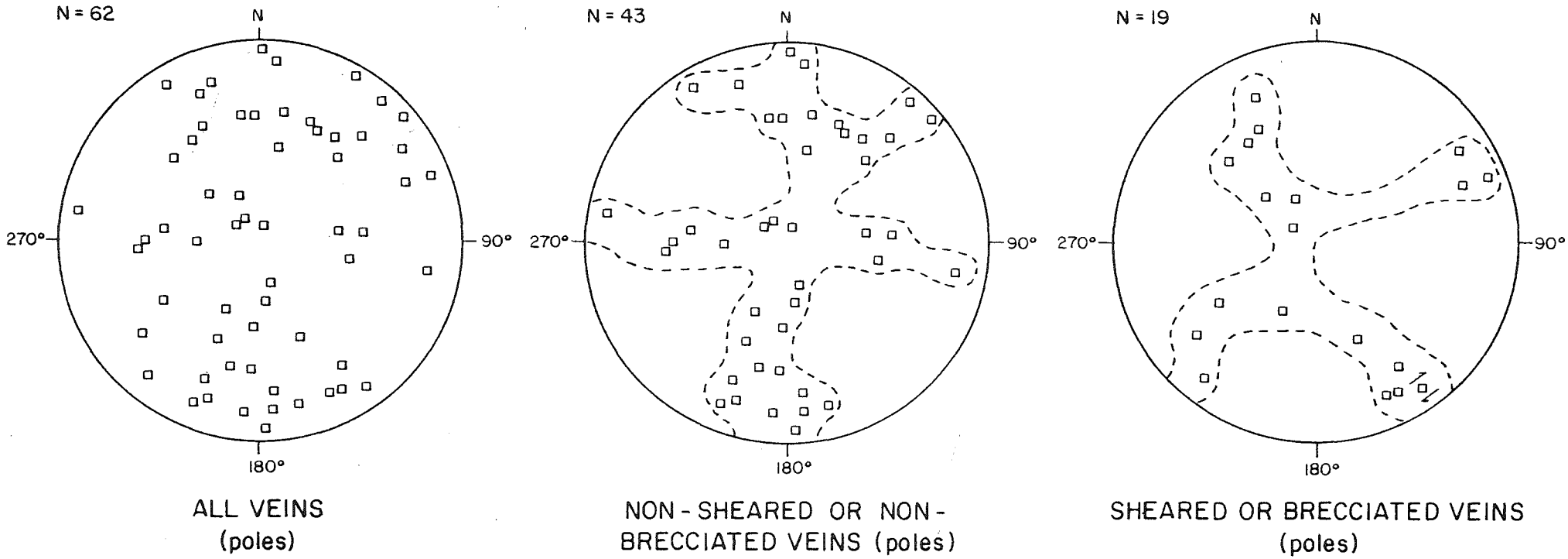

Figure 2.2. Lower hemisphere equal area plots of poles to veins in Torlesse basement. The three nets represent (from left to right) all veins, those veins not sheared or brecciated, and sheared or brecciated veins respectively.

Compression directed to the NNW with extension at the NNE is indicated by these veins. The deformed veins (Figure 2.2, right) are most commonly oriented NW and NE in conjugate relation to the undeformed set. The single motion sense obtained from these structures is consistent with this interpretation. The age of this deformation and mineralization is poorly constrained; the veins occur sporadically over the region and show little sign of concentration near the unconformity nor the range-bounding faults. They are widespread, late-stage and commonly associated with small-scale local slickensiding and faulting, but they are not the youngest of the basement structures. They may well be associated with an inferred phase of late Cretaceous, approximate north-south regional extension (Browne and Field, 1988).

2.2.1.3 Faults and Slickenside Striations

Four well exposed areas of basement were examined for minor slickensided surfaces and yielded a total of 274 faults, mostly with quite scattered orientations of planes and slickenside striations (Figure 2.3, top two rows). Of these, 66 yielded reliable motion sense data and were used for the stress tensor determinations illustrated in the lower half of figure 2.3.

Three patterns of fault distribution were evident during data collection. (1) Widespread, bedding parallel, very minor slickensides found in most outcrops in association with the early folding and bedding plane disruptions. Insofar as possible these were excluded from the main set of measurements. (2) A widespread set of minor faults cross-cutting the bedding parallel system and commonly showing minor mineralization and/or polish. Although locally abundant, these faults

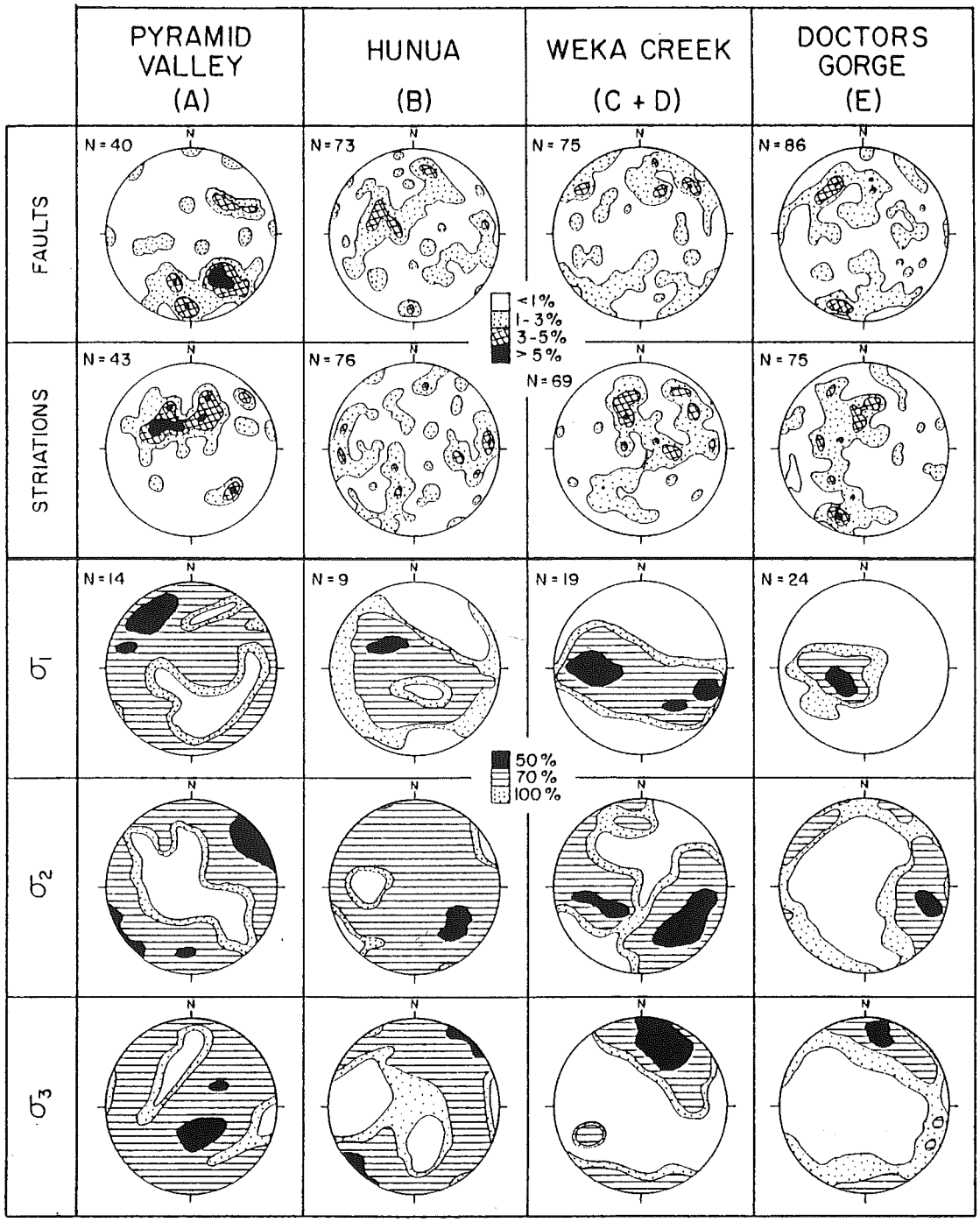

Figure 2.3. Lower hemisphere equal area contour diagrams of poles to faults and the trend and plunge of slickenside striations from four localities within basement are contoured as percentages of the total sample population within a 1% area of the net. Stress tensors (sigma 1,2 and 3) for the same localities derived from these data are contoured to show the total percent of the derived stress tensors within a defined area (see appendix 2B for explanation of stress tensor determination method); where 50, 70 and 100% of the stress axes derived are within the black, black/striped and black/striped/dotted areas

appear to reflect a regional overprint far removed from the young frontal fault structures. (3) Heavy concentrations of slickensided, polished, and shattered surfaces occur in the vicinity of the steeply upturned and faulted range fronts. Local concentrations of these faults also occur within locality B (Figure 2.1) along the projection of a sharp bend in the cover sequence beds. There is no obvious increase in this class of faults below gently tilted portions of the Cretaceous unconformity. Individual faults can rarely be identified with certainty as either class 2 or 3. Accordingly, the faults used for the stress tensor analysis comprise a mixture of these structures.

2.2.2 LATE CENOZOIC STRESS IN BASEMENT

Stress tensors were determined for four of the areas in figure 2.1 and are presented in figure 2.3. In general, the plots show sigma 1 (compression) lying in a NW to W direction and sigma 3 (extension) in a NNE to NE orientation. Plot A (Pyramid Valley) represents the area with the most intense range-front deformation and rotation, and may provide the best indication of late Cenozoic faulting and fault orientation. On the other hand, plots B, C, D and E are mainly from the shallow dipping limbs of the dome structure and may be more indicative of older NNE extension, similar to the stress field indicated by the vein data.

In an attempt to provide better resolution of the data set, areas where the unconformity surface and basement minor faults could be rotated back to a horizontal were combined. Once rotated, the fault data were inverted by the programs described (appendix 2B) to obtain the sigma 1 orientation for the period

prior to, or during, the early stages of dome development (Figure 2.4). The inferred direction of compression is comparable to the sigma 1 direction derived from the entire cover fault population (Figure 2.4, middle) and stylolite columns (parallel to the principal axis of compression during formation) in an Oligocene limestone unit, which has been folded across the dome (chapter 6). A bimodal peak in the basement fault data is interpreted as the result of the older WNW compression associated with the possible late Cretaceous veining events plus the SE compression during the late Cenozoic. The fault data are complemented by supplementary vein and stylolite data, but do not provide an unambiguous stress history in their own right.

The difficulty of deriving a well defined, late Cenozoic stress tensor from these basement rocks is underscored by their complex history of at least two periods of late Mesozoic and Cenozoic brittle deformation and faulting. Without additional stylolite data from the sedimentary cover, this analysis would have been most difficult. Future studies seeking the stress tensor in basement rocks by fault inversion techniques would be well advised to concentrate on the zones of frontal faulting, and to incorporate any available structures from the cover rocks.

2.2.3 LATE CENOZOIC DEFORMATION IN BASEMENT

Observations from this study support Bradshaw's (1975) general conclusion that most late Cenozoic deformation within the Torlesse basement was accommodated by a few large faults, broad warping, and innumerable minor fractures. Within the Doctors Dome, most of the late Cenozoic strain has been released along the large,

approximately north and west-striking range-front faults. These narrow zones (usually less than several hundred metres wide) of deformation comprise at least one major fault (often marked by several metres of gouge) and swarms of minor slickensided surfaces. Away from the influence of these faults, basement deformed into the dome shape primarily by triboplastic mechanisms with widely distributed, small (cm.) movements on many mesoscopic faults and veins; a deformation somewhat analogous to that of a beanbag (see chapter 5, section 5.4.2). Many of these brittle structures are reactivated small-scale Mesozoic features. Further west in the Canterbury mountains, and at structurally lower levels within the Torlesse, small scale (cm. to m.) brittle deformation diminishes rapidly in significance (Bradshaw pers. comm., 1990). Here large faults bound blocks of basement ranging in size from a kilometre to tens of kilometres, which internally contain coherent Mesozoic structures. Bradshaw (1972) mapped some of these Mesozoic structures 20 kilometres to the NW of this study area (See Figure 2.10 for location). This implies that late Cenozoic small scale brittle strain structures are only extensively developed in the top few (1-3) kilometres of basement, and at deeper structural levels the 'beans,' or blocks and bounding faults accommodating the late Cenozoic strain, increase significantly in size.

2.3 FAULTS IN THE COVER SEQUENCE

The cover rocks were largely undeformed prior to the onset of late Cenozoic deformation and provide an important means of assessing the local kinematics of brittle deformation. Two main types of these faults exist: (1) structures associated with large scale faults which extend upwards from the basement, and (2) small

Figure 2.4. A comparison between the principal compression orientation derived from; (a) basement rock faults (with the effects of Tertiary folding removed), (b) cover sequence faults, and (c) late Cenozoic stylolite columns developed in an Oligocene limestone unit (Chapter 6). The derivation of the contours for (a) and (b) is the same as for the stress tensors in figure 2.3, while (c) represents contoured values (as for the faults and striations in Figure 2.3) of the stylolite column trend and plunge.

PRINCIPAL COMPRESSIVE STRESS ORIENTATIONS

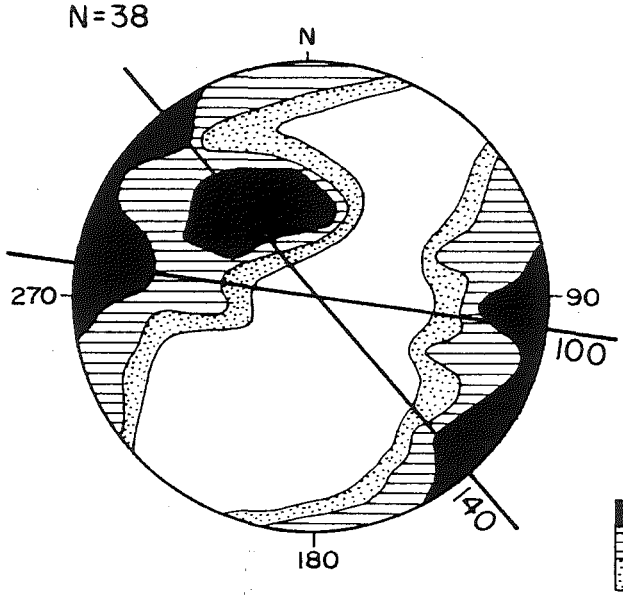

(a) CUMULATIVE BASEMENT FAULT σ_1 STRESS TENSORS

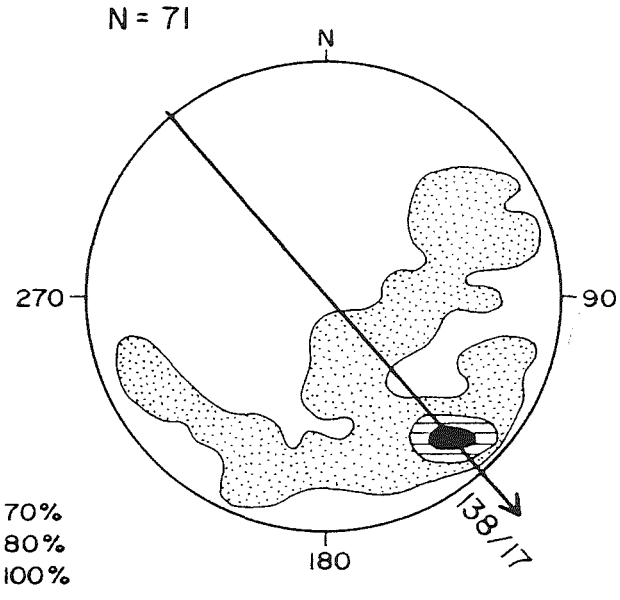

(b) CUMULATIVE LATE CENOZOIC COVER FAULT σ_1 STRESS TENSORS

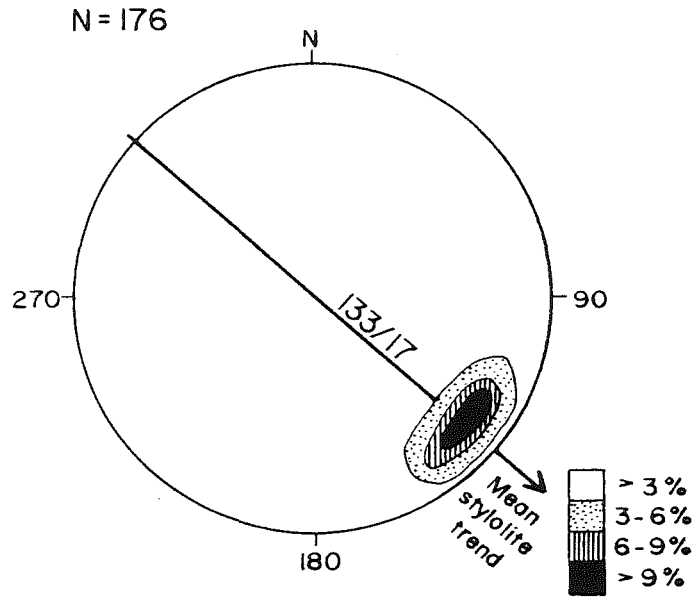

(c) LATE CENOZOIC PRINCIPAL COMPRESSION DERIVED FROM STYLOLITE COLUMNS

outcrop scale faults developed during the folding process. More than 300 faults were sampled within the cover using a combination of widely spaced and concentrated outcrop observations; most were minor faults of type (1). Seven major faults were mapped (Mt Arden, Mt Grey, Pyramid Valley, Birch and Kaiwara faults, and the Karetu Thrust; Figure 2.5), these mainly have vertical displacements of less than 0.6 km. and are described in appendix 2A.

2.3.1 GEOMETRY AND KINEMATICS OF FAULTING

The faults vary in geometry and kinematic character, with two approximately orthogonal orientations and several prominent faulting styles. Poles to fault planes (contoured and in pole form) for the total fault population have been divided into five areas, which progress from west to east, left to right in figure 2.5. This diagram shows a predominance of E-ESE and N-NNE faults, which change in relative significance from E to W (see also Figure 2.6). North-South striking structures dominate the MacDonald Downs and Mt Grey areas to the west, while to the east and south of these areas ESE-ENE faults are most significant.

Three groups emerge from the total fault population. These are: (1) approximate N-S striking oblique-reverse faults, (2) E-ESE striking, steep oblique-normal faults, and (3) E-ESE striking steep to shallow dipping reverse faults (Figures 2.5 to 2.7). North-South striking faults are represented by a broad east-west girdle of poles, and vary in dip from sub-horizontal to sub-vertical (Figure 2.7), whereas the E to ESE striking faults often form steep conjugate sets (e.g. Figure 2.5, Boby's Creek).

Figure 2.5. Fault map showing the orientation and distribution of the major faults (labelled). Fault dip directions are indicated by the thrust teeth and small ticks on the trace, adjacent numbers indicate the amount of dip. Lower hemisphere equal area nets display orientation and distribution of poles to fault planes for reverse, normal and lateral small scale faults within, or immediately adjacent to, cover rocks. Map symbols as for figure 2.1.

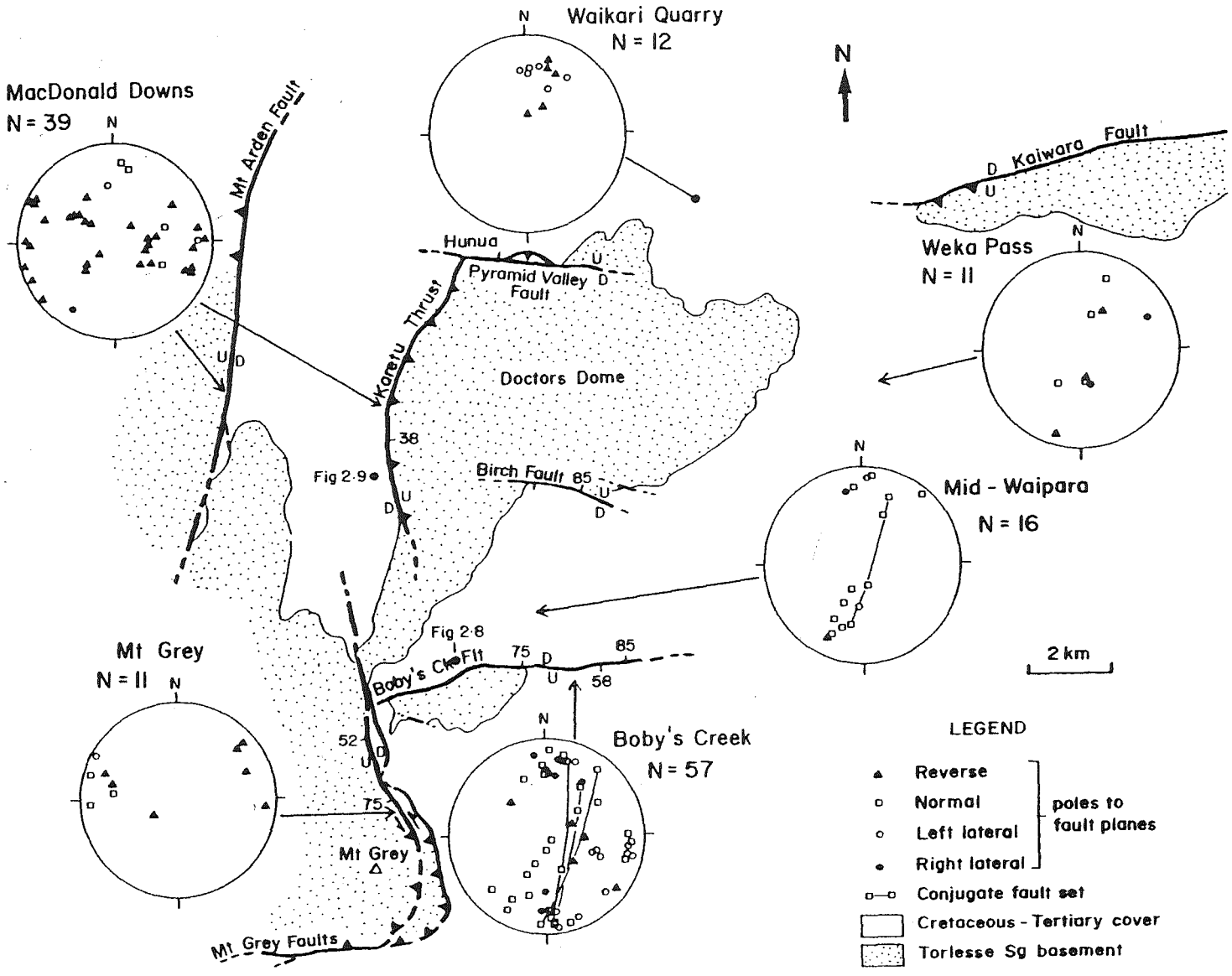

FAULTING MAP

Figures 2.6 and 2.7 present the spatial distribution and geometries respectively for the different types of all faults where a motion sense was observed (about half of the total sampled fault population). Dip-slip faults were characterised by movement vectors orientated at 45^0 or more to the fault strike; strike slip faults imply a motion vector trending at less than 45^0 to the fault strike. Normal, reverse and strike slip faults, were recorded in approximately equal proportions (Figure 2.7). Oblique normal, reverse and lateral (both left and right) movement is associated with E-ESE striking faults (Figure 2.7), although oblique-normal faults with this orientation are most common. Figure 2.8 shows outcrop scale faulting in Boby's Creek, where oblique-normal faults are well developed. This style of faulting is also evident at Weka Pass and Hunua (Figure 2.5). Reverse faults and thrusts that strike approximately E-W occur in the Waikari area and south of Mt Grey. The uneven distribution of ESE-WNW normal and reverse faults reflects local strain partitioning, which is controlled by the style of nearby macroscopic faults. At the respective localities the reverse Kaiwara and Mt Grey Faults and the mainly normal Boby's Creek Fault locally partition strain into compressional and extensional components. Reverse and left lateral faults most often strike N-NNE and have variable dips (Figure 2.7). These faults are most commonly steep oblique-reverse and thrust structures and have accommodated thrusting in E and W directions (Figure 2.5). A good example of contractional faulting is provided by figure 2.9. Left lateral faults were recorded more frequently than right lateral.

Slickenside scratch and groove striations provided motion data for many of the faults. Single fault planes often contained several sets of slickensides with approximately orthogonal trends. Throughout the region the slickenside striations

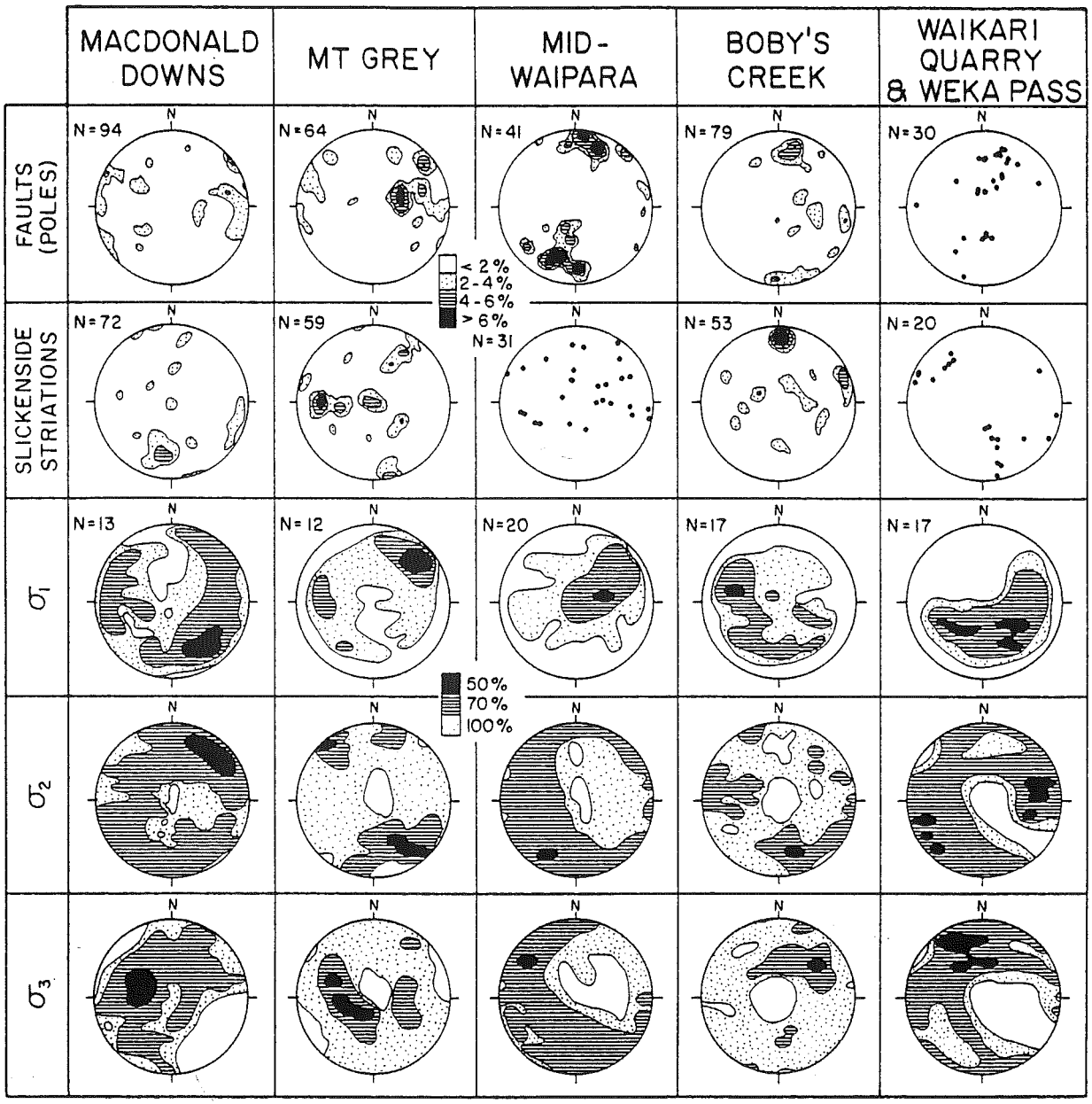

Figure 2.6. Lower hemisphere equal area contour diagrams of poles to faults, trend and plunge of slickenside striations and stress tensors (sigma 1,2 and 3) for five localities within cover rocks (see appendix 2B for explanation of stress tensor determination method). Contours as for figure 2.3.

displayed varying degrees of geometric similarity (Figure 2.6). Within a single sample area single striation orientations may dominate (e.g.Mt Grey, Boby's Creek and Waikari Quarry.) However, in adjacent areas the similarities in striation trend are equivocal. For instance, west trending striations are most abundant at Mt Grey and north trending at Boby's Creek. Oblique-slip faults are most common. In any one area different types of faults may be associated with similarly orientated motion vectors.

2.3.2 LATE CENOZOIC STRESS TENSORS IN COVER ROCKS

Stress tensors were derived using kinematic data measured from 85 faults within the cover rocks. Despite the locally predictable distributions of faults and the similar orientations of some of the slickenside motion vectors, the resulting stress tensors vary considerably in orientation from area to area.

Stress tensor data are presented in the bottom half of figure 2.6, where the contoured areas contain 50,70 and 100% of the stress tensor data derived from the measured faults. The principal stresses are ubiquitously inclined at shallow to moderate plunges, and vary in orientation between localities. The mid-Waipara and Boby's Creek areas are dominated by normal faulting and field evidence implies that they have experienced local extension, mainly in a NNE to NE direction. Consequently sigma 1 tends to be the steepest of the three principal stress tensors. This zone of localised oblique extension is surrounded by areas undergoing compression, confirmed by the predominance of reverse faults, which include the Waikari Quarry-Weka Pass, MacDonald Downs and Mt Grey (Figure 2.5). These are

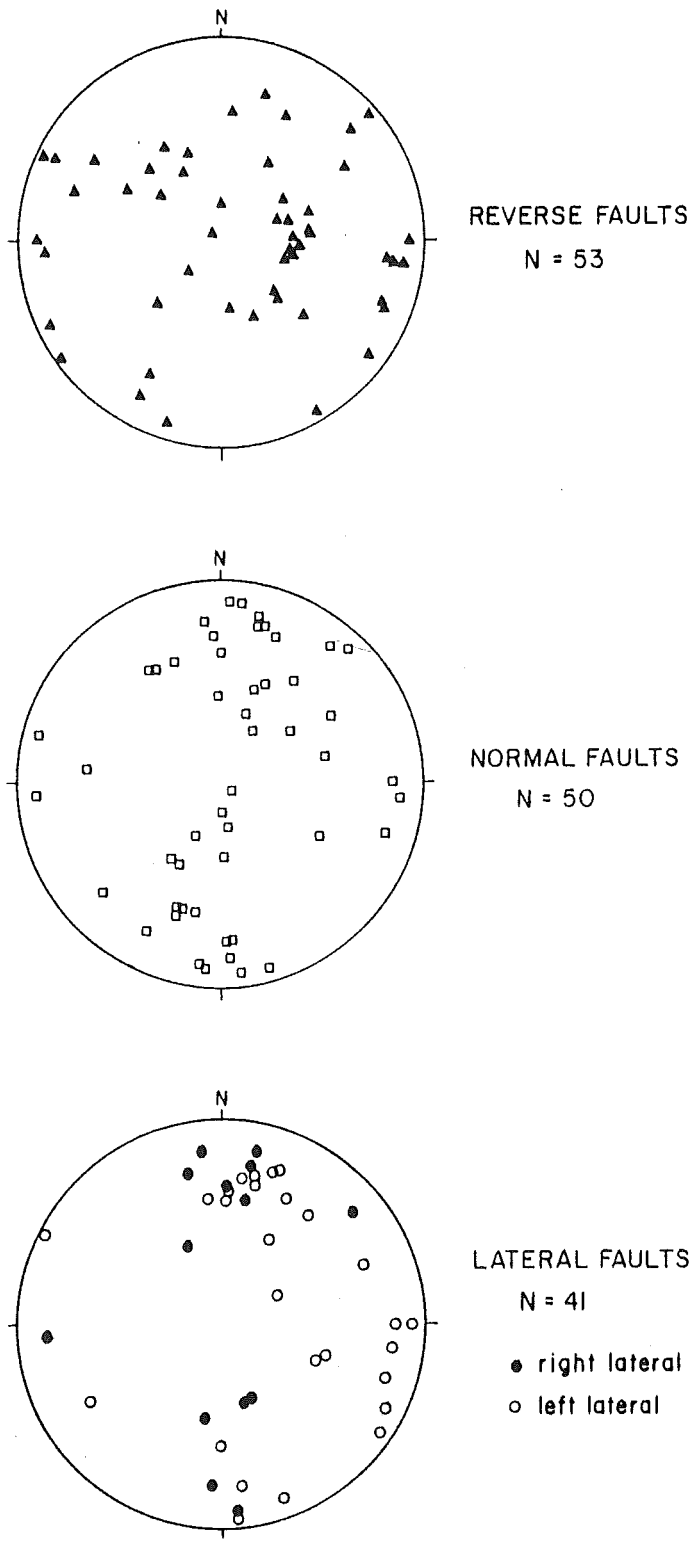

Figure 2.7. Lower hemisphere equal area nets of poles to reverse (top), normal (middle) and lateral (bottom) faults from the entire study area. These represent all faults where a motion sense could be determined and make up about half of the total fault population.

characterised by a sub-horizontal sigma 1 and 2, and a moderate to steeply plunging sigma 3. The results are consistent with fault striation data, and imply that many of the faults are complex structures which have accommodated oblique motion. The orientations of sigma 1,2 and 3 appear to be interchangeable between localities; sigma's 1 and 2 switch between MacDonald Downs and Mt Grey, and sigma's 2 and 3 switch between Mt Grey and mid-Waipara. In both examples the areas are adjacent to each other and imply changes in the relative values of the principal stresses over short (< 1 km.) distances. These changes need not be large because the values of the principal stresses, particularly sigma 1 to 2 in areas dominated by compression and sigma 2 to 3 in areas dominated by extension, may be similar. Close values for sigma 1 and 2 imply that constrictional tectonics (i.e. shortening in two directions) is occurring in areas of compression; a conclusion supported by the synchronous development of interference folding in these areas (Chapter 3). However, despite the likely similarities in the values of two of the principal stresses, the deviatoric stress (sigma 1 minus sigma 3) may to be large, which would imply near uniaxial stress conditions in these areas.

2.3.3 AGE RELATIONSHIPS BETWEEN FAULTS

The history of faulting around the Doctors Dome is complex and the age relationships of the main fault groups are not consistent from area to area. At Boby's Creek and Mt Grey, N-S striking faults truncate and offset E-ESE structures. These age relationships are confirmed by the presence of a SSE striking recent fault trace along the foot of Mt Grey, which truncates the Boby's Creek Fault. To the north, at Hunua (Figure 2.5), the N-S striking Karetu Thrust is apparently

Figure 2.8. Extensional faulting in Boby's Creek (see Figure 2.5 for location). The oblique normal faults (labelled fault) offset Waikari Formation calcareous beds (labelled 1 and 2) by up to several metres. Faults are locally associated with vein (a) and joint sets (b). The clip board is 0.4 m. long.

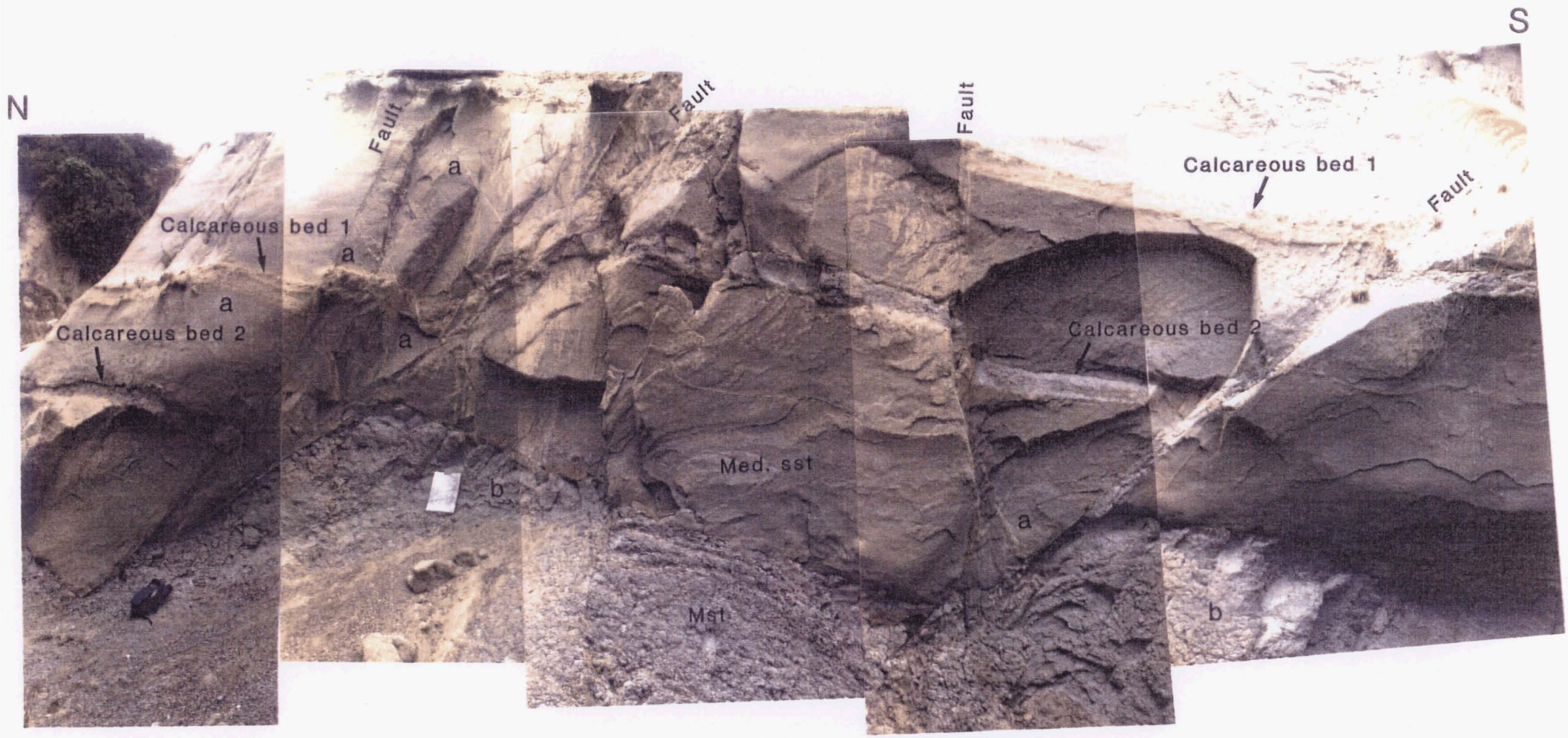

NORMAL FAULTS: BOBY'S CREEK

truncated by the normal E-W striking Pyramid Valley Fault, while at outcrop scale, north striking low angle thrusts are offset by steep normal (E-W) and lateral (N-S) faults. These observations imply that rather than having discrete periods of E-W and N-S faulting, both sets of faults moved intermittently, and in geological terms, have developed synchronously during the late Cenozoic. Fault activity has the appearance of being rather sporadic and spatially random, with movements on short lengths of faults (< 5 km.) separated by distances of 5 to 10 kilometres. Oblique dip-slip motion on one fault group is often recorded as an incipient oblique strike-slip motion on the second group of faults. Thus many fault planes contain two or more sets of slickenside striations. This phenomenon is particularly well developed at Hunua, on the eastern side of MacDonald Downs where oblique-normal movement on the E-W striking Pyramid Valley Fault has been transferred to the N-S striking Karetu Thrust. As a consequence this thrust fault, which has accommodated several hundred metres of dip-slip movement, contains a significant number (about 45%) of strike-slip slickenside striations.

The presence of both E-ESE and N-S fault traces, offsetting Holocene geomorphic features such as streams and fans, indicates that this process continues to the present day.

2.4 INFLUENCE OF CRETACEOUS FAULTS ON LATE CENOZOIC DEFORMATION

The late Cretaceous break up of Gondwana resulted in regional extension over much of the New Zealand continent (Laird, 1981). Lewis et al (1985) and Browne

Figure 2.9. Contractional faulting at MacDonald Downs 350 m. west of the Karetu Thrust (see Figure 2.5 for location). The main thrust in the photo verges eastward and moves extensively deformed Amuri Limestone over Karetu Sandstone. The minimum amount of apparent dip-slip fault displacement is 7 m.

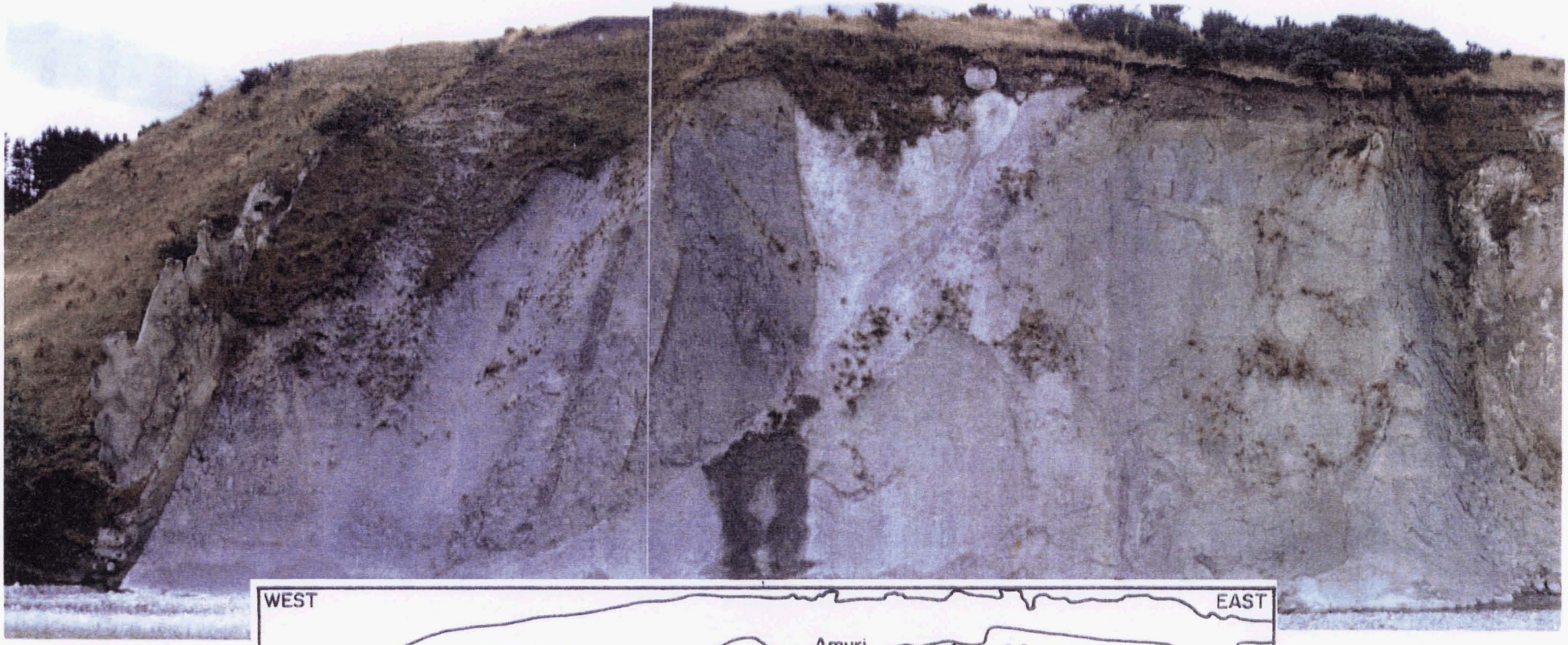
WEST
EAST
vegetation and regolith
Amuri Lmst
back thrust
bedding
bedding
bedding
Waikari Fm (Mst)
Karetu Fm (sst)
main thrust
2m
River bed

and Field (1988) have noted the presence of ENE to ESE trending fault-bounded half grabens on the Chatham Rise. Locally, within basement at the Doctors Dome, faults and veins with a similar orientation also record a pre-late Cenozoic period of NNE extension (see sections 2.2.1.2 and 2.2.1.3). East-southeast striking probable Cretaceous minor faults and veins in basement are complemented by many similarly orientated faults in the cover. Locally the Boby's Creek, Birch and Pyramid Valley faults appear to have been active during the late Cretaceous. Late Cretaceous units become conglomeratic and appear to thicken from 50 to approximately 200 m., against both the Boby's Creek and Birch faults, while late Cretaceous units thin across the Pyramid Valley Fault. All three faults accommodated downthrow to the south during the late Cretaceous, with greater apparent displacement on the southern structures (Figure 2.5). These faults provided zones of basement weakness exploited and reactivated during the present orogeny, a conclusion drawn by Lewis et al (1985) and Browne and Field (1988) for many of the Cretaceous faults on the Chatham Rise. Of the three reactivated faults the Boby's Creek and Pyramid Valley structures have experienced a reversal in the relative upthrown side of the fault, but each is accommodating mainly normal faulting and extension at the present time. The reactivation of pre-existing structures in basement has been widely reported (e.g. Sykes, 1978; Ivins et al, 1990). Reactivation of these E to ESE striking faults seems feasible using Sibson's (1985) considerations, given that the angular difference between the regional principal horizontal compression and the strike of these faults is about 30^0, less than 10^0 from Sibson's optimum of 26.5^0 (for a coefficient of internal friction of 0.75).

While there seems little doubt that E-ESE striking late Cretaceous structures have been reactivated in the late Cenozoic, the same may not be true for N-S striking

structures, which are relatively uncommon in basement. This includes the Esk Head Melange and associated Torlesse bedding to the west (Figure 2.10), which generally strikes NNW to NW (Gregg, 1964; Bradshaw 1972 and 1973). The absence of N-S striking Mesozoic structures in basement implies that N-S faults developed mainly during the present orogeny.

2.5 DISCUSSION

Canterbury is dominated by a NE orientated regional structural grain, which reflects the presence of reverse range-front faults and associated folds. These structures have accommodated differential uplift and facilitated the development of basins between basement cored structural highs (Figure 2.10), controlling the valley and ridge topography of North Canterbury. The regional structural grain is, in the study area, broken up by orthogonal faults striking E-ESE and N-NNE. Figure 2.10 puts the study area in a regional context. The local orientations of these faults appear to reflect regional swings in fault strike away from the Hope Fault and Porters Pass Fault Zone (PPFZ). Several major strands of the PPFZ appear to swing in strike from ENE to NNE (e.g. the fault on the eastern side of Lees Valley) to the west of the MacDonald Syncline (Figure 2.10). The study area straddles the junction between E-ESE striking faults, which diminish in significance westwards, and N-NNE striking, which become less significant to the east.

Valley and ridge topography in the northern South Island is distinct to North Canterbury and contrasts with the style of deformation in Marlborough. In contrast to the major right-lateral faults that form the Marlborough Fault System the main

faults in North Canterbury appear to be predominantly reverse dip-slip structures. This observation in itself is not new as Lensen (1975) has inferred a change from shear to compression dominated deformation from Marlborough to North Canterbury. The most striking aspect of this change is the short distances over which complete changes in the style of faulting takes place. This contrast is exemplified by the local predominance of left lateral minor faults over right lateral. Less than 50 km. south of the Hope Fault, a major strike slip structure, reverse faults dominate and no predominantly lateral macroscopic faults can be observed until the Porters Pass Fault Zone is reached.

These observations are in accord with recent work on the San Andreas Fault in California (Zoback et al, 1987; Namson and Davis, 1988) where strain is partitioned, with almost pure right lateral movement on the fault and thrusting in adjacent areas. In Otago, east of the oblique lateral Alpine Fault and on the 'outboard' edge of the plate boundary zone, Norris and others (1990) suggest that thrusting, which is taking place simultaneously on two orthogonal fault sets, is the dominant form of faulting. The similarities between these examples and North Canterbury suggests that this area too, is presently experiencing compressional faulting indicative of the outboard areas of a plate boundary zone dominated by major lateral fault motion. In fact, the style of faulting in mid-Waipara appears to have more similarities with Otago (Norris et al, 1990) faulting than Marlborough.

Figure 2.10. A regional map of North Canterbury faults showing the style, distribution and regional structural grain of deformation. Structural basins (dotted and blank areas) and areas of basement exposure (shaded) emphasise the differential uplift of North Canterbury.

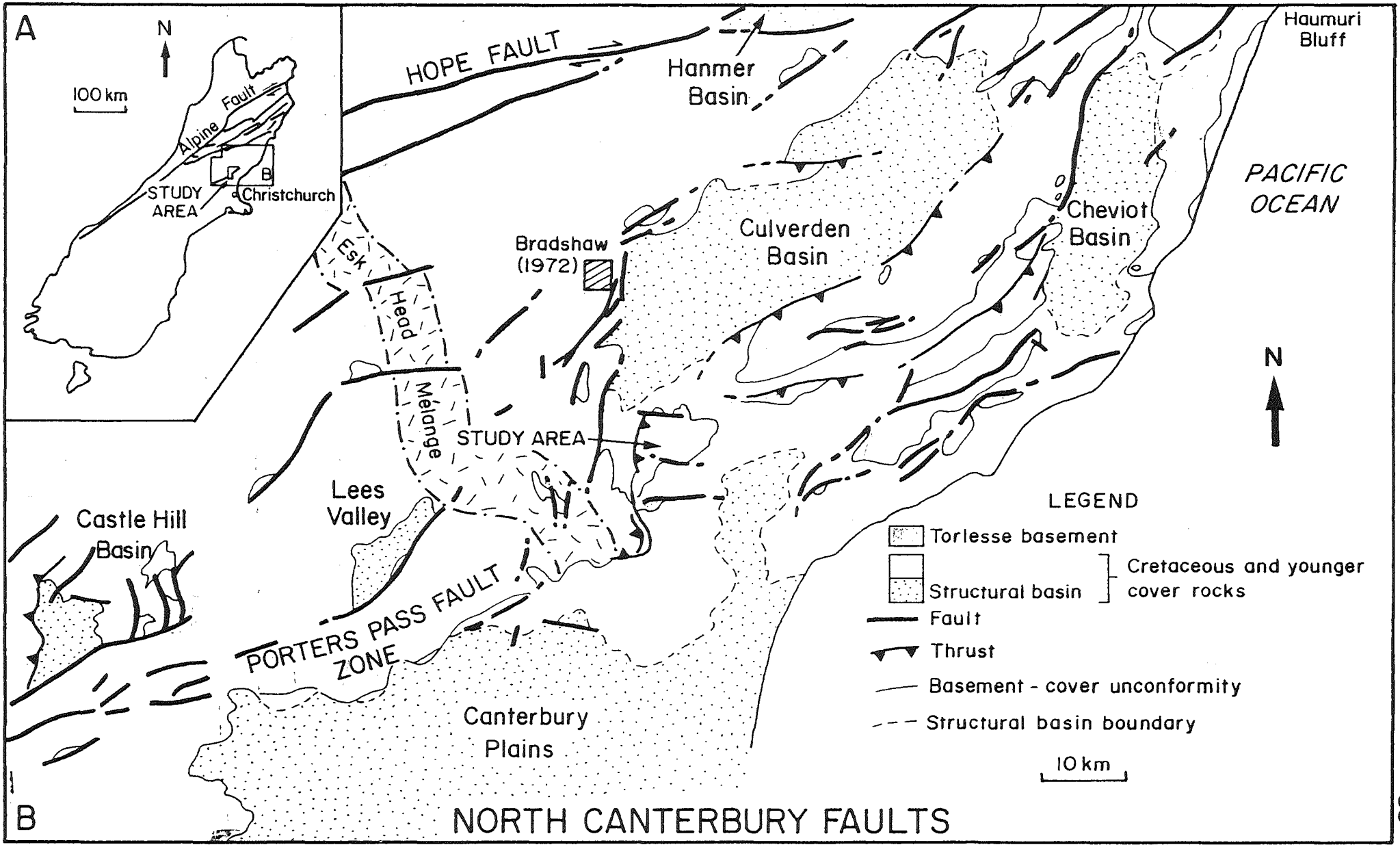
A
N
100 km
Alpine Fault
B
STUDY AREA
Christchurch
HOPE FAULT
Hanmer Basin
Haumuri Bluff
PACIFIC OCEAN
Esk Head
Bradshaw (1972)
Culverden Basin
Cheviot Basin
Mélange
STUDY AREA
N
Lees Valley
Castle Hill Basin
PORTERS PASS FAULT ZONE
Canterbury Plains
LEGEND
Torlesse basement
Structural basin
Cretaceous and younger cover rocks
Fault
Thrust
Basement - cover unconformity
Structural basin boundary
10 km
B
NORTH CANTERBURY FAULTS

2.6 CONCLUSIONS

The style of deformation in North Canterbury is dissimilar to Marlborough between the Wairau and Hope faults. On the southeastern edge of the plate boundary oblique reverse faults and thrusts are most common, while there is little indication of significant right lateral faulting. This is confirmation that strain is being partitioned between the main lateral faults of the Marlborough Fault System and the outer parts of the plate boundary zone in North Canterbury. In the Waikari to Mt Grey area the regional NE structural grain is broken up by E-ESE faults in the east and N-NNE structures in the west. This region is dominated by oblique contractional faults, which thrust and move to the N,S,E and W. Interspersed between steep reverse faults and thrusts are localised pockets of reactivated E-ESE striking normal faults. These two sets of orthogonal faults have been active simultaneously since the early Pleistocene. Interspersed and intermittent movement on members of one set translates incipient movement to the other set.

Locally strain is also partitioned and the minor fault populations mimic the style of faulting established by nearby macroscopic faults. The principal stress axes derived from the analysis of minor fault populations are ubiquitously inclined relative to the horizontal and vertical. These stress tensors imply that the study region as a whole is undergoing NW-SE compression, but locally the principal stress axes have more variable orientations and are more complicated than other studies of the regional data would suggest.

CHAPTER 3 COMPLEX NON-CLASSICAL BASIN AND DOME FOLD INTERFERENCE

3.1 INTRODUCTION

In North Canterbury folding is the most widespread manifestation of late Cenozoic deformation. These folds are non-cylindrical and reflect the interference of two fold sets to form irregular and non-classical (Ramsay, 1962 and 1967) basin and dome outcrop patterns. Although the existence of folding in this region was recognised over a 100 years ago (Haast, 1871; Hector, 1887; MacKay, 1891), the unusual outcrop patterns were variously attributed to the effects of paleotopography (Haast, 1871), present topography on uniformly dipping beds (Marshall et al, 1911) and fault block tilting (Thompson, 1920). Not until Schofield (1949) and later McCulloch (1981) was fold interference inferred.

Fold interference patterns develop where two sets of folds are superimposed on each other, either in succession or simultaneously (Ramsay, 1962). Here two sets of upright folds trending at a high angle to each other interfere to produce complex basin and dome interference patterns (Figures 3.1 to 3.4), which are dissimilar to the classical geometries of superimposed folds (Ramsay, 1962; Thiessen and Means, 1980; Thiessen, 1986). The resulting outcrop patterns are subtle and vary in character from area to area due to the effects of changing fold morphologies and topography.

Figure 3.1. Simplified geological map of the study area showing the location and plunge direction of the main fold axial traces. The major fold axial traces and key structures referred to in the text are named. This figure should also be referred to for chapter 4.

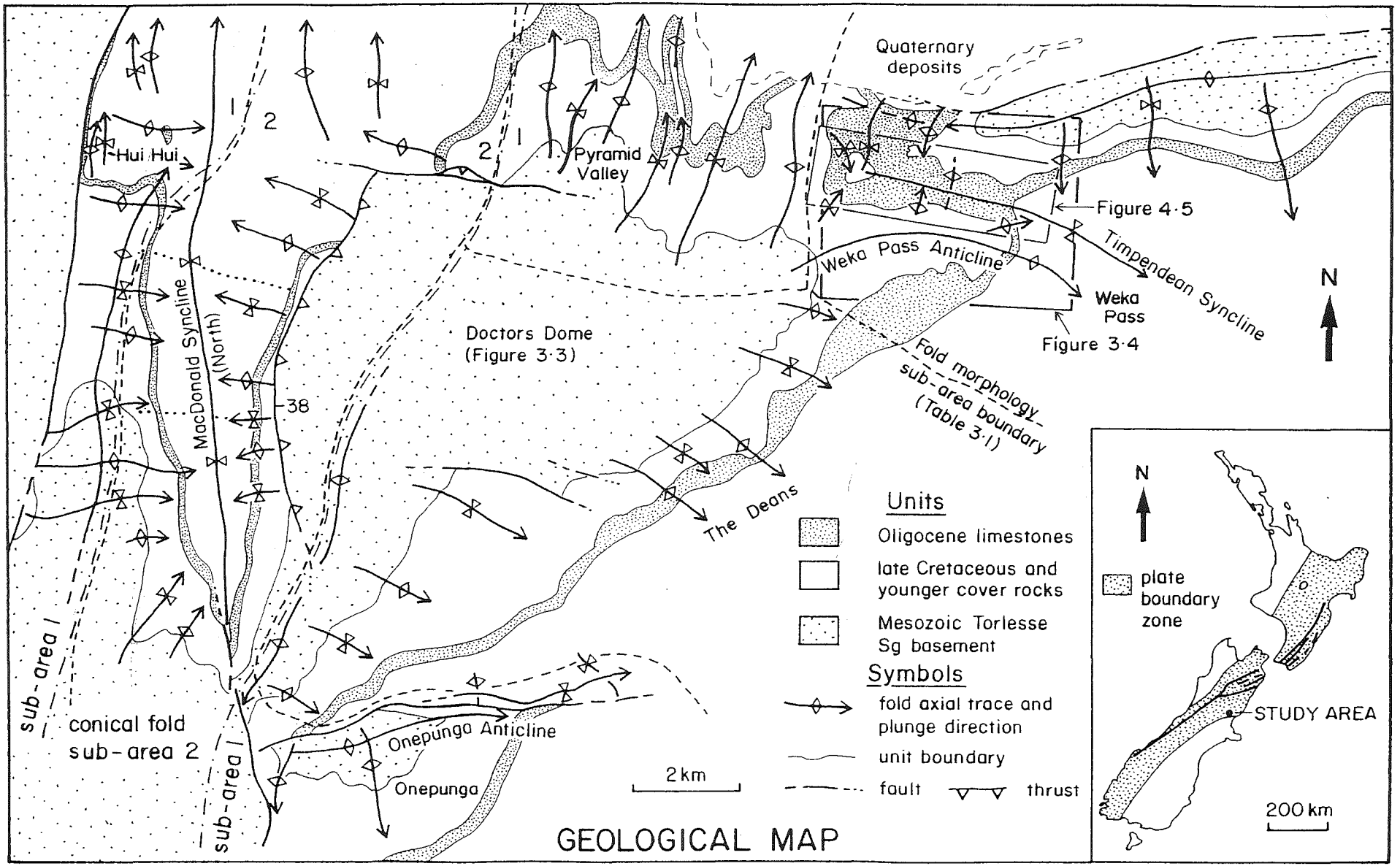
Hui Hui
Pyramid Valley
Quaternary deposits
Figure 4·5
Timpendean Syncline
Weka Pass Anticline
Weka Pass
Figure 3·4
N
Doctors Dome (Figure 3·3)
MacDonald Syncline (North)
38
Fold morphology sub-area boundary (Table 3·1)
The Deans
Units
Oligocene limestones
late Cretaceous and younger cover rocks
Mesozoic Torlesse Sg basement
Symbols
fold axial trace and plunge direction
unit boundary
fault
thrust
sub-area 1
conical fold sub-area 2
sub-area 1
Onepunga Anticline
Onepunga
2 km
plate boundary zone
STUDY AREA
200 km
GEOLOGICAL MAP

The failure of numerous previous workers to recognise fold interference in the mid-Waipara region and the lack of similar fold patterns in the literature provide added significance to the description and discussion of this example. The aim of this chapter is to describe the unusual fold interference patterns, and give some indication as to how and why such patterns should develop.

3.2 FOLD MORPHOLOGY

The folds are defined within a one kilometre thick sedimentary sequence which rests unconformably on basement and is dominated by relatively thick soft marine sandstones and mudstones, with sparse competent limestone units. It is these limestones, particularly the Amuri Limestone and Weka Pass Stone (Browne and Field, 1985), that form resistant ridges and dip slopes that enable the fold geometries to be characterised.

The study area is centred on the Doctors Dome, a 12 by 15 km. basement cored fold interference structure (Figures 3.1 and 3.3). Immediately west of the dome the cover rocks define a sharp, almost isoclinal N-S trending syncline with nearly vertical limb dips. On the remaining three sides of the dome, bedding in the cover dips away from the basement core at relatively shallow angles ($< 30^0$), and the folds are open to gentle (Fleuty, 1964). The fold axes mainly trend approximately N-NNE and E-ESE, but also trend SE along 'The Deans' (Figure 3.1), and locally NE and SE. The folds are mainly upright to steeply inclined, sub-horizontal to gently plunging structures, with straight to conical limbs and angular to sub-angular hinges. Fold

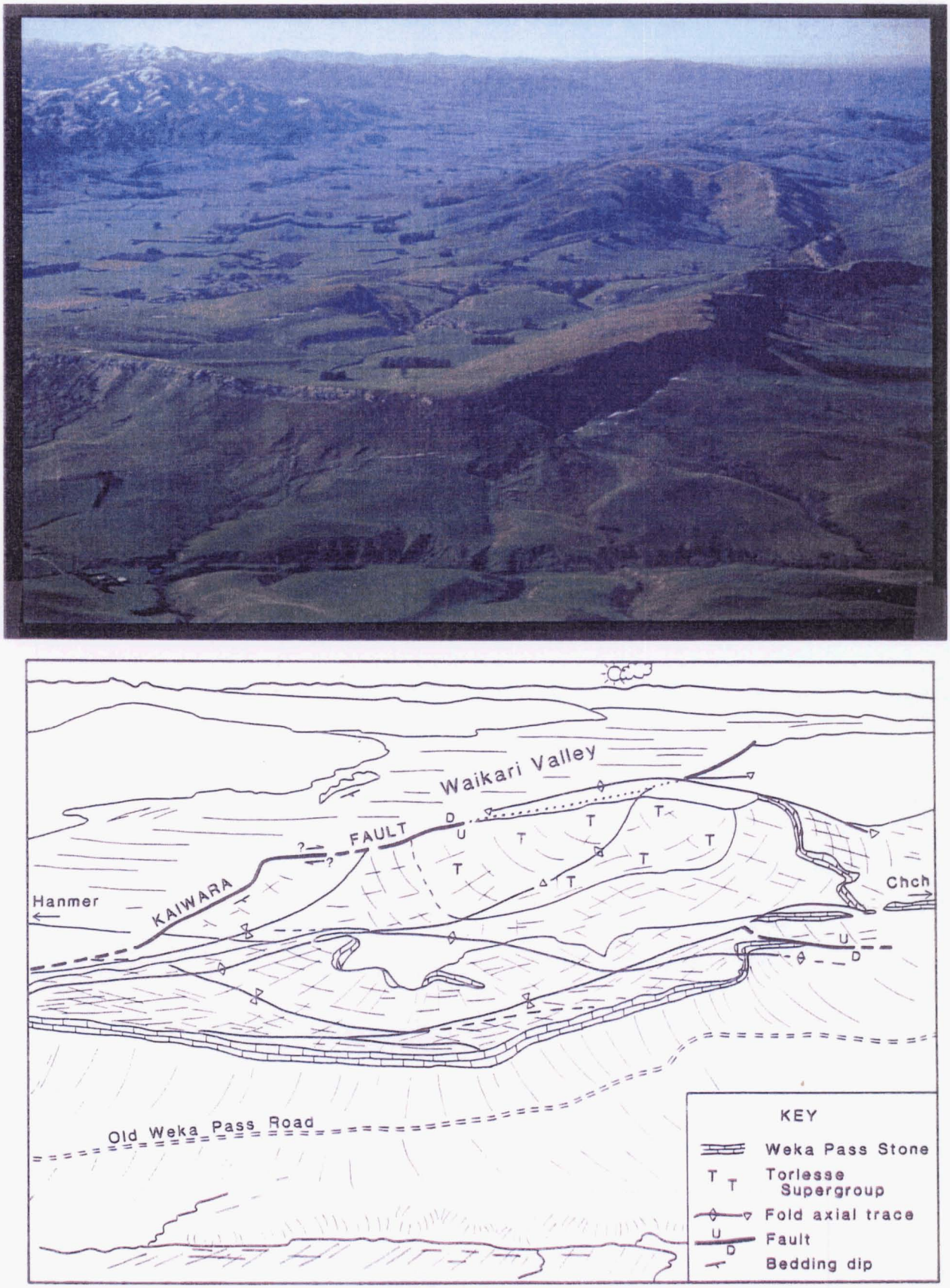

Figure 3.2. Oblique aerial photo and line drawing of fold interference patterns, mainly delineated by the Oligocene limestone units, in the Weka Pass to Waikari area. The main fold in the foreground is the Timpendean Syncline.

amplitudes range from 50 m. to 1.6 km. and account for up to 3 km. of structural relief in the cover sequence. Fold wavelengths of 0.5 to 3 kilometres are most common, while regionally larger structures with 10 to 20 km. wavelengths are abundant (Gregg, 1964).

Approximately 75 macroscopic scale folds are identified by field mapping. These are often well exposed (Figure 3.1) and vary markedly in morphology. Five distinct areas with different fold morphologies, are defined and summarised in Table 3.1.

3.3 INTERFERENCE PATTERNS

Partial irregular basin and dome outcrop patterns are the most obvious product of fold interference. However, due to the gentle nature of folding and the subdued topography (Figure 3.2, photo), these patterns are rarely well expressed. Although some of the effects of fold interference are broadly recognisable on a regional scale (Gregg, 1964), they are most apparent with more detailed observations.

The geometries and styles of interference folding in the study area are illustrated in figures 3.1 to 3.4. The boomerang shaped Doctors Dome is the most prominent fold interference feature in this area (Figure 3.1). Structure contours drawn on the basement-cover unconformity surface (Figure 3.3) show that the dome is asymmetric to the west, and may have a relatively flat top. It is flanked by numerous smaller scale folds which trend sub-parallel, sub-normal and oblique to the main fold sets. Fold interference patterns at Weka Pass are defined by resistant limestone units (Figure 3.2) and are different in geometry to the Doctors Dome example.

Table 3.1. The morphologies of interfering fold sets for five sub-areas within the study area (see Figure 3.1 for location). Included in the Hui Hui sub-area is the MacDonald Anticline (see Figure 8.1), while Onepunga folds form part of the MacDonald Syncline sub-area. The values represent averages derived from between 5 and 20 observations (along single folds and of different structures), of individual fold sets from each sub-area.

Sub Areas	FOLD SET 1				FOLD SET 2			
	DIMENSIONS (km)		INTERLIMB ANGLE (°)	FOLD AXIS TREND (°)	DIMENSIONS (km)		INTERLIMB ANGLE (°)	FOLD AXIS TREND (°)
	Wavelength	Amplitude			Wavelength	Amplitude		
Weka Pass (1)	2·7	0·14	122	98	3·0	0·035	152	356
The Deans (2)	12·0	1·30	140	220	3·4	0·06	158	136
Pyramid Valley (3)	2·3	0·20	105	14	2·3	0·13	120	95
MacDonald Syncline (4)	3·2	0·84	57	355-175	1·7	0·13	146	277-97
Hui Hui (5)	1·4	0·09	140	360	1·3	0·07	157	102

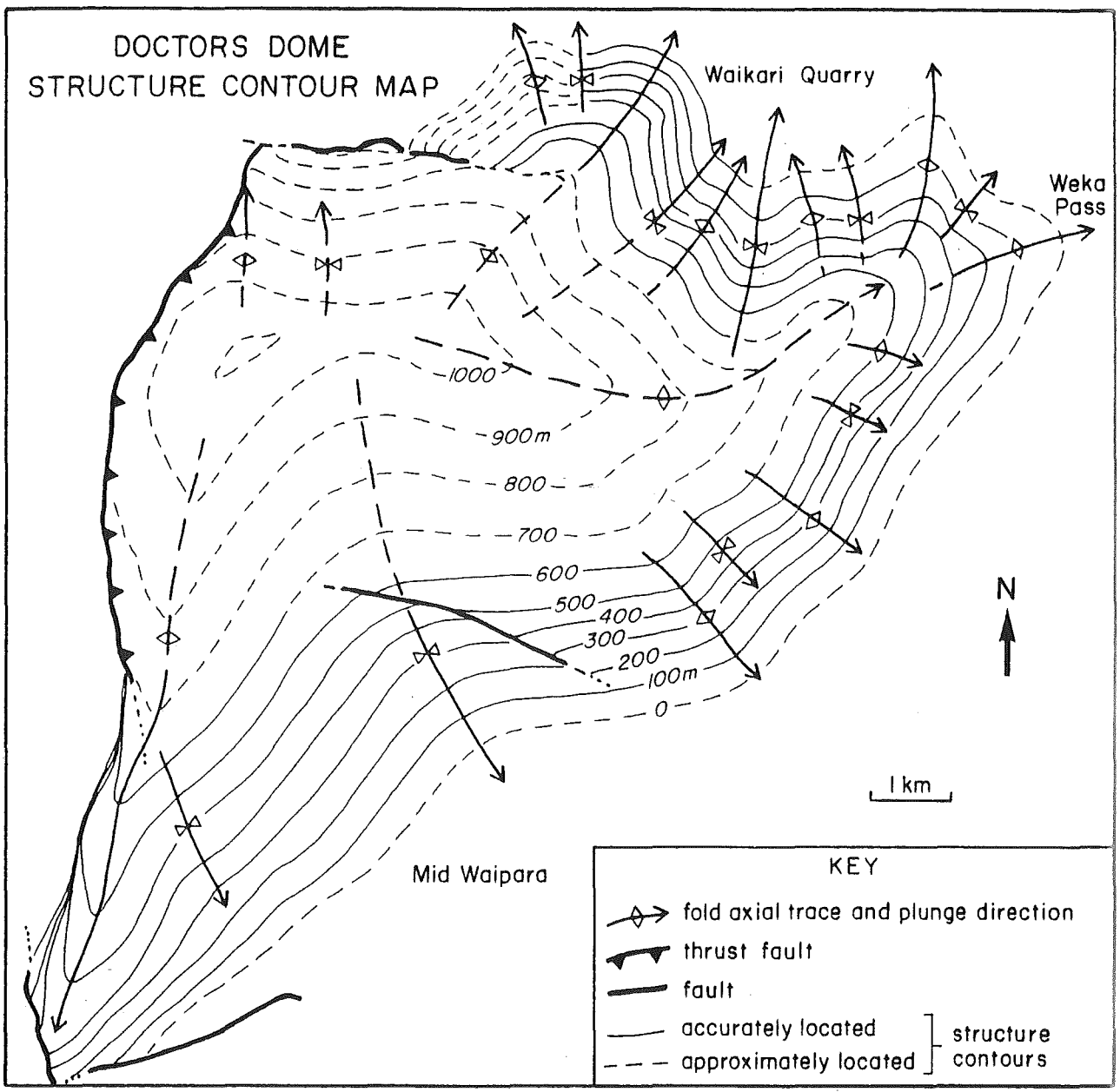

Figure 3.3. Structure contour map of the Doctors Dome fold interference structure. Contours are drawn on the basement-cover late Cretaceous unconformity surface at 100 m. intervals. Elevation control on the datum is provided by altimeter spot heights and 20 m. contours from 1:25 000 topoplots. The unconformity surface is conformable with the overlying cover sequence.

Interference at Weka Pass is mainly due to the development of N-S and E-W trending folds, which display small (< 15^0) local variations in both trend and plunge direction (Figure 3.4). The interference pattern is characterised by angular to sub-angular folding of the limestone datum, with abrupt termination of folds (e.g. west end of the Timpendean Syncline) and secondary folding oblique to the two main fold sets.

Basin and dome interference patterns of this type are not limited to the Doctors Dome and Weka Pass areas. Similar structures are exposed at Hui Hui (appendix 3B, Figure 8.2) and Onepunga (see Figure 5.3), while interference folding with different geometries are also developed along 'The Deans' and in the MacDonald Syncline (Figure 3.1). Bradshaw (1975) also describes similarly irregular folds in the Castle Hill Basin which are non-cylindrical, highly variable in profile, trend and plunge, and associated with basin and dome structures. From the structure contour maps (Figures 3.3 and 3.4) and detailed observations made throughout the study area numerous fold surface geometries are frequently recognised. These are:

(1) two sets of folds trending approximately E-W and N-S (+/- 15^0);
(2) fold axes that change orientation across interfering fold sets;
(3) conical fold surfaces (chapter 4);
(4) boomerang and triangular shaped fold surfaces and outcrop patterns;
(5) corrugated hose shaped fold surfaces and outcrop patterns;

Figure 3.4. Structure contour map of the Weka Pass area, displaying fold interference patterns. Contours are drawn on the mid-Oligocene unconformity surface between the Amuri Limestone Formation and the Weka Pass Stone Member (Omihi Formation) at 20 m. intervals. Elevation control as for figure 3.3. The unconformity surface appears to be conformable with the units above and below in the cover.

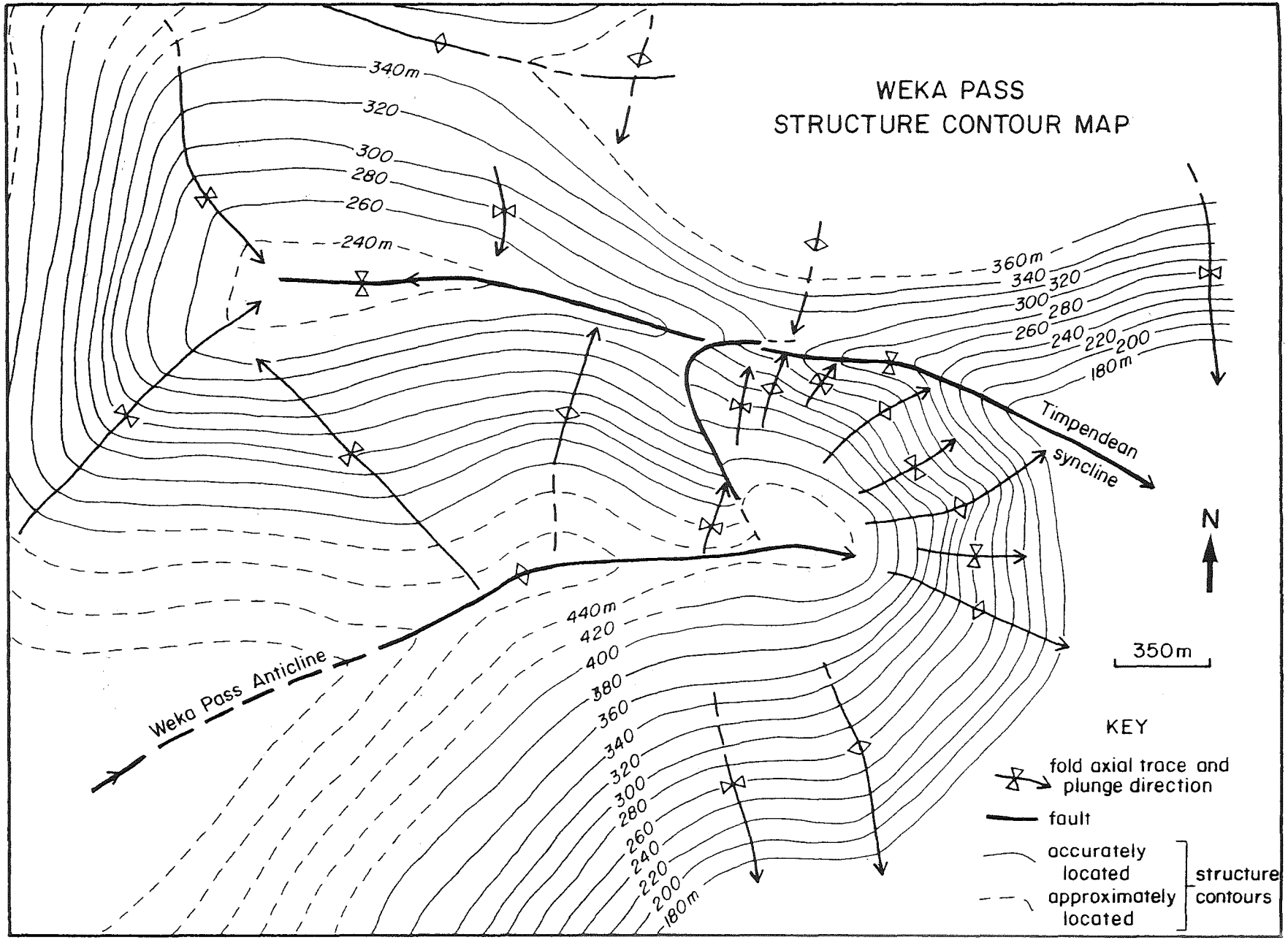
WEKA PASS
STRUCTURE CONTOUR MAP
340m
320
300
280
260
240m
360m
340
320
300
280
260
240
220
200
180m
Timpendean
syncline
N
350m
Weka Pass Anticline
440m
420
400
380
360
340
320
300
280
260
240
220
200
180m
KEY
fold axial trace and
plunge direction
fault
accurately
located
approximately
located
structure
contours

(6) secondary folds that commonly trend NE and SE oblique to, and often bifurcating from, the axial surfaces of the main fold sets;

(7) discontinuous folds, which abruptly terminate against the interfering fold set;

(8) folds that change their geometry along the hinge line in accordance with the position of the interfering fold sets.

The first three features are classical consequences of fold interference (Ramsay, 1962; Wilson, 1967). One and two are illustrated by figures 3.1 to 3.4, while conical fold geometries are described and discussed in chapter 4. Irregular boomerang, triangular and corrugated outcrop patterns, and changes in fold geometry due to fold interference have received little attention in the literature and warrant further discussion.

3.3.1 BOOMERANG AND TRIANGULAR PATTERNS (4)

Fold interference has produced distinctive boomerang (or half star) and triangular (or half diamond) outcrop patterns and fold surface geometries, where anticlines (Figure 3.3) and an anticline and syncline (Figure 3.4) interfere respectively. Figure 3.5 represents the end member interference geometries for like (anticline-anticline or syncline-syncline) and different (i.e. anticline-syncline) fold types.

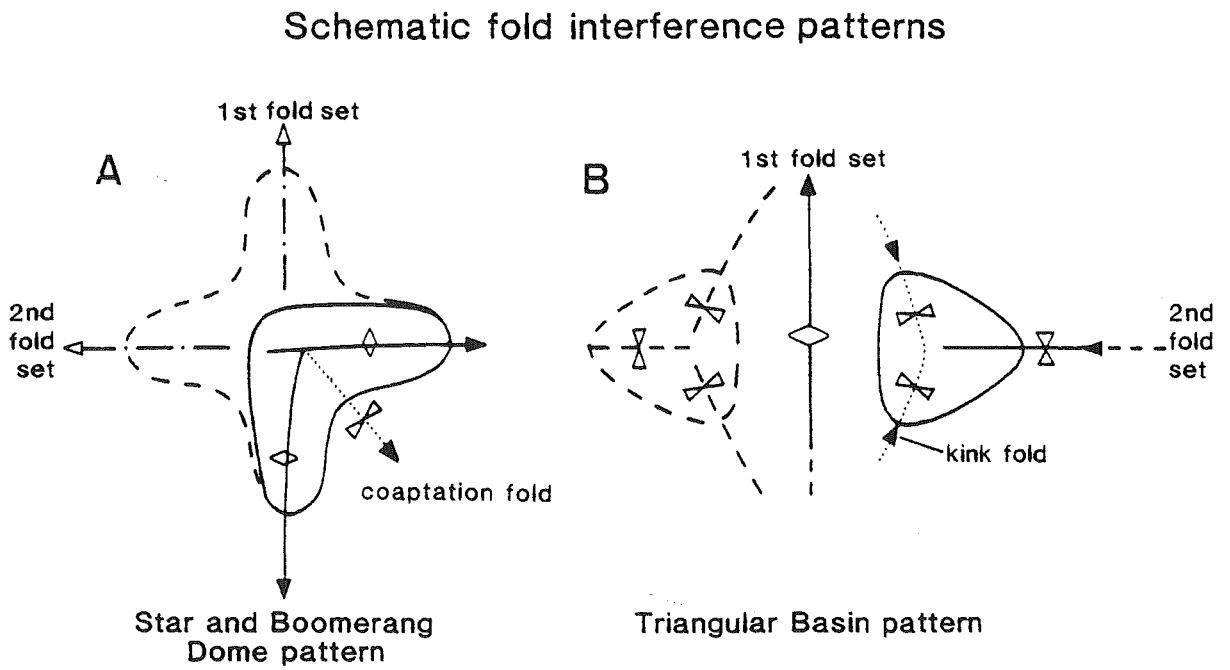

Figure 3.5. Schematic diagrams showing the fold outcrop patterns developed in North Canterbury in association with basin and dome interference of angular folds. The solid lines in (A) and (B) represent simplified versions of the interference patterns in the Doctors Dome and Timpendean Syncline areas respectively.

The interference of like fold types, where fully represented, produces star shaped basins and domes (Figure 3.5a), but, in this example, partial star or boomerang outcrop patterns are more common. The Doctors Dome is the best local example of this interference geometry (Figure 3.3). Potentially this type of interference may result in a number of basin and dome geometries, ranging from the complete star to various 'T' and boomerang shaped (Figure 3.5a) outcrop patterns (Stauffer, 1988), as well as patterns where the greater part of the star is not preserved and only portions of the star points remain.

The interference of different fold types produces an outcrop pattern dominated by triangular or diamond shapes (Figure 3.5b). The pattern is best developed when one of the interfering folds is dominant. For example, the western termination of the Timpendean Syncline results from the interference of the syncline with an adjacent N-S trending anticline to the west (Figure 3.1).

3.3.2 'CORRUGATED HOSE' PATTERNS (5)

'Corrugated Hose' fold interference (Figure 3.6) is developed in situations where the interfering fold sets, trending at a high angle to each other, have markedly different dimensions. Several areas are dominated by relatively large folds (wavelengths 5-30 km., amplitudes 0.5-1.5 km.), which interfere with relatively small scale structures (wavelengths 0.5-3 km., amplitudes 0.05-0.2 km.). This results in an outcrop pattern dominated by the larger of the two fold sets, with interference preserved as small warps on the limbs of the major folds. It produces an interference pattern analogous to a corrugated hose severed in half perpendicular to the corrugations (Figure 3.6a). Locally the best example of this type of interference pattern is produced in the N-S trending MacDonald Syncline (Figure 3.8), but partial 'corrugated hose' patterns are also developed at Onepunga and along 'The Deans' (Figure 3.1). Locally this type of fold interference pattern has developed in association with small amounts of shortening (commonly < 10%) perpendicular to the smallest fold set. As a consequence the fold interference pattern is difficult to detect, and the basins and domes are small (Figure 3.6b).

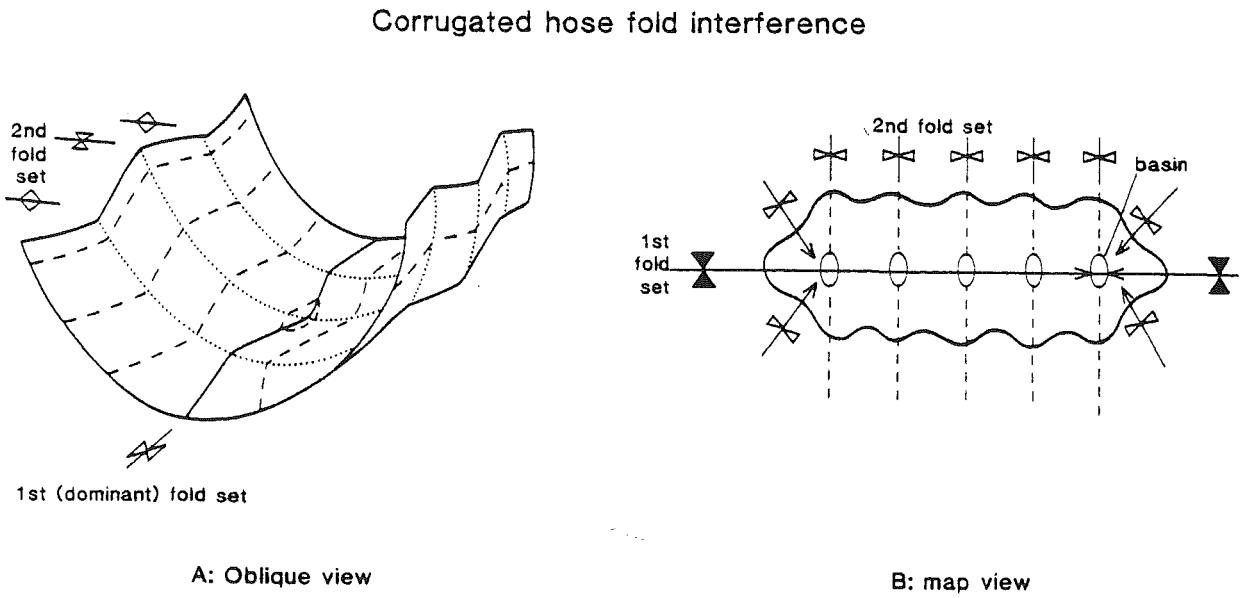

Figure 3.6. Schematic three dimensional oblique (A) and map view (B) representation of corrugated hose fold interference patterns. This pattern is developed where the interfering fold sets have different wavelengths. Locally the MacDonald Syncline provides the best example of this type of fold interference.

3.3.3 OBLIQUE SECONDARY FOLDS (6)

Secondary folds are commonly developed oblique to the main fold sets as an integral part of the interference patterns. These folds most commonly trend NE-ENE and SSE (Figure 3.7), and are generally angular discontinuous folds subordinate to the main fold axes (Figures 3.3 and 3.4). Oblique secondary folds are developed in

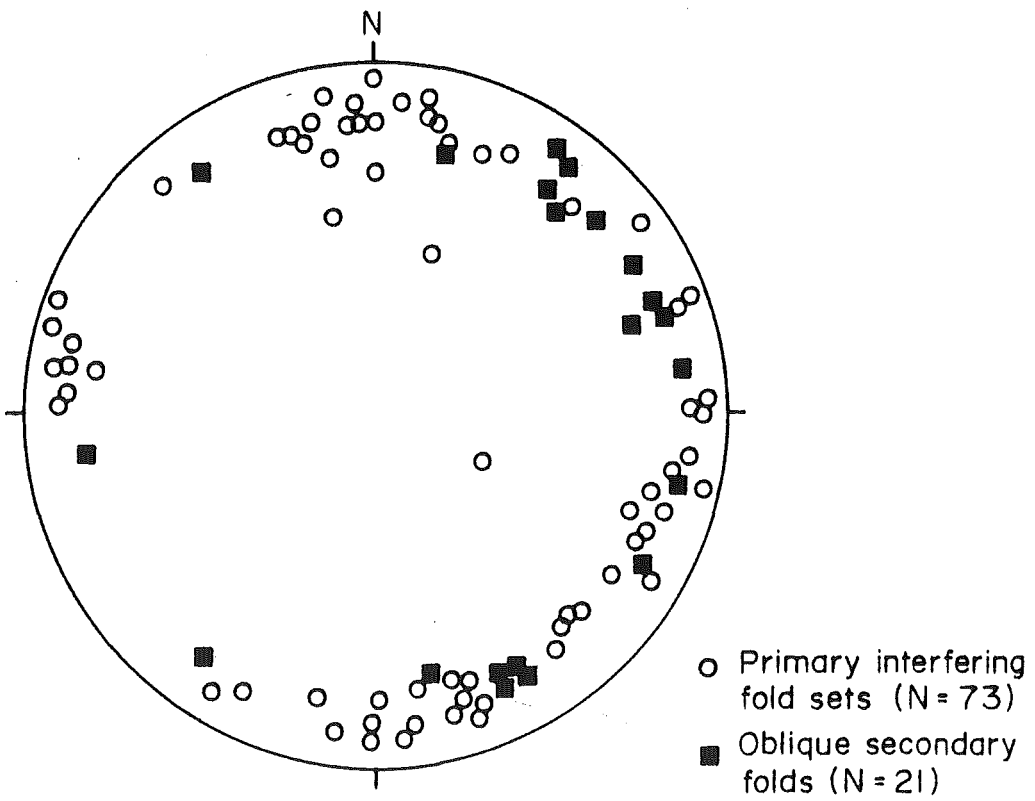

Figure 3.7. Lower hemisphere equal area net of macroscopic fold axes trend and plunge. Primary interfering fold sets and oblique secondary folds are distinguished.

two situations: (1) along the intersection line of the two interfering fold set limbs, referred to as "coaptation folds" by Stauffer (1988); and (2) on the semicircular flanks of basin and dome structures.

Folds that form along the intersection of two interfering fold sets represent sharp changes in the fold surface orientation which bisect the main fold sets, commonly trending NE and SE. The presence of two such fold orientations precludes the possibility that S and E trending folds represent a single refolded structure. Folds developed along the intersection of two fold sets are preserved as both discrete (Figure 3.3) and bifurcating structures (Figure 3.4). Stauffer's (1988) suggestion that "coaptation folds" are most commonly formed where like folds interference may just

reflect that it is easier to locate these folds when they are associated with prominent basins and domes. Discrete oblique secondary folds are produced where like fold types interfere and radiate away from, and towards dome and basin structures respectively. They appear never to reach the dome culmination or basin depression (Figures 3.3 and 3.5). Secondary folds which bifurcate from the main fold axes, forming a triple junction of fold axial traces (Figure 3.4), are consistently developed where different fold types interfere (Figures 3.5b). Oblique secondary folds formed due to the interference of an anticline and syncline bifurcate from the terminating fold axis (Figure 3.5b). In figure 3.4, at the western end of the Timpendean Syncline, the syncline fold axis bifurcates as it is terminated against the adjacent and dominant anticline.

Secondary folds developed on the flanks of basin and dome structures are illustrated at the eastern end of the Weka Pass Anticline (Figure 3.4) and the Waikari Quarry area (Figure 3.3). In these areas the fold surface is hinged about numerous folds, including the main fold sets, which are spread evenly around the partial interference structures. These folds are short, discontinuous structures which converge towards the dome apex or basin low. They represent numerous bends in the folded surface at varying angles to the main fold sets, and are analogous to pleats or flutes.

Some debate exists as to the origin and nomenclature that should be used for folds identical to the ones described here. Stauffer (1988) suggests that folds form along the intersection line of the interfering fold sets, as a geometric consequence of fitting together the two fold forms, and introduced the term "coaptation fold" for these structures. However, Lisle et al (1990) suggest that this type of fold pattern develops

to accommodate curvature on the flanks of basins and domes, and that the term "curvature accommodate fold" is more appropriate. The secondary oblique folds described here appear to accommodate curvature of the fold surface imparted by fold interference. Therefore, in the broad sense both fall within the group of 'curvature accommodation folds'. However, the coaptation folds of Stauffer (1988) represent a sub-group which is geometrically distinct and common. The term 'coaptation fold' should be retained.

Potentially a single interference structure may contain both 'pleat' and 'coaptation' curvature accommodation folds. The Doctors Dome provides a good example of this, with its large SE trending coaptation fold and numerous 'pleats' in the Waikari Quarry area. In this example each type of oblique secondary fold is developed at a different scale on different surfaces. The 'pleat' folds are formed in highly competent thin limestone units, as suggested by Lisle and others (1990), and the coaptation on the basement-cover unconformity (Figure 3.3).

3.3.4 CHANGES IN FOLD GEOMETRY (7 and 8)

Locally and within the Castle Hill Basin (Bradshaw, 1975) folds display variations in morphology along their hinge lines (Figures 3.8 and 8.3). These changes appear to result mainly from fold interference and/or the termination of folds both along the hinge line and vertically through the sequence.

Changes in fold cross sectional shape (Figure 3.8) appear to be influenced by the position and morphology of the interfering folds. Field observations suggest that fold interference of like folds produces an increase in the fold wavelengths associated

Figure 3.8. Changes in cross sectional shape along the hinge line of the MacDonald Syncline (see Figure 3.1 for location). The solid fold outline represents the shape of either the top of the Mt Brown Formation or the Weka Pass Stone Member. The distances along the hinge line are measured from south to north and begin where the fold axial trace intersects the Mt Grey Fault. The cross sections have been drawn E-W, parallel to and often coincident with, the interfering fold set.

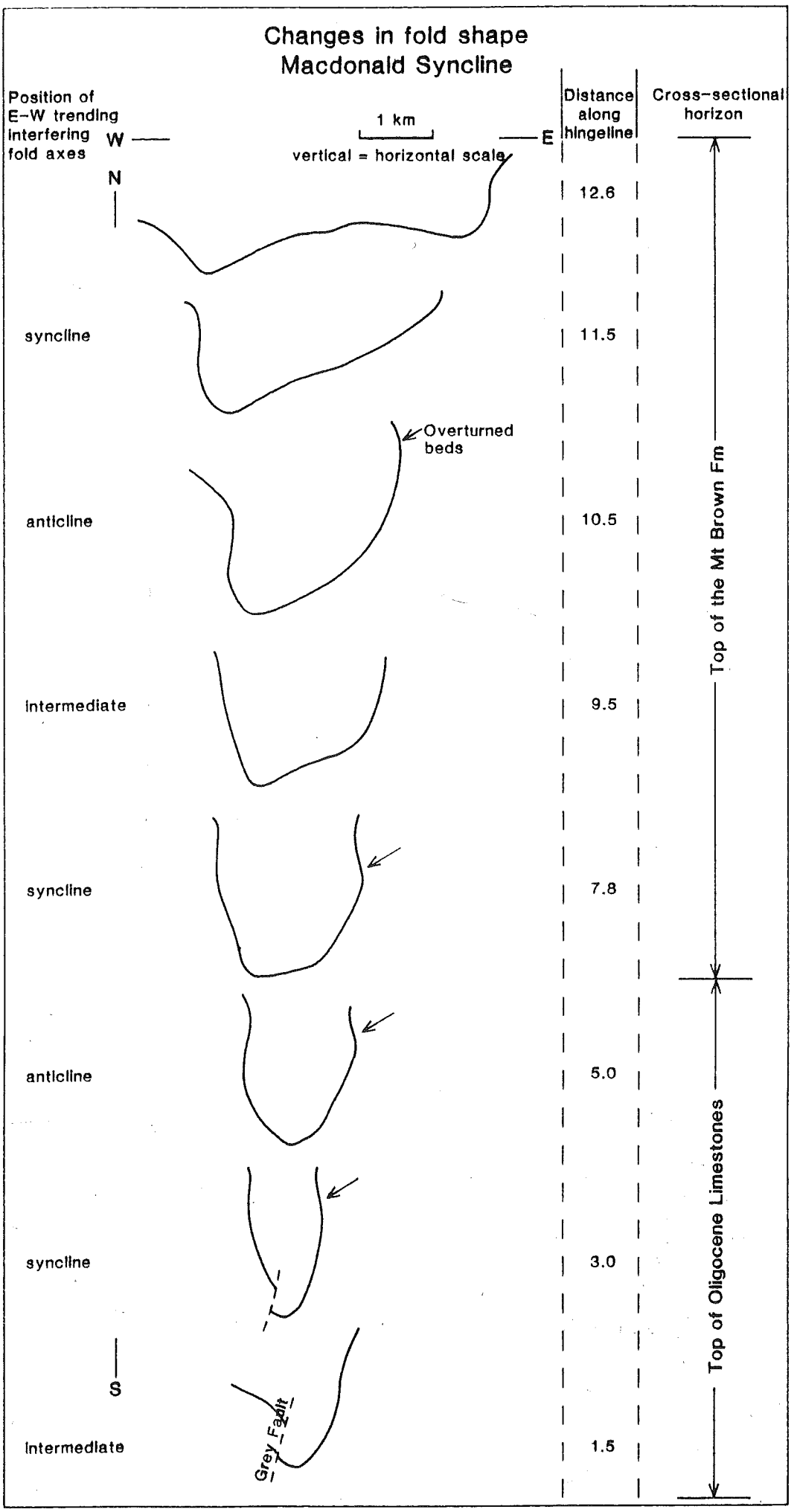
Changes in fold shape
Macdonald Syncline
Position of E-W trending interfering fold axes
W
E
1 km
vertical = horizontal scale
N
S
Distance along hingeline
Cross-sectional horizon
12.6
11.5
10.5
9.5
7.8
5.0
3.0
1.5
syncline
anticline
intermediate
syncline
anticline
syncline
intermediate
Overturned beds
Grey Fault
Top of the Mt Brown Fm
Top of Oligocene Limestones

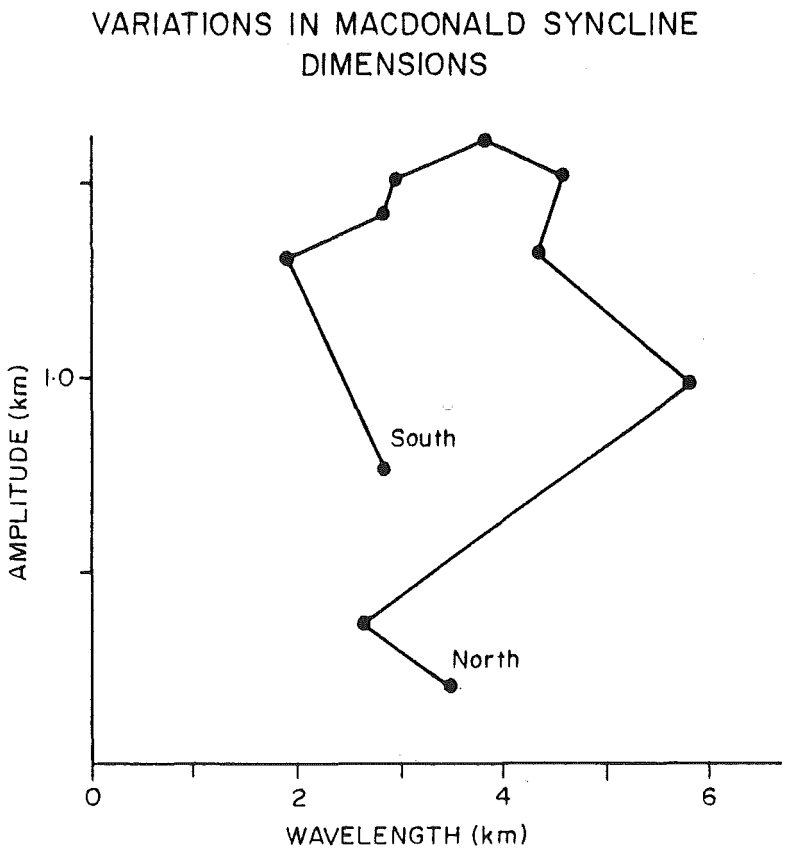

Figure 3.9. A graph showing the variation in fold dimensions from south to north along the MacDonald Syncline. Note that the fold reaches a maximum amplitude in the central parts of the observed structure, while the wavelength maximum is closer to the northern end. The data for this diagram was extracted from a number of cross sections drawn across the syncline, which are partly reproduced in figure 3.8.

with broad basin and dome structures, while interference of different folds produce restricted saddle structures with reduced wavelengths. However, this is not convincingly portrayed by figure 3.8, although changes in the cross sectional shape of the Timpendean Syncline (Figure 8.3) are in accord with field observations. Figure 3.8 does show that bedding on the eastern limb of the MacDonald Syncline is apparently only overturned in the hinges of the interfering fold sets.

These changes are generally superimposed on the effects of fold termination, which may occur abruptly over several hundred metres or gradually over several kilometres. Along the MacDonald Syncline both fold dimensions change (Figure 3.9), but while the fold wavelength reaches a maximum close to the northern limit of fold observations, amplitude is at its greatest in the central portions of the structure. Abrupt lateral fold terminations are also common (e.g. west end of the Timpendean Syncline, east end of the Weka Pass Anticline and the north end of the MacDonald Anticline; see Figure 3.1). Fold termination of this type is commonly associated with the development of an adjacent fold at a high angle to the terminating structure.

3.4 CONCLUSIONS

Basin and dome interference of folds trending approximately N-S and E-W has produced irregular and complex outcrop patterns. These non-classical interference patterns vary locally and are characterised by numerous fold surface geometries ranging from half star (boomerang) to newly recognised triangular and corrugated hose outcrop patterns.

These patterns reflect directly the morphologies of the interfering fold sets and the types (e.g. anticline-anticline or anticline-syncline) of folds interfering. The interference of like fold types (e.g. anticline-anticline) produces patterns dominated by partial star (boomerang) shapes, while interference of different fold types forms triangular and diamond outcrop patterns. In situations where the interfering fold sets are markedly different in size a third interference pattern, dominated by the largest fold set and characterised by small basins and domes, is formed. This has been

termed'Corrugated Hose' fold interference. As a further consequence of interference, discontinuous secondary folds form obliquely to the main fold sets. These folds have no kinematic significance and develop to accommodate curvature of the surface deformed by fold interference.

Discontinuous faulting is attributed to the discontinuous nature of folding and the resulting partial and irregular fold interference geometries. These irregular interference geometries are only likely to form where the folded units are competent enough to accommodate bending without changes in the unit thicknesses.

Similar fold interference patterns could be abundant in orogenic belts where angular folds are developed at shallow crustal levels in response to faulting. However, they are likely to be discontinuous and irregular and may not be readily recognised due to their non-classical geometries. Because of the irregular geometries, vertical and lateral extrapolation of fold data needs to be approached with caution.

CHAPTER 4 CONICAL FOLDS PRODUCED BY BASIN AND DOME FOLD INTERFERENCE

4.1 INTRODUCTION

Conical folds comprise a small, special part of the larger category of non-cylindrical folds, but unlike many folds in this group they are easy to define geometrically with the aid of stereographic or equal area net projections. A folded surface defined by a mathematical cone must have its geometric axis oblique to the surface (Haman, 1961; Stauffer, 1964; Systra and Skornyakova, 1980). The orientation and curvature of a conical fold surface can be defined by the inclination of the cone axis and the angle between this axis and the folded surface, which is half the apical angle of the cone (Figure 4.1a and Table 4.1). Cylindrical folds may be regarded as conical folds with an apical angle equal to zero. These parameters are measured directly from equal area plots of poles to the folded surface (bedding in this case), which are distributed along small circles (Figure 4.1b). Conical folds commonly develop in two situations; (1) at the termination of a cylindrical fold (Webb and Lawrence, 1986), and (2) as a consequence of fold interference (Systra and Skornyakova, 1980).

Inhomogeneous shortening and associated conical fold development are implicit in basin and dome fold interference, and it is widely recognised that conical folds develop in association with fold interference (e.g. Ramsay, 1962; Wilson, 1967; Systra and Skornyakova, 1980). However, not all basin and dome fold interference patterns are characterised by conical folds, irregular and non-cylindrical forms are common (e.g. Stauffer, 1988).

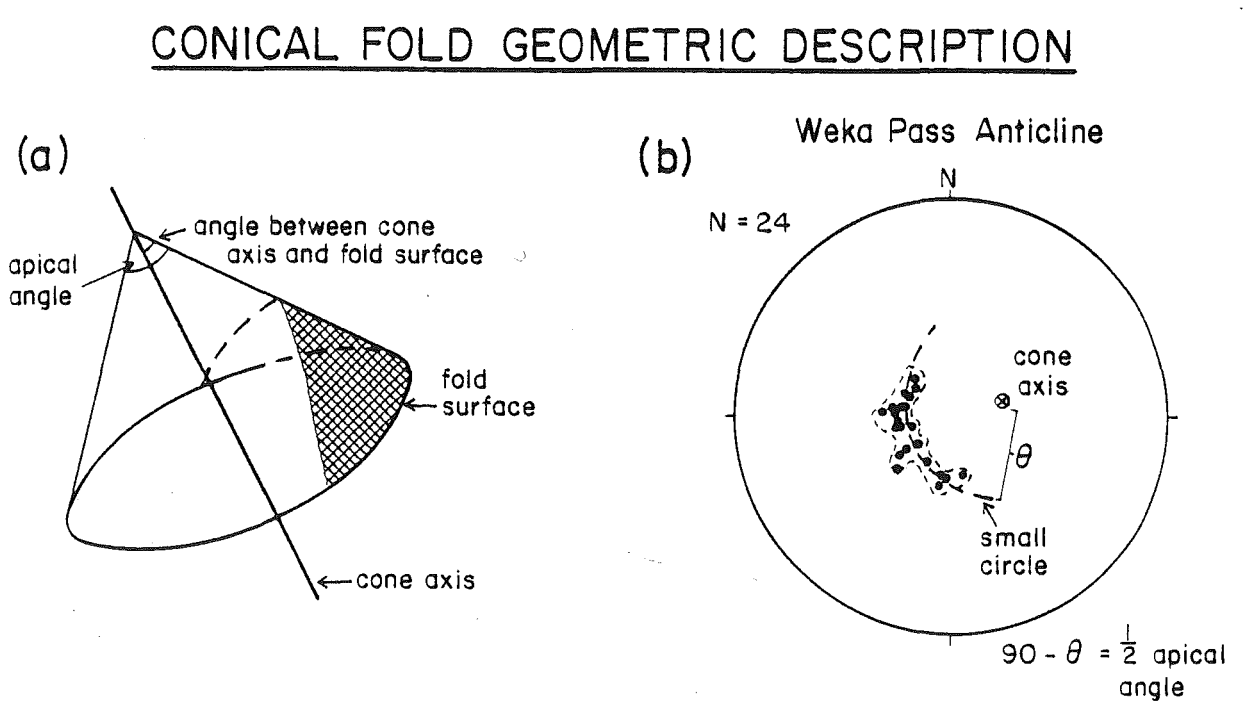

Figure 4.1. Geometric description of conical fold surfaces. (A) Cone shape and geometric elements, including cone axis and apical angle, for the Weka Pass Anticline, North Canterbury. (B) The same structure is represented in a lower hemisphere equal area plot of poles to bedding.

Detailed analysis of well defined, non-cylindrical, angular macroscopic folds in North Canterbury suggests that these structures are made up of conical elements that change systematically with variations in the development of interfering fold sets. This study examines the geometric relationships between the interfering fold sets which produce basin and dome fold interference and conical folds. The resulting cone

geometries are complex and often difficult to detect, which may explain the apparent absence of conical folds in some areas of basin and dome fold interference.

4.2 CONE GEOMETRIES

Table 4.1 provides a summary of the conical fold geometries from each sub-area (see Figure 3.1 for sub-area location). The MacDonald Syncline (sub-area 2) is dominated by steep cone axes and small (30-60^0) apical angles, while everywhere else (sub-area 1) fold surfaces are mainly characterised by steeply inclined cone axes (60-80^0), and large apical angles (ranging from 100-130^0). Folded limestone surfaces are commonly composite shapes which are represented by several cone surfaces.

4.3 VARIATIONS IN CONE GEOMETRY

Conical folds vary in geometry both across and along interfering fold sets. This variation is intimately related to changes in the morphology of each fold set. Geometric parameters of each of the interfering fold sets contributing to the shape of the conical fold surfaces include the curvature of the hinge zone, fold tightness (a function of the fold amplitude-wavelength ratio), and limb dips. These features are first discussed separately, although their effects are cumulative. Where possible, fold surfaces influenced by fold terminations have been excluded.

Table 4.1. A summary of all conical fold data and interfering fold set interlimb angles for the North Canterbury area of study. All numbers represent averages, in degrees, for each subarea. The location of both subareas is indicated on figure 3.1.

	Cones Axes Plunge	Cone and Fold axis angular separation	Apical Angle	Interlimbs (using Fleuty 1964)	
				Fold Set 1	Fold Set 2
Subarea 1	75	55	114	132	154
Subarea 2	67°	69°	45°	43°	146°

4.3.1 HINGE ZONE CURVATURE

Upright folds commonly display a reduction in dip of the fold surface towards hinges. The interference of two folds at a high angle to each other results in a flattening of the fold surface into basin and on to dome structures. Figure 4.2a depicts the expected change in cone geometry and distribution of poles to the fold surface into a rounded fold interference basin. As limb dips decrease towards the basin (or dome) the apical angle of a cone which describes the fold surface (marked by the heavy line in Figure 4.2a, schematic diagram) must increase and the small circles describing the cones decrease in diameter (Figure 4.2a, equal area

plot, and Table 4.2). When rounded folds interfere, although the cone axis may remain steep, the cone apical angle must continually change to accommodate the curvature of the fold surface, and many cones may be required to geometrically describe the surface. Angular folds, such as the ones preserved in North Canterbury, prove much easier to describe and the number of cones required to approximate the fold surface curvature imparted by the interfering hinge zones is limited to one or two (Figure 4.2b). The effects of hinge zone curvature on cone geometries are often under represented because hinge zones are commonly undersampled. The effects of hinge zone curvature are best observed on the limbs of the second fold set, particularly if the interfering folds are rounded.

4.3.2 FOLD SET TIGHTNESS

The ratios of fold amplitudes to wavelengths and the subsequent tightness of respective fold sets has a profound affect on the fold interference cone geometry. Figure 4.3 demonstrates the expected change in cone geometry with different combinations of fold set interlimb angles. Only if both fold sets are upright and have similar interlimb angles do the resulting cones have an apical angle approximately equal to the interlimb angles (Table 4.1, subarea 1), with a steep cone axis and circular cross section (Figure 4.3, cones 1,5,8 and 10). Increasing the interlimb angles (i.e. increasing the amplitude to wavelength ratio), increases the apical angle.

When the folds are upright and the interlimb angles of the interfering fold sets are different (Table 4.1, subarea 2), the resulting cones become flattened (with an elliptical cross section) perpendicular to the trend of the tightest fold set. The

HINGE CURVATURE AND CONE GEOMETRY

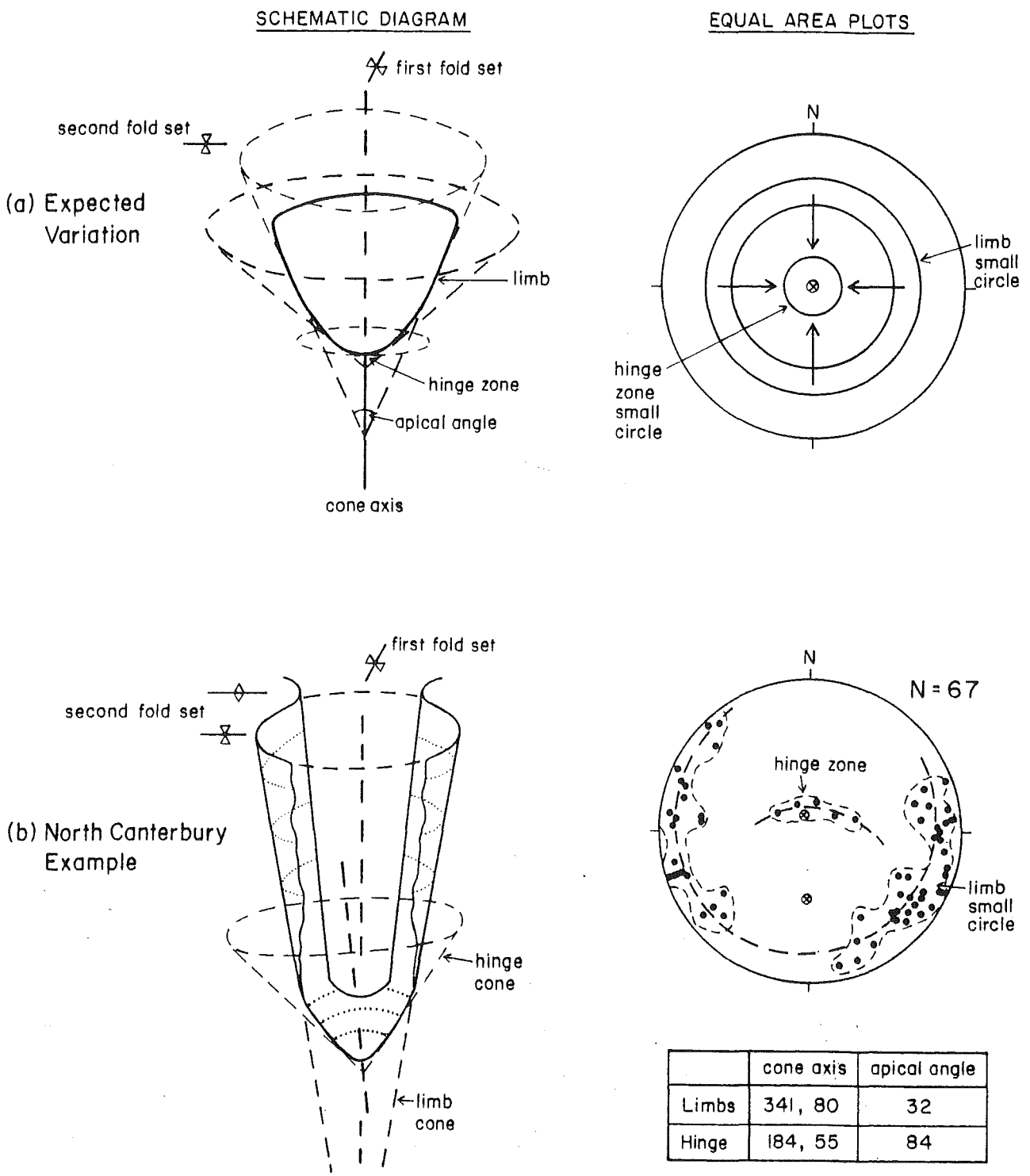

	cone axis	apical angle
Limbs	341, 80	32
Hinge	184, 55	84

Figure 4.2. Schematic diagrams and equal area plots demonstrate the expected (a) and observed (b) changes in cone geometry into fold interference basin structures. The arrows on the upper equal area net indicate the reduction in small circles size into the basin.

flattening becomes more pronounced as the difference between fold set interlimb angles is increased, and the fold surface geometry can no longer be defined by a single cone. Cone flattening is most obvious in the top row (cones 1-4) of figure 4.3. The flattened cone becomes best described by several partial cone surfaces with increasingly inclined axes, particularly the two axes parallel to the axial surface of the tightest fold set. The apical angle of the cone surface approximately parallel to the axial surface of the tightest (1^{st}) fold set increases and the surface approximately parallel to the axial surface of the 2^{nd} fold set decreases (Figure 4.3, inset). Interfering folds with large differences in their interlimb angles are most accurately described by several cone surfaces, but may be approximately periclinal and exhibit short, cylindrical middle sections, and conical terminations. The fold surfaces in the MacDonald Syncline (Table 4.1, subarea 2) approach this extreme (Figure 4.3, cone 4), with interlimb angles of 43^0 and 146^0 respectively, generating steep limb cone axes and inclined hinge cone axes (Figure 4.2b). This example emphasises the cumulative effects of the fold hinge zone and interlimb effects, with small cone apical angles on the limbs and large cone apical angles in the hinge zone. As the interlimb angle of one fold set tends to zero or 180^0, the second fold set becomes approximately cylindrical. Slightly "flattened cones" with elliptical cross sections can be expected as the commonest form associated with fold interference.

4.3.3 LIMB DIPS

The geometry of fold interference cones varies where limb dips differ for one or both of the fold sets. An upright fold with variable limb dips subject to interference folding will have different cone geometries on each limb (Figure 4.4 and Table 4.2). As the

Figure 4.3. Predicted changes in the geometry of conical folds produced by changes in the tightness of the interfering fold sets. These changes in the fold set interlimb angles are inferred for areas of basin and dome fold interference where fold limb dips are equal. Hinge zone curvature effects are neglected.

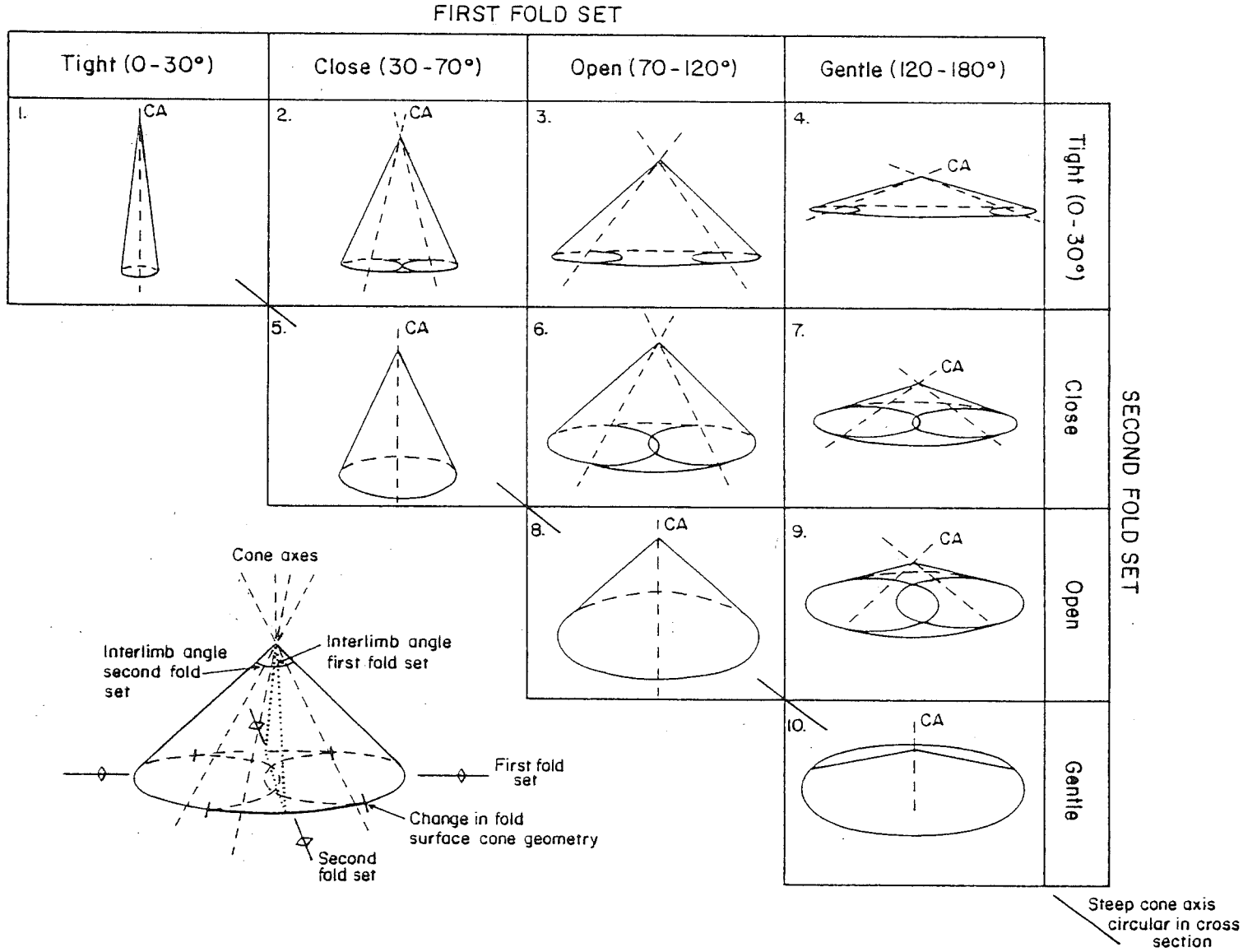

INTERFERING FOLD SET TIGHTNESS AND CHANGES IN CONE GEOMETRY

limb dips increase the apical angle of the conical fold surface on that limb must decrease, if the cone axis remains steep. In North Canterbury, however, the geometry is more complex and the steepest limb of one fold set (Figure 4.4a, north limb) is commonly characterised by a conical surface with a steeply plunging cone axis and a relatively large apical angle, and the shallower limb (Figure 4.4a, south

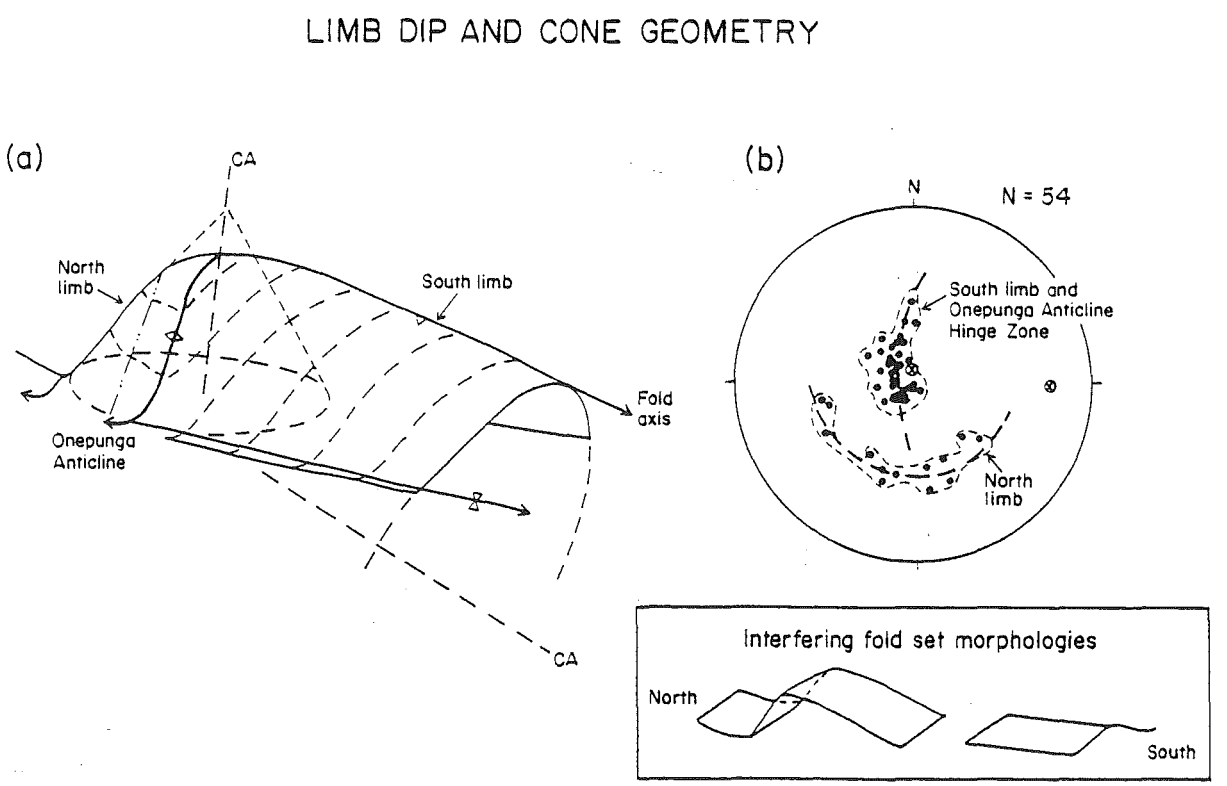

Figure 4.4. Variation in cone geometry with changes in limb dip for the Onepunga Anticline, North Canterbury. The diagram includes a 3 dimensional representation of the fold (with cones superimposed), an equal area plot of poles to bedding, and inset, morphologies of the interfering fold sets.

limb) by a shallow cone axis (trending parallel to one of the fold sets) and a smaller apical angle. With increases in the dip of the steepest limb the apical angle of the cone describing that limb decreases (Table 4.2, limb dips of steepest limb increase from top to bottom). In the MacDonald Syncline the dip of the steepest limb is 70^0 and the apical angle is similar for each limb, but the cone axes maintain dissimilar plunges (Table 4.2, bottom row).

Table 4.2. A summary of conical fold geometries for three folds with different limb dips on one of the interfering fold sets. The locations of the Onepunga and MacDonald folds are indicated on figure 3.1, while sub-fold area 2 of the Timpendean syncline is indicated on figure 4.5. The Onepunga Anticline conical geometries are illustrated in figure 4.4. Hinge zone cone geometry data is included.

Fold		Limbs						Hinge		
		Steepest limb			Shallowest limb					
		Bedding Dip	Cone Axis Plunge	Apical Angle	Bedding Dip	Cone Axis Plunge	Apical Angle	Fold Axis Plunge	Cone Axis Plunge	Apical Angle
Timpendean Syncline	Subarea 1	25	80	116	9	25	30	20	80	116
	Subarea 2	25	85	134	18	20	34	3	20	34
Onepunga Anticline		45	80	84	20	25	32	11	25	32
MacDonald Syncline (North)		70	65	52	35	10	68	14	70	116

4.4 COMPOSITE CONE GEOMETRIES

The recognition of conical folds is reliant on having a well exposed regional conical structure or repeated small folds of similar cone geometry. However, conical folds that reflect the combined effects of interference morphologies may be irregular and apparently non-conical. The cumulative effects of these variables produce conical fold shapes that change both across and along the fold. An example of changes in the resultant fold surface geometry due to slight variations in the morphology of the interfering fold sets is demonstrated by the Timpendean Syncline (Figure 4.5). The fold geometry is mainly defined by cones with steep axes and large apical angles (Figure 4.5), but the fold surface varies in shape from a simple conical fold (sub-fold areas 3 and 4), to a fold defined by two distinct conical surfaces (sub-fold area 1 and possibly 2). Whereas sub-fold area 3 mainly reflects the influence of the fold set tightness, sub-fold area 4 shows the effects of a fold termination, with a reduced apical angle. Conversely, sub-fold area 2 is influenced by the different limb dips of the main syncline, and the steeper limb has a steeper cone axis and larger apical angle than the shallower limb.

Plotting all of the data on a single equal area net (Figure 4.5, all data) produces a bedding-pole distribution that is more diffuse than those of the sub-fold areas and, although there is some indication that the folds are conical, it is difficult to define a cone geometry. If in this example more bedding data had been sampled from the hinges of the individual fold sets the sub-fold area plots and particularly the composite plot of all data would prove difficult to interpret. This would be particularly so for rounded folds that are well exposed.

Figure 4.5. Map and inset equal area nets displaying the changes in fold interference cone geometries along the Timpendean Syncline, North Canterbury. Structure contours are drawn on the mid-Oligocene paraconformity surface. Poles to limestone bedding are presented on lower hemisphere equal area nets.

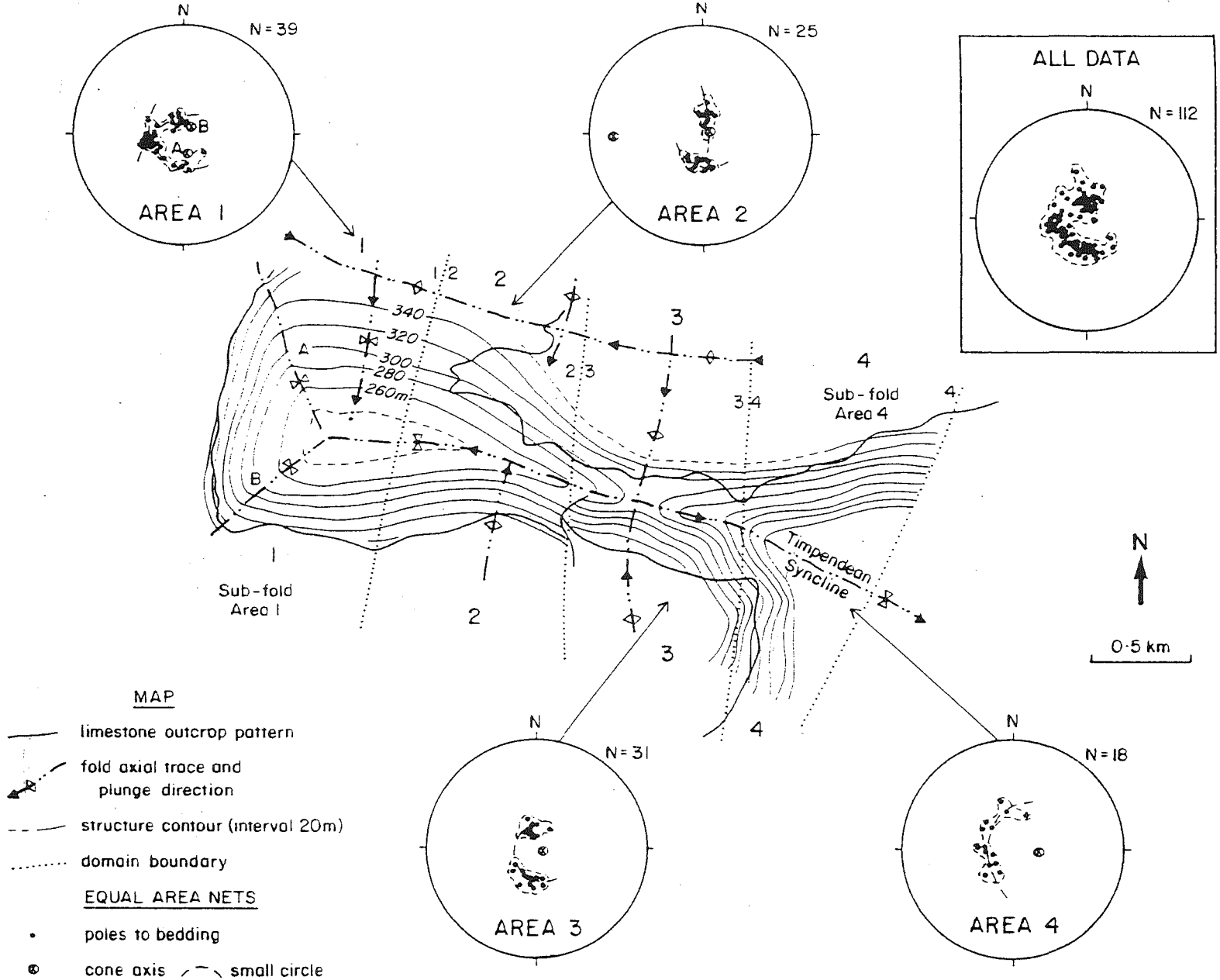

VARIATIONS IN CONICAL FOLD GEOMETRY - TIMPENDEAN SYNCLINE

4.5 ANALYTICAL RECOMMENDATIONS

As a first approximation to geometrically describe composite conical folds developed in association with basin and dome fold interference a two stage filtering process is required. Firstly, the fold must be subdivided into sub-fold areas which define parts of the fold with a common geometry. Initially this can be done by defining fold domains, bound approximately by the inflexion lines of the interfering fold sets. The dominance of the Timpendean Syncline has meant that it was only necessary to define N-S domain boundaries in the example given (Figure 4.5).

Having defined geometrically distinct portions of the fold surface it may be necessary to separate measurements from the fold hinges and limbs. This will allow the effects of the hinge zone curvatures and limb morphologies to be assessed independently. Clearly angular folds with confined hinges and straight to slightly curved limbs will be much more amenable to this type of analysis than rounded structures. Only when the fold is divided into domains can the true geometry imposed by fold interference be determined.

Early recognition of the presence of basin and dome fold interference may provide the key to recognising the presence of conical folds and separating out the cone geometries. Conversely, conical folds may provide a pointer to previously unrecognised fold interference.

4.6 CONCLUSIONS

The irregularity and non-cylindrical geometry of surfaces effected by basin and dome interference folding are normally regarded as being ambiguous and unrewarding to analysis by stereographic methods because poles to the folded surface produce diffuse distributions. Conical folds previously recognised as associated with fold interference are simple structures represented by single small circles. However, as shown by North Canterbury examples, interference surfaces are commonly characterised by several cone geometries which change, both across the fold and along the hinge line. Recognising that interference folds are composite surfaces made up of conical segments with varying apical angles and cone axes allows the geometry of the folds to be more fully described and quantified than in previous accounts. The variations in cone geometry defined by analyses of sub-fold areas relate directly to changes in the hinge curvature, interlimb angle and limb dips of the interfering fold sets, and therefore provide information about these characteristics, which otherwise would be overlooked.

CHAPTER 5 FAULT-RELATED FOLDING AND THE DEVELOPMENT OF COMPLEX INTERFERENCE PATTERNS.

5.1 INTRODUCTION

Folding in the late Cretaceous-early Pleistocene cover sequence is characterised locally by two sets of folds trending at a high angle to each other, which interfere to produce complex outcrop patterns (Chapter 3). These fold sets appear to have developed synchronously in response to macroscopic faulting in the basement and cover (Chapter 2). Folds within the cover rocks appear to develop in two situations; (1) in direct response to fault displacement, and (2) within the blocks bound by the major faults. Fault-related folds (1) are the largest and most prominent of the two fold types and form the focus of this study.

Much work has been conducted on fault-related folds, using surface and sub-surface field mapping (e.g. Berg, 1962; Stearns, 1971; Reches, 1978; Cook, 1983), and theoretical modelling (e.g. Friedman et al, 1976; Reches and Johnson, 1978; Chester et al, 1988). This work has led to the recognition of four main types of folds associated with vertical fault-displacement. These are: drag folds, fault-bend folds, fault-propagation folds and drape folds (Suppe, 1985).

In the Waikari to Mt Grey region faults are often observed to disappear into the cores of folds, forming fault-propagation folds. Fault-propagation folds develop due

to the deformation that takes place just in front of the propagating fault surface (Suppe, 1985). These are complemented locally by limited drape folds, which form by flexure over buried faults (Suppe, 1985), and minor drag folding along the major faults. Folding has been achieved primarily by buckling, with associated brittle fracture, mesoscopic faulting and minor bedding plane slip, which becomes more significant with greater bedding dips, particularly within the mudstone units.

The aim of this chapter is to characterise the geometric and genetic relationships between the young and complex folding patterns in the cover rocks, and macroscopic faulting. Faults and folds are developed at the same structural levels, making it possible to test the relationships between these structures and look closely at the controlling influence of the faults.

5.2 FAULT-RELATED FOLD MORPHOLOGIES

5.2.1 FOLD ORIENTATIONS

Throughout Canterbury (Gregg, 1964) macroscopic folds and faults display similar orientations, a feature also noted by Bradshaw (1975). Figure 5.1 shows that in the area comprising this study faults and folds share common orthogonal N-NNE and E-ESE orientations. The local relationships between the orientations of the macroscopic faults and fold axes are displayed on the four equal area nets in figure 5.1. With the exception of the Weka Pass area these nets show that the major faults strike parallel to the dominant and most abundant fold sets. The Weka Pass area represents a block between main faults, and in this region the trend of the folds is

Figure 5.1. Fault and fold spatial and geometric relationships throughout the study area. The lower hemisphere equal area nets show the geometric relationships between the poles to the major faults and fold axes in four areas. Note that the poles to these macroscopic faults trend at approximately 90^0 to the main folds. The open arrows represent the trend and plunge, with the amount of plunge indicated by the adjacent number, of the principal compressive stress.

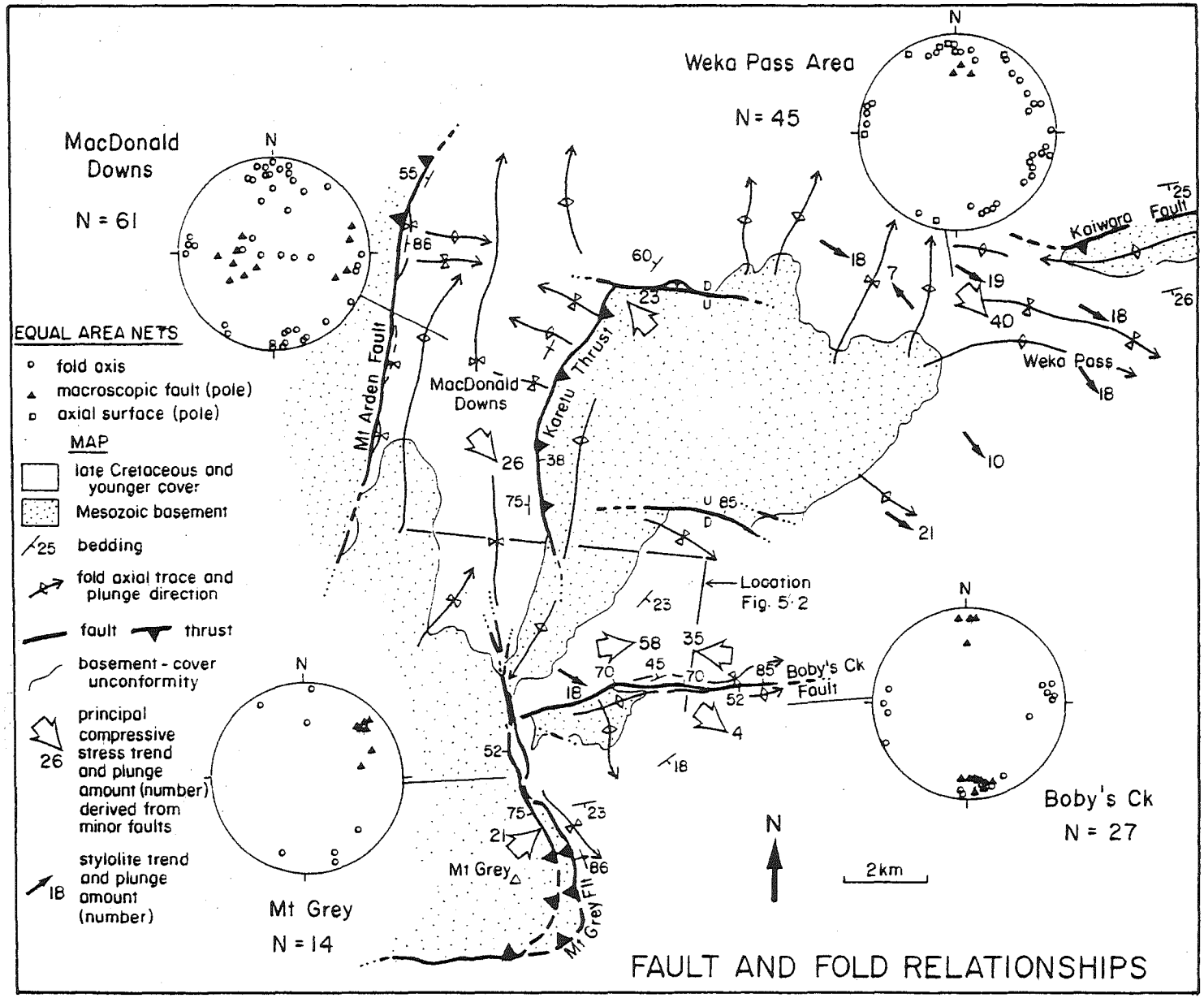
Weka Pass Area
N = 45
MacDonald Downs
N = 61
Mt Grey
N = 14
Boby's Ck
N = 27
EQUAL AREA NETS
fold axis
macroscopic fault (pole)
axial surface (pole)
MAP
late Cretaceous and younger cover
Mesozoic basement
bedding
fold axial trace and plunge direction
fault
thrust
basement - cover unconformity
principal compressive stress trend and plunge amount (number) derived from minor faults
stylolite trend and plunge amount (number)
Mt Arden Fault
Karetu Thrust
MacDonald Downs
Kaiwara Fault
Weka Pass
Boby's Ck Fault
Mt Grey Fault
Mt Grey
Location Fig. 5.2
2km
FAULT AND FOLD RELATIONSHIPS

variable (Figure 5.1 equal area net). However, adjacent to the northern edge of this block several of the main folds are parallel to the Kaiwara Fault, a major structure of regional extent. North to North-northeast faults and folds predominate to the W at MacDonald Downs and Mt Grey, and E-ESE structures are most important to the E in the Weka Pass and Boby's Creek areas.

5.2.2 FOLD SHAPE

Fault-related folds are generally asymmetric and verge towards the relative downthrown side of the fault, with one shallow ($<30^0$) and one moderate to steeply dipping limb (Figure 5.2). Folds with this shape have developed in association with the Mt Grey, Boby's Creek and Mt Arden Faults, and the Karetu Thrust (Figures 5.1 and 5.2).

Faults that develop in association with folding frequently show close spatial relationships to an anticline-syncline pair (e.g. Berg, 1962; Reches, 1978; Cook, 1988). This has been observed in North Canterbury, where each fold in the pair commonly rest on the opposite sides of the fault (Figures 5.1, 5.2 and 5.3). The syncline is always on the relative downthrown side of the fault, although the syncline fold axial trace may be truncated by the fault plane (see the Mt Arden Fault, Figure 5.1, and the Boby's Creek Fault, Figure 5.3). At Boby's Creek both the anticline and syncline are truncated by the main fault (Figure 5.3), while a second set of folds orthogonal to the dominant set, is only well developed on the northern downthrown side of the fault.

Figure 5.2. A scale block diagram showing the fault and fold relationships across the mid-Waipara and MacDonald Syncline areas. The folds result directly from drape and fault-propagation folding due to displacement of the mainly normal Boby's Creek Fault and the predominantly reverse Karetu Thrust respectively. See figure 5.1 for the location of the diagram.

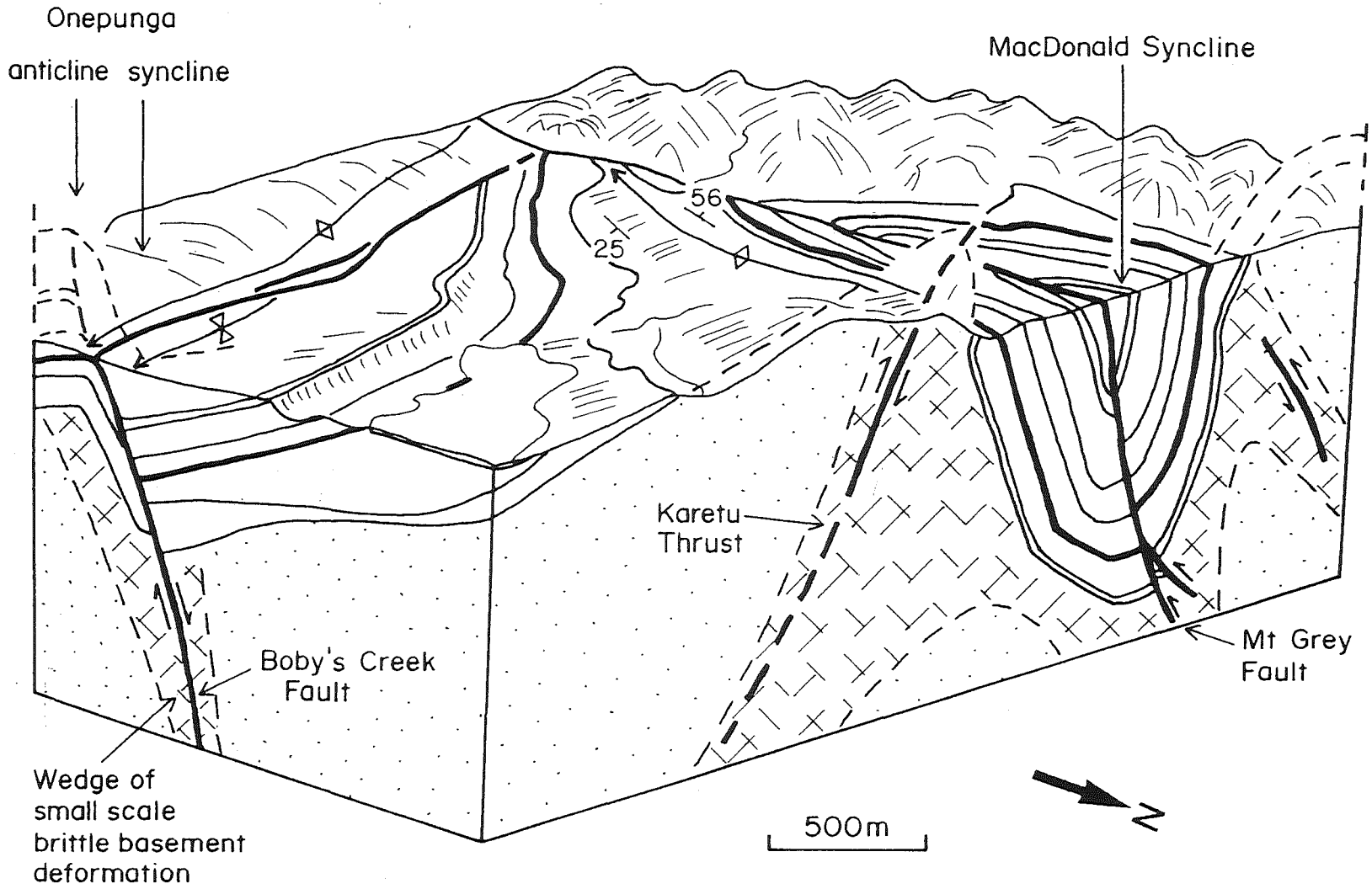

MID-WAIPARA STRUCTURES

5.2.2.1 Fold Hinge Angularity

Angular folds that have developed in association with faults are well documented (e.g. Stearns, 1978; Suppe, 1983 and 1985; Cook, 1988). The folds within the sedimentary cover sequence of North Canterbury are mainly angular structures. Cover rocks form a thin veneer (1 km.) dominated by thick incompetent sandstone and mudstone lithologies interspersed with sparse competent limestones of variable thickness (see Figure 1.2). Locally the competent layers are thin (often < 3 m.) and lensoid, with variable vertical separation distances and commonly have competent layer thickness to fold limb length ratios of > 1:20. Consequently fold angularity is unlikely to have resulted from deformation of a multilayered system with units of contrasting competence (cf Ramsay, 1974). Similarities between these macroscopic folds and small scale angular folds on the Kaikoura Peninsula, which appear to owe their geometry to variations in bedding thickness and competence contrast, may be somewhat fortuitous. Fault-bend folds are commonly angular (Suppe, 1983), but no such folds can be positively identified in this area. Rather, fold angularity may reflect the passive response of a thin cover sequence to late Cenozoic strains localised in basement by faulting.

5.2.3 FOLD DIMENSIONS

The dimensions of the folds reflect directly their location with respect to the main faults. Folds developed within the blocks defined by the main faults are relatively small structures with wavelengths of 0.5-3 km. and 0.05-0.2 km. amplitudes, while fault-related folds often have wavelengths of 5-20 km. and amplitudes of 0.5-1.6 km.

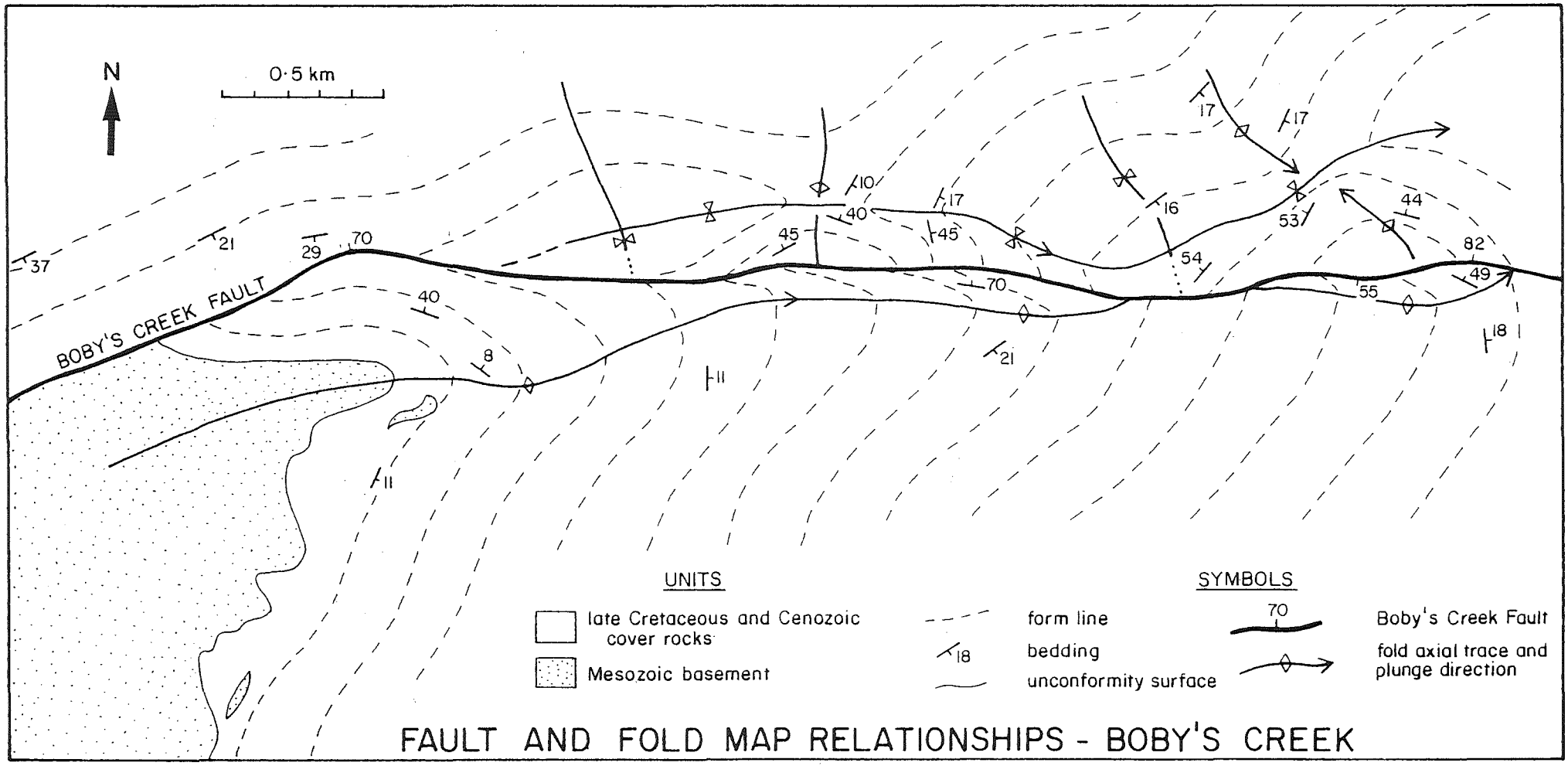

Figure 5.3. A detailed examination of the spatial and geometric relationships between the Boby's Creek Fault and the closely related Onepunga Anticline and Syncline.

The dimensions of the fault-related folds are clearly influenced by the main faults. Their wavelengths appear to be controlled by the distance normal to strike between adjacent major faults and amplitudes by vertical fault displacement.

5.2.3.1 Fold Amplitude

The relationship between fault displacement and fold amplitude is a positive one, and as the fault displacement increases, so must the fold amplitude. However, because faults nucleate and die out at structurally lower levels than their related folds (see Figure 5.6a), the relationship is likely to vary at different structural levels.

In an attempt to better describe this relationship, fold amplitudes are plotted against vertical fault displacement for 15 fault-related folds from North Canterbury. These structures are most commonly high angle reverse faults or thrusts associated with fault-propagation folds asymmetric in the direction of dip-slip fault movement. The error bars represent the level of certainty for each measurement. The graph, figure 5.4, shows a crude positive relationship between the two variables and not unexpectedly implies that faults with the largest vertical displacement are associated with larger amplitude folds. Although the resolution of the graph is poor there is some indication that the slope of the estimated mean line of the data (Figure 5.4) decreases with increased fault displacement. If this is so, it may be indicative of a decrease in the rate of fold growth with respect to fault displacement. In the early stages of the structural evolution fold growth is greater than fault displacement. Immediately above the developing fault vertical displacement is zero and fold amplitude greater than zero (see Figure 5.6a). The data on the graph (Figure 5.4)

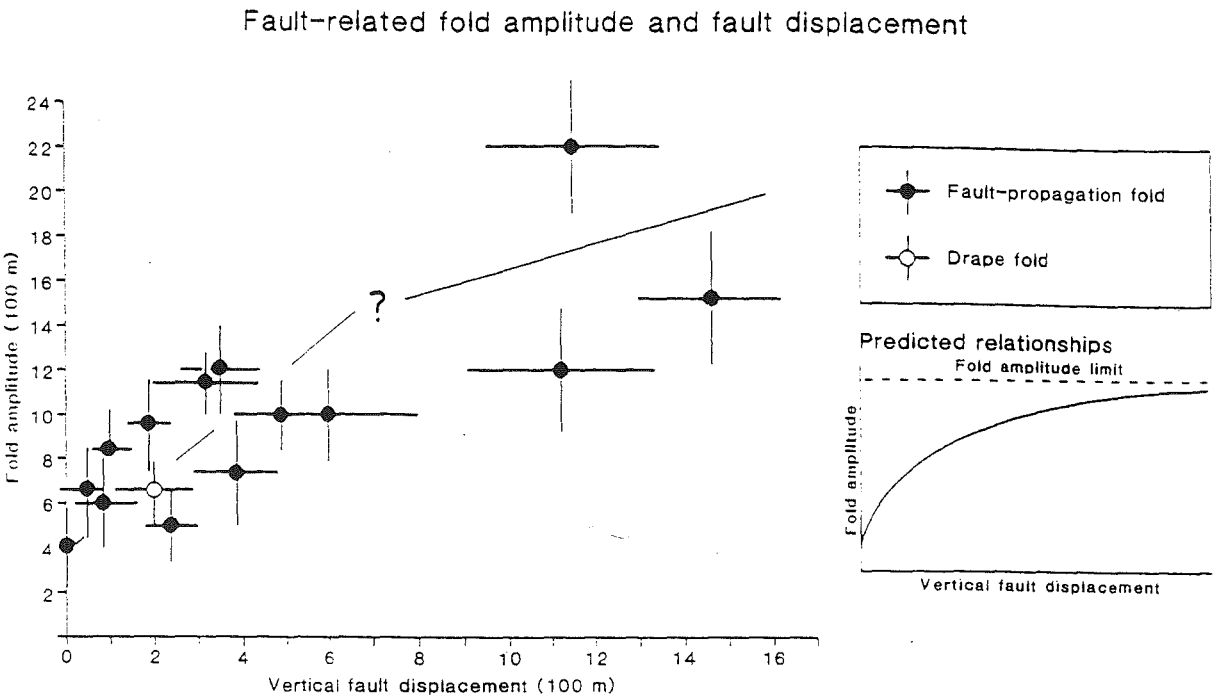

Figure 5.4. The graphical relationships of vertical fault displacement and fold amplitude for 15 fault-related folds from North Canterbury. The data were extracted from cross sections constructed normal to the structural grain from this study and from detailed mapping by Wilson (1963), Maxwell (1964), Yousif (1987) and Barrel (1989). Inset is the predicted conceptual relationships for these variables. The amplitude limit represents the limit of folding by buckling and bed over bed slip.

suggests that fold amplitude may reach values of one to three hundred metres before the stratigraphy is displaced by faulting. With time, fold growth slows as the limit of folding by buckling and bed over bed slip is reached, while fault movement

may continue. The inset in figure 5.4 shows the predicted conceptual non-linear relationship between these two variables.

5.3 KINEMATICS

5.3.1 STRAIN

The orientation of strain accommodated by folding and the macroscopic faulting has been determined for the MacDonald Syncline area using fold axial surface and fault slickenside striation data (Figure 5.5). Shortening on the major faults is crudely resolved into two E-W and N-S slip directions approximately parallel to the fold shortening directions. The slickenside striations developed within the MacDonald Syncline, due to bed over bed slip, also show a crude, but not a total parallelism with the macroscopic fault slickensides (Figure 5.5). The main fault slickensides, formed on mainly steep faults, frequently plunge more steeply than the fold shortening directions of the upright folds (Figure 5.5). This is to be expected given that strain is accommodated by folding of sub-horizontal anisotropic bedding and movement on moderate to steeply dipping faults.

The main E-W trending folds in Boby's Creek imply an approximate N-S sub-horizontal shortening associated with fold development. However, analysis of the faulting in this area (Chapter 2) clearly shows a predominance of normal faulting associated with sub-horizontal NNE-NE extension (see Figure 2.6), approximately parallel to the shortening direction derived from the folds. The E-W trending folds in the Boby's Creek area are drape folds developed in response to steeply inclined

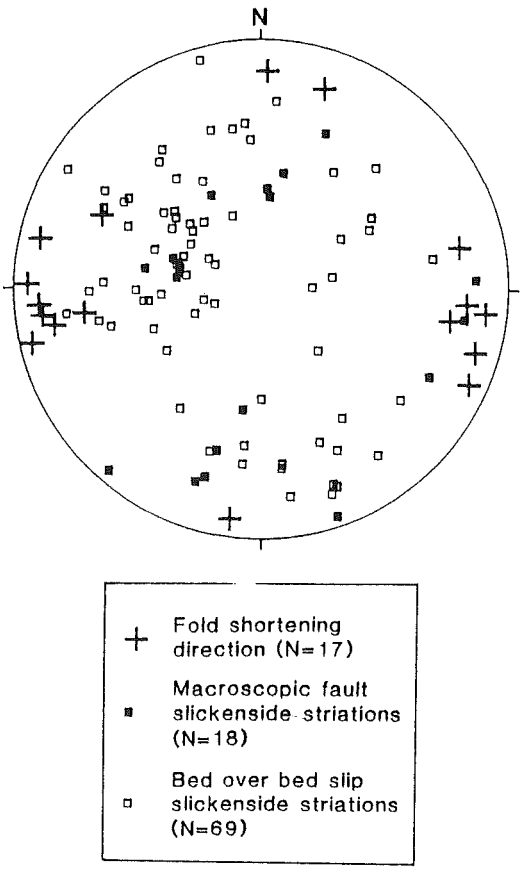

Figure 5.5. Fault and fold shortening directions for the MacDonald Downs area inferred by slickenside striations and the orientation of the axial surface of the MacDonald Syncline. Each is a lower hemisphere equal area net. See figure 5.1 for location.

compression and movement on the predominantly normal Boby's Creek Fault. To correctly interpret fold shortening it is clearly important to differentiate whether folding is indicative of vertical or horizontal compression (Brown, 1988). In Boby's Creek no basement shortening is required to produce E-ESE trending folds and the constrictional tectonics implied by having two sets of folds developing synchronously at a high angle to each other is not real. Clearly it is important to study the faulting and related folding before drawing any conclusions about the kinematics.

Locally the amount of shortening recorded by folding in the cover varies from <2-70%, but is most often between 10 and 30%. The cover is deformed by a combination of faulting and folding and is not detached from basement. Where large faults cut through the entire cover sequence the total strain may be considerably more than that measured by folding.

5.3.2 PRINCIPAL COMPRESSIVE STRESS

The principal compression directions derived from minor fault populations (Chapter 2) and stylolite column trends (Chapter 6) have been placed on figure 5.1. The principal compression stress is ubiquitously inclined to the horizontal, and often trends NW-SE. With the exception of the Boby's Creek area, where the plunge of the principal compressive stress is at its greatest, compression is oblique to the main structural elements. The main N-S and E-W structures are most commonly bisected by NW-SE trending principal compression.

5.4 SUB-SURFACE STRUCTURES

As faults and folds are exposed at the same structural level in North Canterbury it may be possible to make inferences about the presence and style of faulting, and the nature of basement "folding" at depth, below regions where only folding can be observed or exposure is poor.

5.4.1 FAULT ACTIVITY AT DEPTH

It is widely known that folds are frequently the surface expression of large scale faults at depth (e.g. Yeats, 1987a and 1987b; Stein and King, 1984). However, in many cases these macroscopic faults either do not reach the surface, or are poorly expressed in outcrop. In these situations it may be possible to place some constraints on the nature of the faulting at depth by analysing the morphologies of folds exposed at the surface. To use folds in this way it must be established that the faults and folds are genetically related, and demonstrated that consistent geometric relationships exist between these structures.

In Canterbury it cannot be assumed that all folds are directly related to faulting. However, in all cases where asymmetric folds with one steep to moderately dipping limb were located, the folds were closely associated with a macroscopic fault. In these instances the trend of the fault-related folds is approximately parallel to the strike of the fault (Figure 5.1) and fault dips are most often, but not always moderate to steep away from the steepest fold limb (Figure 5.6). The faults shear through the steep fold limb, and the relative upthrown side of the fault is indicated by the position of the anticline hinge. The total amount of relief from the syncline to anticline hinge is likely to be considerably larger than the displacement close to the fault tip (Figure 5.6).

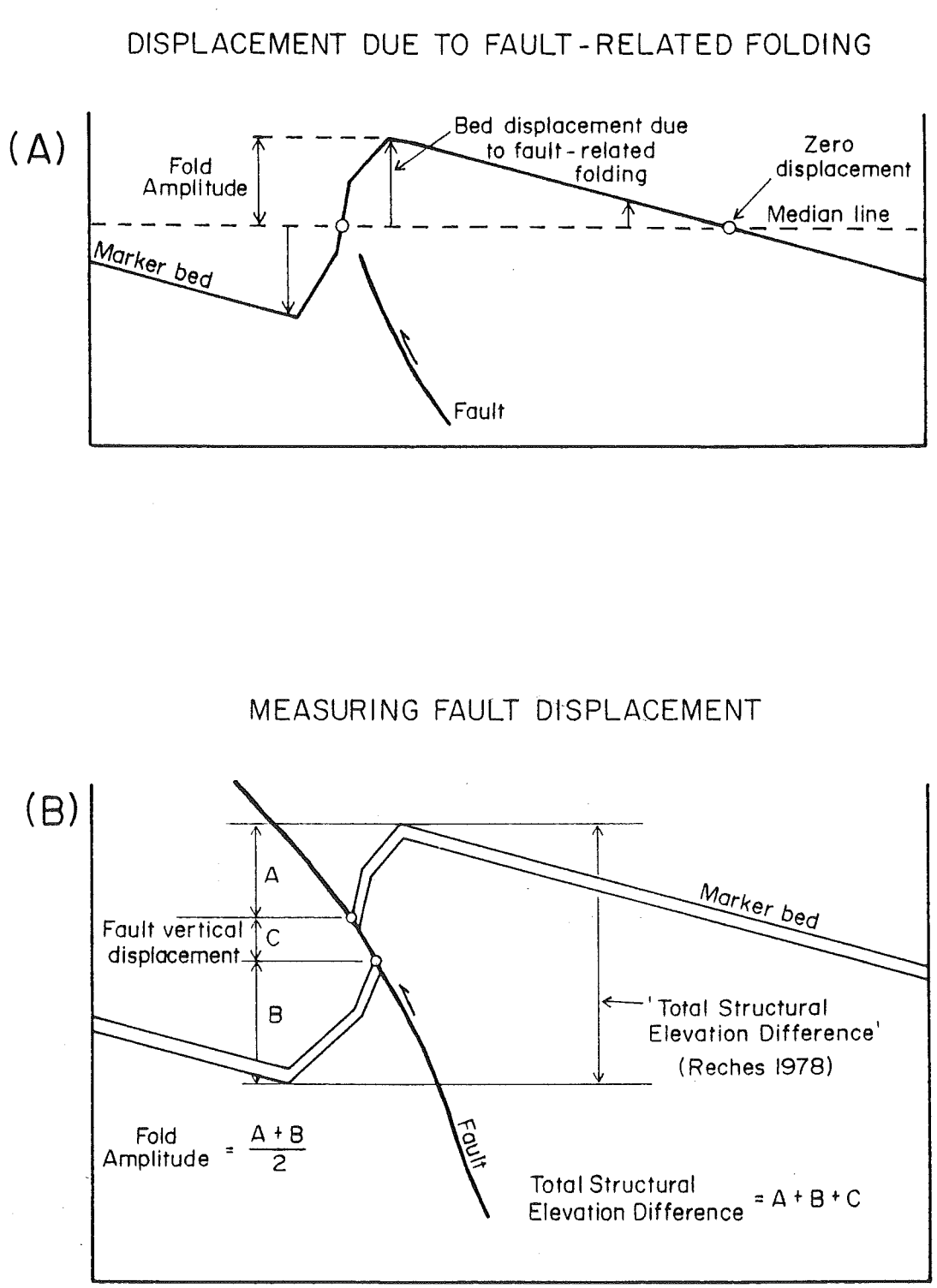

Figure 5.6. The measurement of fault related displacement by faulting and folding. (a) Fault-related fold displacement due to buckling and bed over bed slip can be measured from the fold median line. Prior to the displacement of the marker bed 2 (fold amplitude) = the 'total structural elevation difference' (Reches, 1978) across the fault. (b) After the fault has displaced the marker bed the 'total structural elevation difference' = fault displacement + 2 (fold amplitude) (see text).

5.4.1.1 Fault Displacements

When faults develop in conjunction with fault-related folds, fault displacement constitutes only a portion of the total structural elevation difference accommodated across the fault, which is characterised by faulting and folding (Figure 5.6). Where the fault has developed in association with a macroscopic fold it may be more appropriate to state the "total structural elevation difference" across the fault (Reches, 1978). For asymmetric fault-related folds this is equal to the fault displacement plus two times the fold amplitude (Figure 5.6b). Estimates of the fault displacements in North Canterbury may be more indicative of the "total structural elevation difference". For example, Wilson (1963) failed to identify the Onepunga anticline-syncline pair in Boby's Creek and consequently over-estimated the vertical displacement (extracted from his cross section) on the Boby's Creek Fault, but his estimate was close to the "total structural elevation difference". Similarly, where basement is faulted against cover rocks, because folding has accommodated some fault-related strain, it may be erroneous to equate the elevation difference between the cover rocks and adjacent basement range heights with the minimum fault displacement.

5.4.2 BASEMENT "FOLDING"

Basement is not detached from the cover rocks and the unconformity on the Mesozoic metasediments of the Torlesse Supergroup have been "folded" to conform to the shape of folds in the cover. However, the folds in basement (Chapter 2, section 2.2.1.1) are truncated by the unconformity surface, and Torlesse bedding

has not been refolded by late Cenozoic deformation. Basement has not folded sensu stricto, but rather has deformed in a brittle fashion by movement on large range-front faults and many small scale faults, similar to the operation of a beanbag (Chapter 2, section 2.2.3).

The distribution of small scale beanbag type deformation in basement appears to occur in confined zones adjacent to the main faults and close to the late Cenozoic fold hinges (see Chapter 2, 2.2.1.3). Small scale faults which appear to have accommodated late Cenozoic movement, are not abundant beneath the gently dipping limbs of the cover folds and do not offset the unconformity at these localities. Brittle basement deformation appears to be largely confined to an envelope of brittle deformation defined by the causal fault and the adjacent anticline-syncline fold hinges (Figure 5.2). Rait (pers. comm., 1990) suggested that similar brecciation and small scale fault deformation occurs at the propagating tip of late Cenozoic faults on the East coast of the North Island. Friedman et al (1976) and Chester et al (1988) have identified envelopes of small scale deformation in fault rock models of basement-cored folds, while Cook (1983 and 1988) has inferred similar wedge shaped zones of small scale brittle deformation in basement cored fault-related folds. In Canterbury small scale brittle deformation decreases rapidly in significance to the west at lower structural levels, which implies that this zone of deformation is wedge shaped (Figure 5.2, cross hatched zones), decreasing in width with depth and increasing confining pressures. Small scale late Cenozoic deformation of the Torlesse is facilitated by the extensive suite of pre-existing Mesozoic joints and faults. This is distinctly different to the block jointed granitic and granulitic rocks of the Rocky Mountain Foreland, and should be taken into consideration before comparisons between the two areas are made.

5.5 INTERFERENCE FOLDING EVOLUTION

5.5.1 INTERFERING FOLD SET GEOMETRIES

Many of the major folds in the mid-Waipara region have developed in direct response to fault propagation and/or displacement. Although there is a crude correlation between fault and fold shortening the main influence on fold orientation appears to have been provided by fault strike. Throughout North Canterbury the main fold sets are everywhere parallel to the major faults (Gregg, 1964), this is despite the fact that several of the larger faults in this region have accommodated oblique slip motion. This explains the disparities between the apparent fold shortening and the principal compressive stress. Folding has developed parallel to the major faults in response to their vertical components of movement, rather than their oblique movement which is indicative of the regional NW-SE compression.

The fold interference patterns in this area owe their geometries to the development of E-W and N-W striking fault sets. These orthogonal faults are thrusts, reverse and normal faults. North-south striking faults are contractional and E-W faults represent a combination of discrete normal and reverse faults and/or hybrid faults with dip reversals. The resulting folding patterns are formed due to interference of two contractional fault-propagation fold sets or contractional fold sets and extensional drape folds. Individually these folds may verge N,S,E or W, and have developed in response to thrusting in four directions. Locally, compression is interrupted by approximate N-S extension in Boby's Creek.

Fault motion on these two orientations of macroscopic scale faults has not occurred in two distinct phases, but rather has been synchronous (Chapter 2). The pattern is one of intermittent movements along short sections (< 5 km.) of both orthogonal fault sets, with the orientation of the fault accommodating the last major motion varying from area to area. The inference is that E-W and N-S fold sets are also developing synchronously, with intermittent growth of both fold sets over distances in the order of five kilometres. Synchronous fold development is also implied by apparent warping of Holocene terrace surfaces about both N-S and E-W axes, at the northern end of the MacDonald Syncline.

5.5.2 IMPLICATIONS FOR FAULT DEVELOPMENT

The presence and geometry of fold interference patterns has important implications for determining the orientation of the dominant fault(s) and the degree of orthogonal fault set activity. In areas where one fold set dominates, and a corrugated hose interference pattern (Chapter 3, section 3.3.2) has evolved, one dominant set of faults, parallel to the main fold set, is implied. This can be observed within the MacDonald Syncline, which is jammed between, and sub-parallel to, two reverse, approximately N-S striking, range-front faults (Figure 5.1). In the MacDonald Syncline, with the increasing influence of the E-W fault to the north at Pyramid Valley, E-W folding becomes more pronounced (Figure 3.1). Thus while the major folds are controlled by the faulting pattern, in the blocks between these faults, shortening is also accommodated by folding, but the folds are not directly related to fault displacement. In regions where two well developed orthogonal fault sets can be observed, for example in the Boby's Creek area (Figure 5.1), both of the

interfering fold sets are well developed and produce approximately equant interference patterns.

Fold and fault shortening directions provide short and long term indications, respectively, of the local strain history. Crude similarities in the shortening directions of these structures and genetic relationships between fault and fold growth, suggest that the long term faulting history (implied by folding) is compatible with short term movements determined from slickenside striations and the offset relationships of the different fault sets.

5.6 CONCLUSIONS

Faults and folds have developed synchronously since the early Pleistocene. Complex basin and dome interference folding in the late Cretaceous-Tertiary cover sequence results directly from the propagation and movement of N-NNE and E-ESE striking faults extending up from the basement. The major folds are developed parallel to the main faults and oblique to the principal compression, in association with a complex array of orthogonal thrusts and normal faults. In the blocks between these main faults secondary smaller scale folding is accommodating shortening. Fault-related folds, including fault-propagation and drape structures, are commonly angular and asymmetric with N,S,E and W vergence. The amplitude and wavelength of these folds appears to be controlled by the fault vertical displacement and the strike-normal distance between the main faults, respectively. Where the faults do not reach the surface or are poorly exposed it may be possible to make inferences about faulting from the adjacent individual and/or interfering fold set geometries.

CHAPTER 6 OLIGOCENE LIMESTONE TECTONIC STRUCTURES

6.1 INTRODUCTION

Deformation of two Oligocene limestones in North Canterbury has resulted in the development of multiple joint, stylolitic pressure solution seam and mesofault sets (Table 6.1). These mainly small scale structures provide a means of assessing the timing and kinematics of the local deformation. Similar brittle microtectonic structures have been used extensively, particulary by the French, to characterise regional deformation (e.g. Arthaud, 1969; Jaroszewski, 1972; Choukroune, 1976; Letouzey and Tremolieres, 1980). These structures are indicative of small strains (Segall and Pollard, 1983) and have proven most useful in rocks that have experienced only mild deformation. They have been found to be reliable kinematic indicators, being variously used to provide unambiguous data on the directions of shortening and dilation (e.g. Bahat, 1979; Fletcher and Pollard, 1981), and stress trajectories (e.g. Engelder and Geiser, 1980; Buchner, 1981; Angelier, 1984).

Small scale brittle tectonic structures are rarely examined closely in rocks deformed at convergent plate boundaries. This is mainly because these early small strain structures are generally overprinted and deformed in rocks that may have complex strain histories. In North Canterbury these microtectonic structures provide progressive snap shots (Table 6.1) of local late Cenozoic deformation, enabling a coherent tectonic history to be established. Here the rocks are variably deformed,

and also provide a good opportunity to assess the extent of local variation in the geometry and kinematics inferred by the small scale structures.

6.1.1 LIMESTONE LITHOLOGIES

Within the mid-Waipara area Oligocene limestones are composed of two units: the Amuri Limestone Formation and Weka Pass Stone Member of the Omihi Formation (Browne and Field, 1985). These units lie in the middle of a one kilometre thick late Cretaceous to early Pleistocene sequence which rests unconformably on Mesozoic Torlesse Supergroup basement. The Amuri Limestone extends 700 km from the Waitaki River in the south, through North Canterbury, across the plate boundary and onto the east coast of the North Island (Figure 6.1). The Formation is dominated by a fine even micritic lithology, rich in coccoliths and foraminifera, which thins and becomes progressively younger both to the NE and SW of central Marlborough (Browne and Field, 1985; Browne, 1987). Locally the Amuri Limestone is early to mid-Oligocene in age, with bed thicknesses of 0.3 to 1.5 m. and varies in total thickness from 0 to 30 m. The mid-late Oligocene Weka Pass Stone Member is dominated by a massive to poorly bedded (beds 5-10 m. thick) very fine to medium, sandy glauconitic limestone lithology. This unit occurs only in North Canterbury and locally varies in thickness from 10-110 m. The Weka Pass Stone rests unconformably on the Amuri Limestone, producing a combined average limestone thickness of 20 to 40 m.

Table 6.1. A summary of the brittle microstructures, their relative sequence of development and estimated ages.

Tectonic Structures	Absolute Age	Deformation Event
Low Angle Joints	mid-late Oligocene	Weak tectonic sub-horizontal compression associated with the initiation of the plate boundary as through-going transform (?).
Bedding-parallel pressure solution seams	Pliocene	Uniaxial gravitational loading by overlying sedimentary cover.
Steep Orthogonal Joints	late Pliocene	Initiation of uplift associated with dominant NE-SW dilation and NW-SE shortening, at the outer edge of the plate boundary zone.
Bedding-normal pressure solution seams and stylolites.	early Pleistocene	Onset of NW-SE principal horizontal compression.
Macrofractures	early Pleistocene to Recent	Onset of folding. Mainly associated with N-S and E-W shortening and fracture development.
Mesofaults	early Pleistocene to Recent	Continued folding, N-S and E-W shortening. Joints, fractures and bedding planes activated and become mesofaults.

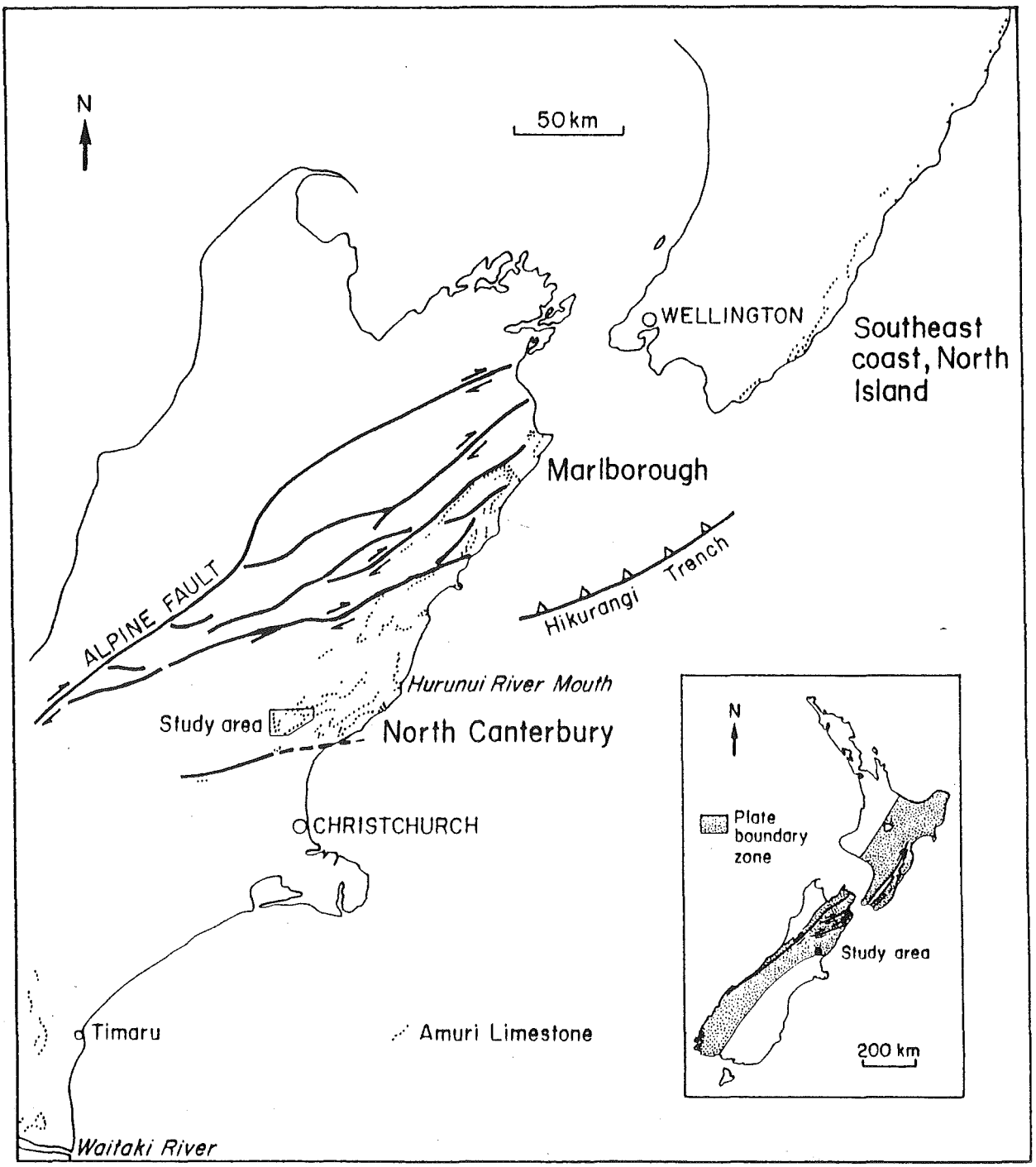

Figure 6.1. Study area location in relationship to the Alpine Fault and other plate boundary features. The location of the Amuri Limestone is marked by the dots; data collated from the 1: 1 000 000 geological maps, Browne (1987), Lewis (pers. comm., 1990), Pettinga (pers. comm., 1990) and this study.

6.2 TECTONIC STRUCTURES

6.2.1 JOINTS

The term joint refers to a barren or closed fracture with no measurable slip or dilation (Hancock, 1985). Joints represent the most abundant and widespread microtectonic structures in the limestones of North Canterbury. They are pervasively developed, and spaced at intervals of less than 8 cm. throughout the limestone horizons rich in micrite, but may have spacings of 1-2 m. Despite the often close spacings of these fractures the term joint is preferred to fracture cleavage, due to the variability of the fracture spacings and their obliquity to folding. At least four joint sets are recognised and divided into two groups. (1) Low Angle Joints, which form at angles of less than 35^0 to bedding, often in conjugate sets symmetrical about the bedding. (2) Two steep Orthogonal Joint sets that strike NE and NW, and form at a high angle ($> 60^0$) to bedding. Figure 6.3a displays both groups within a single massive bed of Weka Pass Stone, here dipping into the outcrop face at 20^0.

6.2.1.1 Low Angle Joints

Low Angle Joints dip at angles of between 7 and 20^0 to bedding, and show little effect of pressure solution. In outcrop (Figure 6.3a), they form conjugate joint sets symmetrically disposed about bedding, with dihedral angles ranging from 7 to 25^0, spacings of 6-20 cm, and moderate planarity.

Figure 6.2. Geological map of the study area with stylolite column trend from 15 locations. Rose diagrams were generated using a computer program written by Wise and Fleischmann (in prep.). Each rose represents between 10 and 47 stylolite column trend observations. The total data set is approximately 300.

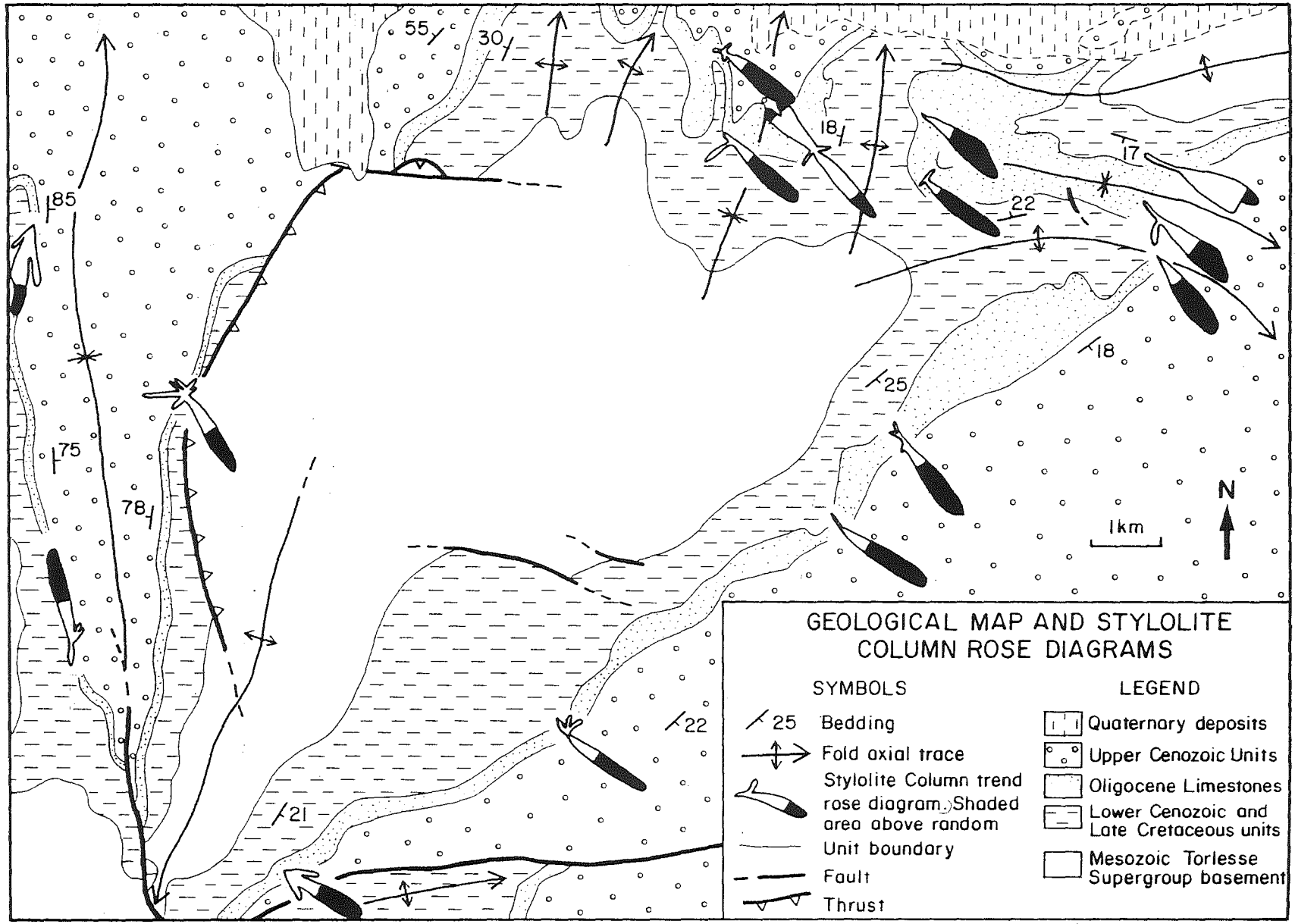
55
30
18
17
22
85
18
25
75
78
1km
N
22
21
GEOLOGICAL MAP AND STYLOLITE COLUMN ROSE DIAGRAMS
SYMBOLS
25 Bedding
Fold axial trace
Stylolite Column trend rose diagram. Shaded area above random
Unit boundary
Fault
Thrust
LEGEND
Quaternary deposits
Upper Cenozoic Units
Oligocene Limestones
Lower Cenozoic and Late Cretaceous units
Mesozoic Torlesse Supergroup basement

Within two metres of the unconformity surface these joints are frequently coincident with Thalassinoides borings. Lewis and Ekdale (in prep) suggest that these borings were formed after the joints during the development of the mid-Oligocene unconformity. Paradoxically Low Angle Joints have also been noted in the Weka Pass Stone above the unconformity surface, which is contradictory evidence to the timing of joint development (discussed further in section 6.3). Low Angle Joints most often strike NNE and ESE-WNW (Figure 6.4, top left), and adjacent joints dip in opposing directions. They abut, and are older than, the steep Orthogonal Joint sets described below (Figure 6.3a). The angular relationships between bedding and Low Angle Joints are maintained irrespective of bedding dip (see Figure 6.6), which suggests that they also developed prior to measurable folding. Locally Low Angle Joints represent the oldest small scale tectonic features (Table 6.1).

6.2.1.2 Orthogonal Joints

These joints are commonly steep (> 60^0), where bedding dips at less than 30^0, and strike NE-SW and SE-NW forming orthogonal (85^0 azimuth difference) joint sets (Figure 6.4, middle left). Joint sets that strike NW-SE are approximately twice as abundant as NE-SW structures. Both joint sets are widespread, but not ubiquitous, and can vary by up to 15^0 in strike between stations (Figure 6.5, top). These joints display poor to good planarity, with spacings of 2-7 cm. in the Amuri Limestone and 1-1.5 m. in the Weka Pass Stone. They are frequently less than 2 m. in length, often abut (Figure 6.3a) and post date joints inclined at a low angle to bedding. Orthogonal joints appear to have been extensional in character and are indicative of NE-SW (normal to the principal horizontal compression inferred by stylolite

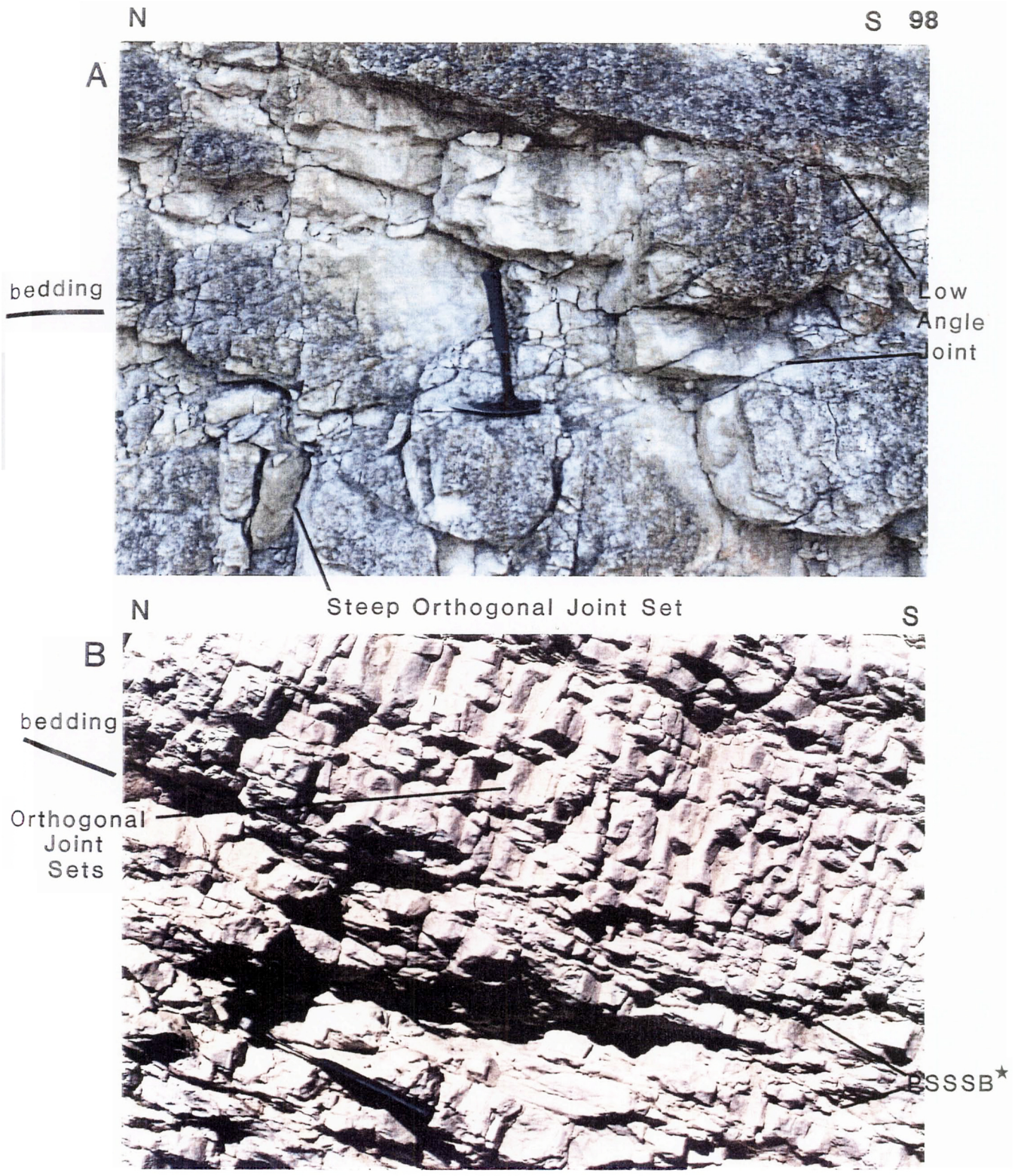

Figure 6.3. Photographs of brittle fractures within the limestone units. (A) Low Angle Joints and steep joints (labelled) within the Weka Pass Stone in the road cut at Weka Pass. (B) Orthogonal Joints and pressure solution seams sub-parallel to bedding (labelled)in micritic Amuri Limestone, Weka Pass Stream.

★PSSSB = Pressure Solution Seam Sub-parallel to bedding

columns) and NE-SW dilation. Where folding is gentle (limb dips are < 30^0), these joints generally bisect the N-S and E-W fold axes and strike at between 20 and 40^0 to the fold trend (Figure 6.7). Local variation in fold orientations can cause intermittent joint-folding parallelism (Figure 6.5a). Where bedding dips are steep (> 60^0), Orthogonal Joint sets become difficult to detect and all fractures are commonly rotated into the plane of flattening associated with folding (Figure 6.4, bottom left). Figure 6.6 demonstrates that with the exception of Low Angle Joints, all joints including orthogonal structures, display repeated, but not ubiquitous, high angle relationships to bedding, and decrease in dip with increasing bedding inclination. Orthogonal Joints sampled from gently dipping beds (Figure 6.4, middle left) proved to be less scattered in orientation when bedding dips were removed. Collectively these observations suggest that most Orthogonal Joints pre-date early Pleistocene to Recent folding.

6.2.2 PRESSURE SOLUTION SEAMS

Fractures that have been subject to pressure solution are here referred to as solution seams (after Hancock, 1985). They are best developed as uneven, undulating and discontinuous fractures within micritic Amuri Limestone horizons deficient in clay, and often contain stylolite columns and slickolite striations (appendix 4). Two distinct sets of solution seams occur: (1) sub-parallel to bedding, and (2) normal to bedding (Figure 6.4, right column). Both sets contain stylolite columns which vary in distribution, size and shape.

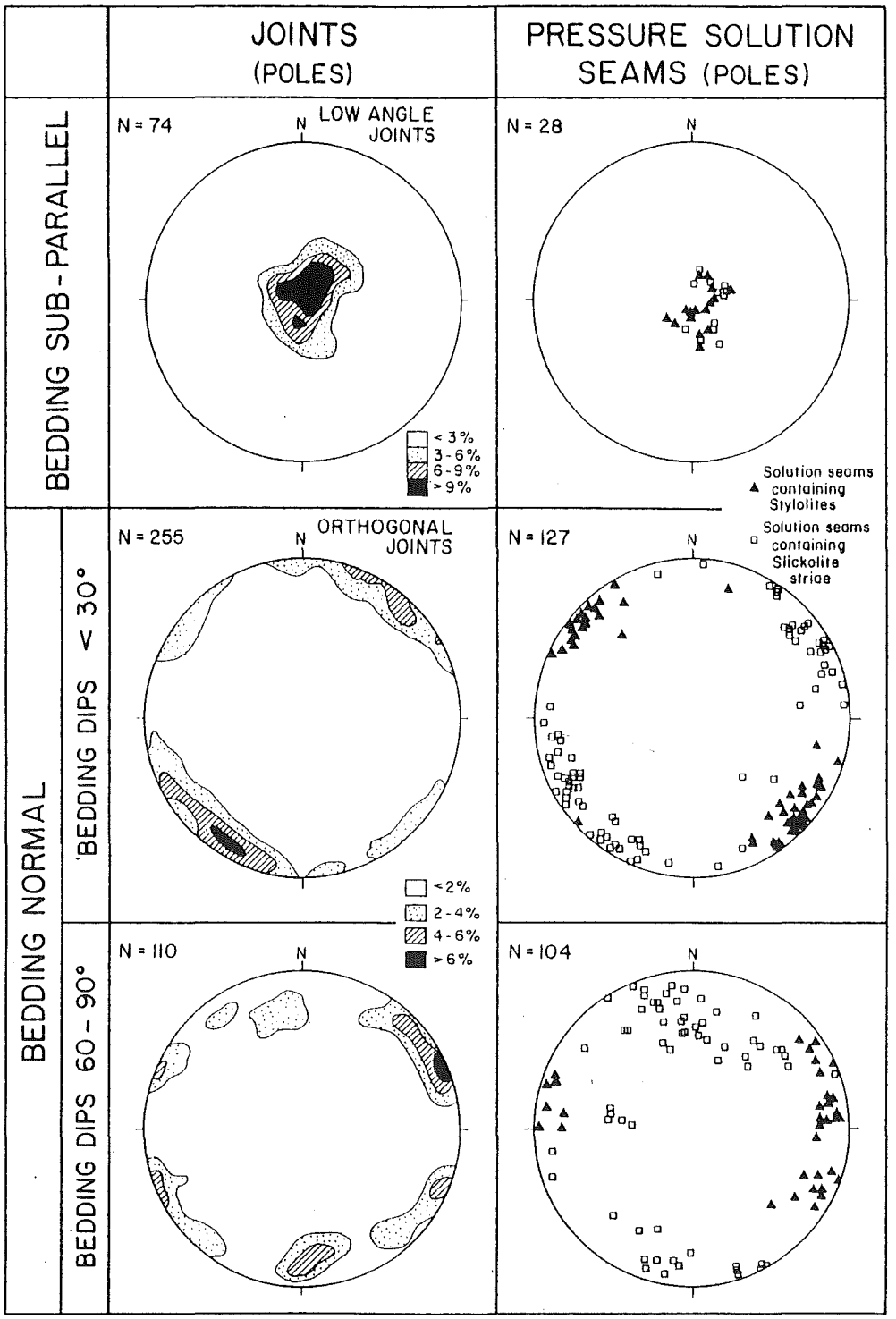

Figure 6.4. Lower hemisphere equal area plots of poles to pressure solution seams (right side of diagram) and spherical gaussian contoured poles to joints (left side of diagram) that are both sub-parallel (top row) and normal (middle row) to bedding, where bedding dips are less than 30^0. The bottom row represents bedding normal data collected from areas where bedding dips exceed 60^0. Few data were sampled from beds with dips between 30 and 60^0. Bedding dips have been removed for all nets.

Solution seams sub-parallel to bedding are variably developed and show a gradation from well preserved discontinuous anastomosing fractures in Amuri Limestone beds rich in micrite, to Low Angle Joints in the Amuri Limestone beds rich in clay and in Weka Pass Stone (compare Figure 6.3a and 3b). These solution seams form at a low angle (between 5 and 20^0) to bedding and give outcrops a lozenged or flaggy appearance (Figure 6.3b). They contain bedding normal stylolite columns up to 3 mm. long and SE trending slickolite striations (appendix 4), while incipient column parallel slickolite striations are also occasionally developed on steep fractures at a high angle to bedding. Solution-seam fractures sub-parallel to bedding most commonly strike ESE-WNW, similar to the dominant strike of Low Angle Joints (Figure 6.4, top row). Gradation from Low Angle Joints to solution seams sub-parallel to bedding, infers that these solution seams developed preferentially on previously formed Low Angle Joints. This pressure solution is most obvious in fine, carbonate pure Amuri Limestone lithologies. Pressure solution seams with this orientation probably formed due to uniaxial compression imposed by the overlying accumulating sedimentary sequence, which reached thicknesses of 1 to 1.5 km. during the Pliocene (inferred from local and regional maximum thicknesses of 0.7 and 1.2 km. respectively for the Kowai Formation; plus an average of 0.3 km. for the remaining units in the sequence above the limestones). Bedding-normal stylolites and slickolite striations generally post-date and are older than SE trending bedding parallel stylolites and slickolite striations. Solution seams sub-parallel to bedding have previously been termed "stylobedding" by Browne and Field (1985). The term, as introduced by Long and Semeniuk (1976), applies to solution seams that are not necessarily related to unit lithological variation, but rather have the appearance of a 'bed'. However, "bedding" sensu stricto implies a primary lithologic bedding/solution seam relationship, which is not the case here. It is more

appropriate to refer to these structures as 'pressure solution seams sub-parallel to bedding'.

Solution seams normal to bedding have identical orientations to, and are sporadically interspersed with, NE-SW and NW-SE striking Orthogonal Joints (compare Figure 6.4, middle left and right). Northeast-southwest striking solution seams frequently contain stylolite columns (up to 7 mm. long) which are normal to the solution surface and parallel to bedding (Figure 6.4, middle right). These stylolites regionally trend SE-NW and mainly plunge away from local gently folded anticline hinges (Figure 6.2). Slickolite striations with NW and SE trends are also frequently developed on NW-SE striking fractures (Figure 6.4, middle right). Stylolite columns and related slickolite striations, formed on solution seams which strike NE-SW, represent uniaxial strain indicative of a paleostress (cf Buchner, 1981) dominated by horizontal SE-NW principal compression. Removing the effects of folding characteristically restores stylolite plunges to the horizontal (+/- 5^0), which suggests that much of the pressure solution on surfaces normal to bedding developed prior to, or during, the early stages of folding. This pressure solution event occurred over a short period of time after Orthogonal Joint formation and before the onset of folding. Solution seams sampled from steeply dipping beds (Figure 6.4, bottom right) generally strike N-S and E-W, approximately parallel and normal to the local MacDonald Syncline fold axial surface, and imply a ENE-ESE principal horizontal compression that reflects the influence of the local folding.

6.2.3 MACROFRACTURES AND MESOFAULTS

The term macrofracture refers to fractures tens of metres long, that could not be differentiated either as faults or joints. Steep macrofractures with spacings of 5-25 m. and strike lengths of 20-250 m. were identified and measured from aerial photographs in areas where unvegetated limestone dip slopes, dipping at angles of less than 30^0, are exposed. In the field these fractures are characteristically dissolution fissures picked out by surficial weathering. They display a wide variation in strike both regionally and at individual localities (Figure 6.5, bottom). A comparison of macrofractures and steep joints in figure 6.5 shows that with the exception of stations 5 and 9 these structures vary in orientation at individual locations. Macrofractures of three main types can be determined. (1) Macrofractures that strike NW-SE parallel to the regional principal compression, and fractures that strike normal (2) and parallel (3) to local fold axes, to form extensional AC and AB macrojoints (Turner and Weiss, 1963). Macrofractures on the NE striking limb of the Waipara Syncline, at the bottom of figure 6.5, are both normal to the local fold axis and parallel to the NW-SE regional principal compression. Figure 6.5 (bottom) shows a predominance of macrofractures that strike parallel, and normal to, the local fold axes. These structures appear to have developed in conjunction with early folding.

Mesofaults are observed with displacements ranging from 1-2 cm. to 2-3 m. on a centimetre to metre scale within the limestone units and occasionally pass into the units above and below. They form two groups. (1) Widespread dip-slip faults parallel and sub-parallel to bedding (see Figure 6.8), which appear to have activated bedding planes and Low Angle Joint surfaces to accommodate small layer over

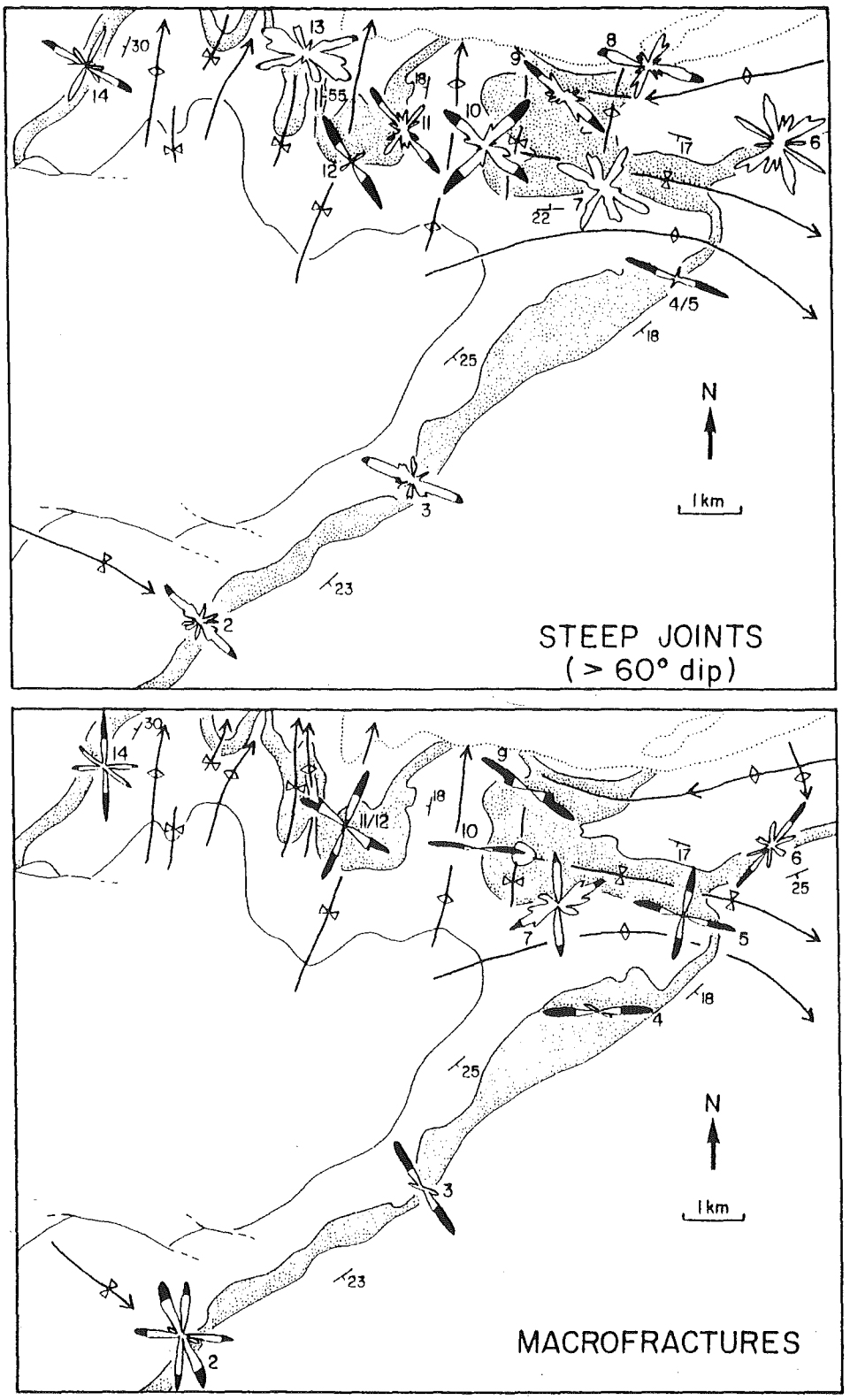

Figure 6.5. Fracture strike rose diagrams for steep joints (top) and macrofractures (bottom) sampled from 14 stations (numbered); beds predominantly dip at 30^0 or less. The dotted area shows the outcrop pattern of the Oligocene limestones, while the symbols are the same as figure 2. Each station represents between 10 and 55 fracture strike measurements. The total data set is approximately 500.

layer slip during folding. (2) Steep to moderately dipping dip-slip and strike-slip faults that mainly strike E-SE (Figure 6.8a). Both fault groups are characterised by narrow (1-10 cm.) zones of brecciation, pressure solution or polishing. These mesofaults are late-stage structures that disrupt and often exploit previously formed steep macrojoints, Orthogonal Joints, Low Angle Joints and bedding. In the Waikari Quarry (see Figure 2.5 for location), figure 6.8b, steep right lateral strike slip mesofaults sporadically reactivate macrojoints and Orthogonal Joints with identical orientations.

6.3 OLIGOCENE DEFORMATION

Low Angle Joints occur regionally within Oligocene limestone units of North Canterbury and Marlborough, while solution seams, inferred to have developed on these joint surfaces, are equally widespread. These structures appear to be intimately related in time to the regional North Canterbury mid-Oligocene unconformity surface. At Weka Pass joints inclined at a low angle to bedding are developed both above and below the unconformity, while exposures in Weka Creek, at the Hurunui River mouth and Gore Bay (Figure 6.1), reveal that similar fractures within the upper 2 m. of Amuri Limestone are infilled with the overlying sediments and not developed above the unconformity surface. These observations suggest that Low Angle Joints at various localities are both older and younger than the unconformity surface. This observation requires that either there are two unconformity surfaces or two periods of joint development. At present there is not enough data available to distinguish between these two options. The unconformity(s) appears to have developed during the upper Whaingaroan over a 2-3 ma period (Hornibrook pers. comm. to D.W.Lewis, 1990). This infers a probable mid-late

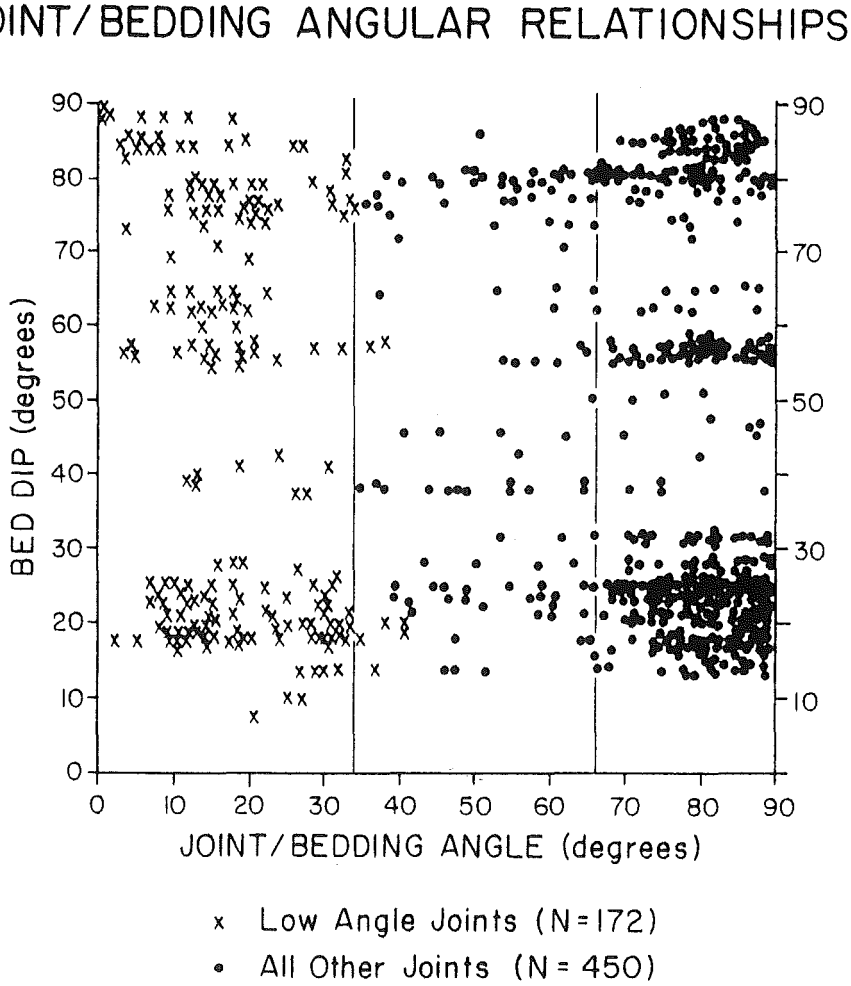

Figure 6.6. Joint/bedding angular relationships for Low Angle Joints and all other joints (differentiated in the field). Ninety six percent of all Low Angle Joints fall within the area left of the line on the left side of the graph, while 77% of all other joints fall right of the line on the right of the graph. Indicating that the majority of joints can be clearly discriminated at any outcrop and that internal bedding/joint angular relationships are maintained irrespective of bed dip.

Oligocene age for the Low Angle Joints. A weak tectonic event of this age is in agreement with the observations of several other workers (Lewis et al 1979; Prebble, 1980; Lewis, in prep) who have also postulated the advent of mild tectonism during the Oligocene. The origin of these joints is uncertain, although it is clear that they formed close to the surface (under low confining pressures) and that parts of the Amuri Limestone must have lithified prior to deposition of the Weka Pass Stone,

while parts of the Weka Pass Stone and all of the Amuri limestone must have lithified prior to the deposition of the overlying units. It also seems likely that Low Angle Joints developed in response to sub-horizontal shortening. They record a weak deformation that extended over much of the present plate boundary zone in North Canterbury and Marlborough, and represent the first indication of Tertiary compression in this area. This deformation appears to have occurred about the time that the plate boundary developed as a through-going transform system (Molnar et al, 1975; Carter and Norris, 1976; Kamp, 1986; Cooper et al, 1987), and may signify this event. Lewis (in prep) also suggests that gentle warping during the Oligocene may reflect the initial development of the plate boundary through New Zealand.

6.4 PLIO - PLEISTOCENE MICROSTRUCTURE DEVELOPMENT

Many of the structures described, including Orthogonal Joints, pressure solution seams normal to bedding (and related stylolites), and a number of the macrofractures and mesofaults, record an early, low strain and mainly brittle period of deformation during the late Pliocene to early Pleistocene. The timing of this deformation is constrained by the early Pliocene to early Pleistocene age (Wilson, 1963; Browne and Field, 1985) of the uppermost unit in the Cretaceous-Tertiary sequence, which locally appears to have been subjected to folding during deposition south of the study area. Stylolites and bedding-normal solution seams, Orthogonal Joints and bedding-parallel solution seams all developed prior to the initiation of folding during the early Pleistocene, but after the Oligocene development of Low Angle Joints. However, bedding-parallel solution seams, developed due to loading

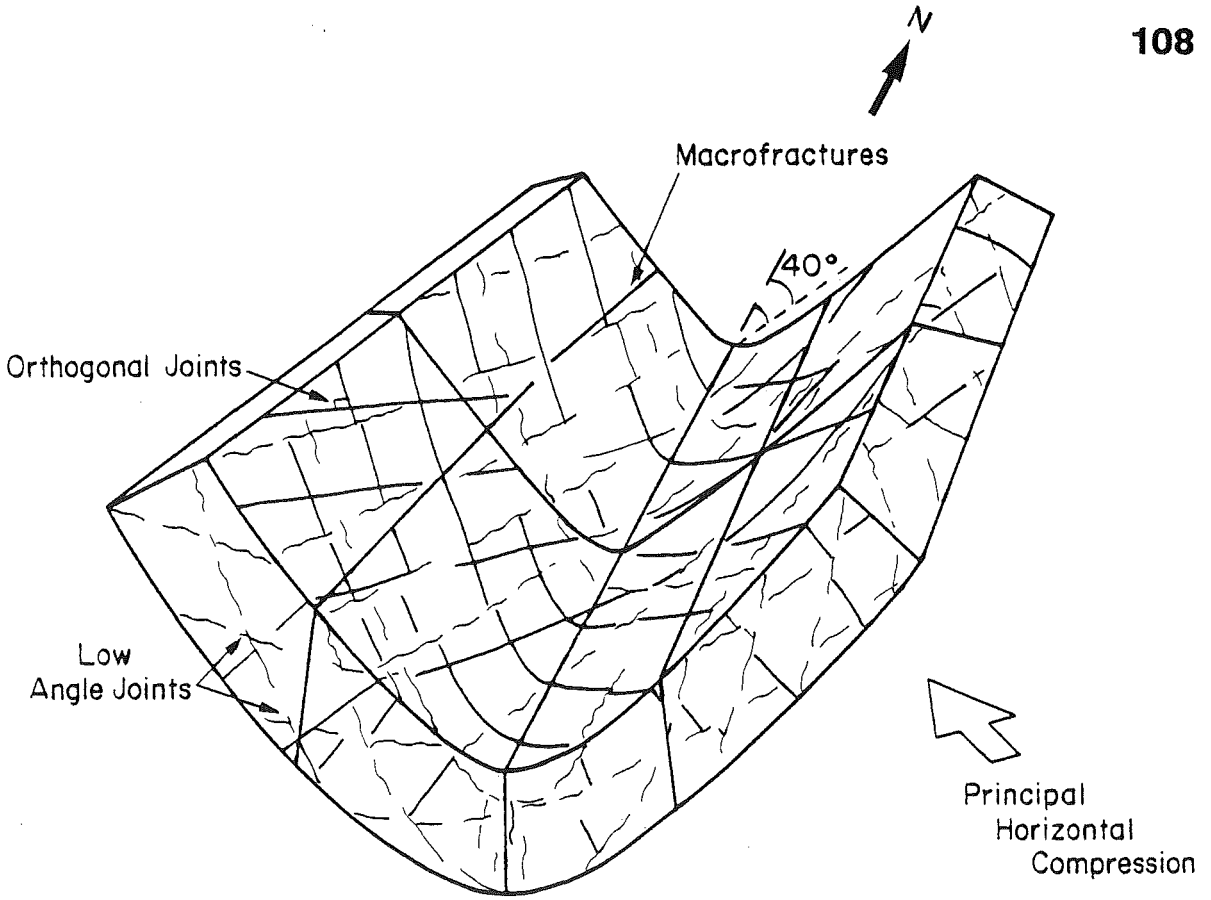

Figure 6.7. Schematic diagram that shows the general geometric relationships between folding, jointing and the macrofractures.

of the overlying sedimentary pile, probably formed mainly during the Pliocene when the sediments overlying the limestones appear to have been thickest.

During the Pliocene to early Pleistocene, lithified Oligocene limestone units, initially buried and being compressed by the overlying sediments, began to experience the effects of gentle regional uplift and subsequent erosion of the overlying Pliocene cover. Orthogonal Joints represent the first microstructures developed during this period of deformation. The relative ages of the Orthogonal Joint sets have not been resolved here, although both sets probably developed early in the uplift history of

the area, prior to the formation of pressure solution seams normal to bedding and the onset of folding. Some constraints can be placed on the mechanics of orthogonal joint formation. Both joint sets appear to be extensional, which implies a 90^0 change in the minimum principal stress between joint forming events, a widely observed phenomena (e.g. Price, 1966; Ramsay and Huber, 1987). The primary kinematic control, as indicated by the restored pre-fold orientation of stylolite columns and the dominant joint set, was provided by a horizontal NW-SE principal compression. A second much more incipient compression is indicated by a small number (6% of the total measurements for bed dips $<60^0$) of stylolite columns that trend NE. This compression may be related to NE-SW joint development. Elastic modelling for vertical systems of orthogonal fractures by Price (1966) indicates that during the formation of such joints the maximum principal compression is commonly vertical and the intermediate and minimum principal stresses are in the horizontal plane. Hancock and others (1987) extended this view by suggesting that orthogonal fractures form under switching principal stresses when the intermediate and minimum principal stresses are nearly equal. These conditions may have been achieved during the early stages of deformation, when the horizontal compressive stress was smaller than the stress imposed on the limestones by the overlying rocks. These conditions are likely to have been short lived given that the rocks overlying the limestones were probably relatively thin (<1.5 km.) and the vertical compression small.

Orthogonal Joint formation was closely followed by horizontal uniaxial compression and stylolite development. Under conditions of uniaxial compression the principal intermediate and extension stresses (sigma 2 and 3) are commonly negligible relative to the value of principal compression (sigma 1) and the differential stress is

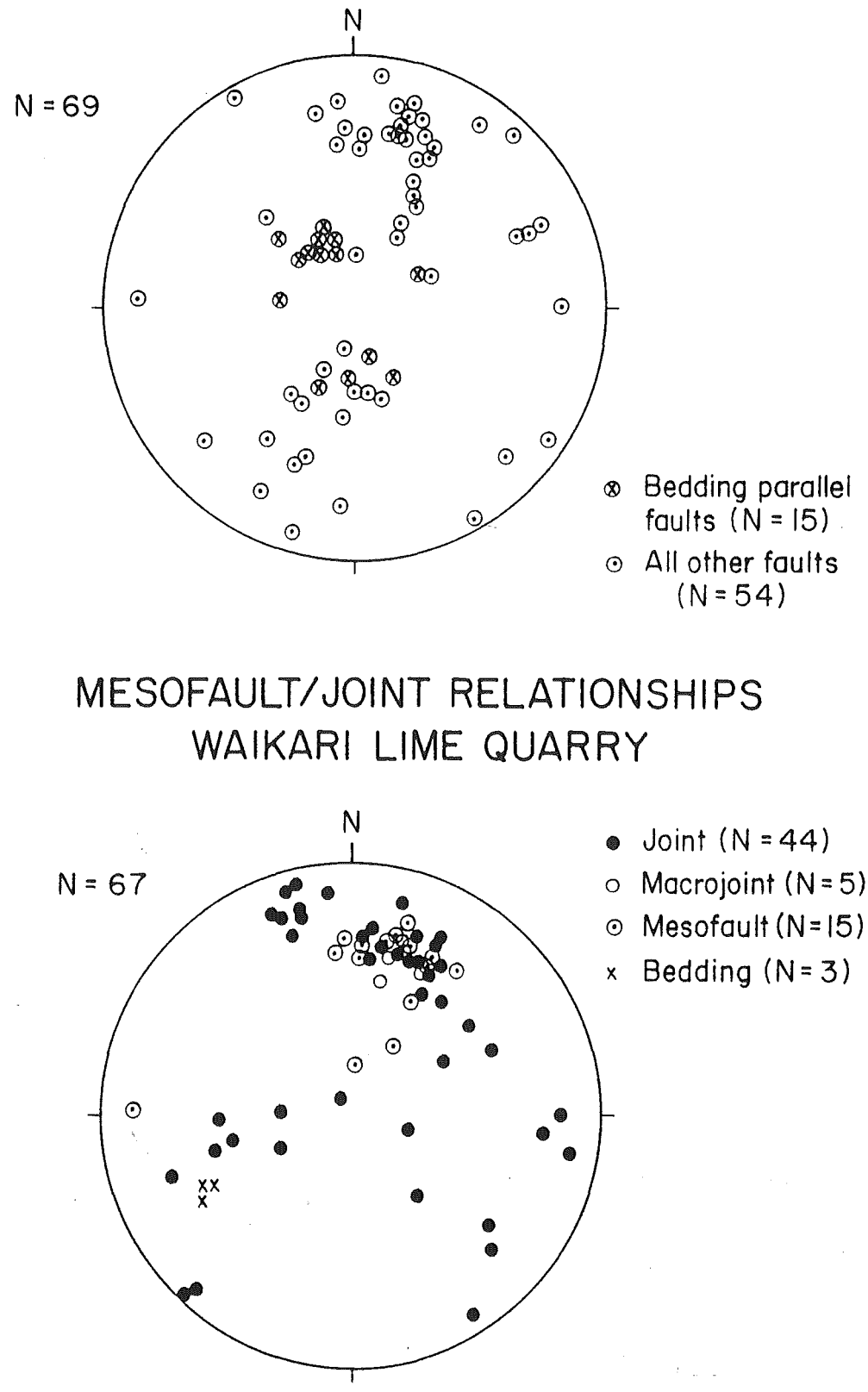

Figure 6.8. Mesofaults within Oligocene limestones (A) and their geometric relationships to jointing in the Waikari Lime Quarry (B).

large relative to the principal horizontal extension. These conditions signify the end of the probable Orthogonal Joint forming period and an increase in the magnitude of the maximum principal stress. Orthogonal Joint surfaces provided a medium on which to record compression, in the form of stylolite columns on sporadic pressure solution seams. These solution seams accommodated a small amount of NW-SE uniaxial shortening strain prior to the onset of folding and faulting, which may have overprinted earlier formed bedding normal slickolite striations and NE-SW stylolites. Calculations suggest that NW-SE pressure solution seams probably developed in association with <5% shortening.

Unlike the Orthogonal Joints and bedding normal solution seams folding began developing in response to N-S and E-W shortening. The early stages of folding may have been responsible for the formation of AC and AB macrojoints, developed in association with shortening of thick (5-10 m.) massive Weka Pass Stone beds. With continued folding macrojoints and other pre-existing fractures were subsequently activated into mesofaults. These faults are particularly abundant in limestones with bed dips of greater than 20^0 subjected to shortening of greater than 10%. The fold geometry and development is primarily controlled by large scale faulting within Mesozoic basement (Chapter 5). Consequently the folds are parallel to the strike of the causal fault and oblique to the principal compressive stress and earlier formed fractures. Warped river terraces and anomalies in the drainage patterns suggest that active folding, already demonstrated to the east by Campbell and Yousif (1987) is also occurring here. Up to the present between 2 and 70% (12-20% estimated mean) cumulative strain has been accommodated by folding locally.

6.5 PLATE BOUNDARY DEFORMATION IN NORTH CANTERBURY

Microstructures within Oligocene limestone units indicate two periods of plate boundary deformation in North Canterbury. Firstly, a period of weak regional deformation, associated with small strains and sub-horizontal shortening, during the mid-late Oligocene. This deformation appears to be related to the initial development of the Alpine Fault as a through-going transform, and provides the only indication of Miocene and older plate Boundary deformation in this part of Canterbury.

The second period, began during the late Pliocene in North Canterbury and early Pliocene in Marlborough, with the onset of compressional tectonics. Microtectonic structures formed during this period developed at shallow depths (< 2 km.) in crustal rocks of the Pacific Plate and reflect mainly brittle deformation at the outer edge of the plate boundary zone. Initially, the magnitude of tectonic paleostresses appear to have been comparable to the loading stresses imposed by the overlying rocks. The sequence of Orthogonal Joint, pressure solution seam and stylolite development, folding and finally faulting testifies to the increasing magnitude of NW-SE compression (Figure 6.9) in this region. The sequence of microstructure development displays a progressive increase in the intensity of deformation as the plate boundary deformation zone widened and migrated southwards across northern Canterbury with time. Lateral spreading and widening of the boundary zone deformation appears to reflect directly the increased plate convergence across the northern South Island during this time. Similar southward migration of activity on the faults of the Marlborough system (Campbell, 1973) may indicate that the pre-Pliocene Alpine Fault was at that time located close to the present Wairau Fault.

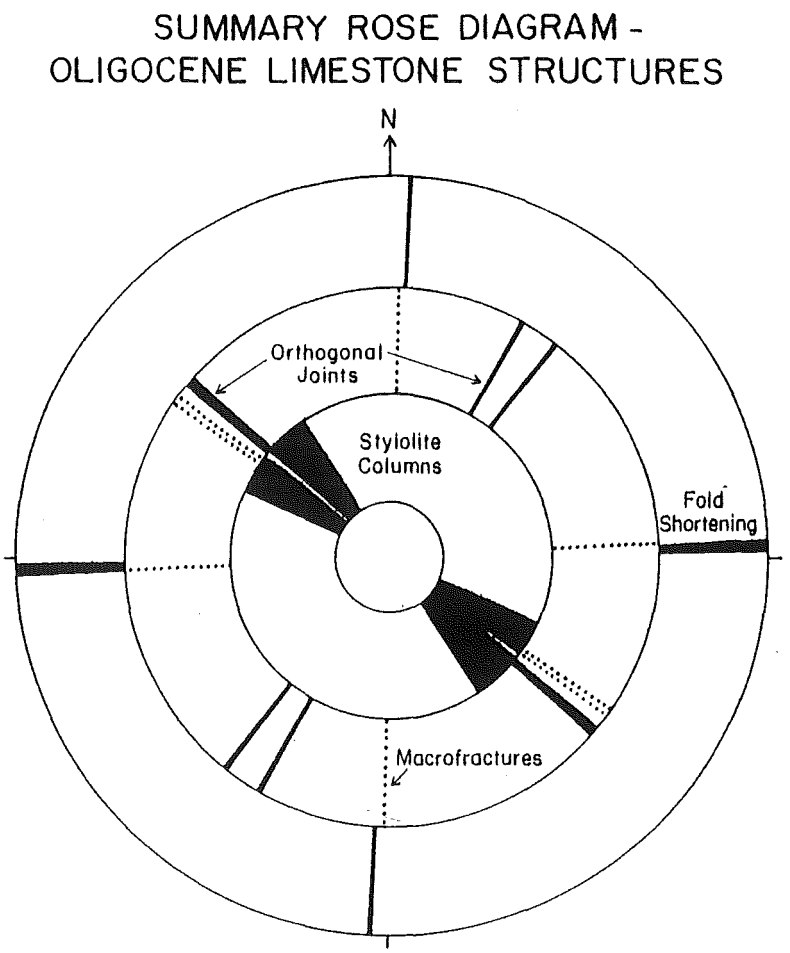

Figure 6.9. A summary composite rose diagram for all Oligocene limestone structural data collected from beds with dips less than 30^0. Orthogonal Joints and macrofractures rose orientations represent the discontinuity strike and the stylolite and fold data trends. The orientation of the rose petals represent the mean value for all histogram peaks above random, while the petal width is proportional to the petal area above random.

The stylolite columns and the dominant Orthogonal Joint sets collectively imply that plate boundary deformation was driven by horizontal NW-SE principal compression with mainly horizontal NE-SW principal extension (Figure 6.9). Since the onset of late Cenozoic tectonics, the orientation of the principal compression driving deformation has not changed. The compression inferred from solution seam stylolite columns is

similar to the focal mechanism data (Rynn and Scholtz, 1978; Walcott, 1978) determined for this part of the plate boundary.

6.6 CONCLUSIONS

Small scale tectonic structures in Oligocene limestone units on the outer edge of the New Zealand Plate Boundary developed in response to small strains in shallow crustal rocks. The structures indicate two periods of deformation, (1) weak regional mid-late Oligocene compression and (2) NW-SE Pliocene to Recent compression. Post Pliocene deformation is characterised by two phases, initial NW-SE shortening followed by N-S and E-W shortening, each associated with geometrically similar brittle structures. Consequently closely spaced Orthogonal Joints and stylolites bisect the fold axes. In North Canterbury since the late Pliocene NW-SE compression has increased progressively in intensity and implies a rapid widening of the plate boundary zone in the last 2-3 ma.

This study reiterates the finding of numerous earlier workers in suggesting that where limestone beds dip steeply ($>60^0$), the small scale structures are rotated into the plane of fold flattening. In such cases the microstructures record local strain imposed by folding and are of little use in determining the regional tectonics. However, folded limestones with bedding dips of at least 30^0 contain brittle microtectonic structures that maintain a regional significance after bedding dips are removed.

CHAPTER 7 SYNTHESIS AND REGIONAL TECTONICS

7.1 SYNTHESIS OF MID-WAIPARA DATA

In the mid-Waipara region on the edge of the New Zealand Plate Boundary, shallow (< 2 km.) crustal deformation has resulted in the development of structures within a thin (< 1.5 km.), late Cretaceous-early Pleistocene sequence of sedimentary rocks. The main structures were initiated or reactivated during the early Pleistocene (see section 6.4), and continued seismicity testifies to the ongoing strain. The development of faults and folds are intimately related and locally structures are parallel, with mainly E-ESE and N-NNE orientations. This contrasts with the regional NE-SW structural grain of Canterbury.

Faulting is dominated by oblique-reverse and thrust faults with north, south, east and west vergence. There is no clear evidence of major right-lateral faulting. Locally, E-ESE striking faults accommodate mainly oblique normal motion, and are inferred to be reactivated late-Cretaceous structures. Offsets across the major faults are generally less than 0.6 km., which may indicate that the faulting is very recent or that slip-rates are low. The orientation of the principal stress axes, derived from minor fault populations (Figures 2.3 and 2.6), most frequently plunge at shallow to moderate angles. The stress tensors indicate a predominant NW-SE compression (azimuth 130-140^0) across the region between the southern end of the Culverden Basin and Mt Grey. However, local stress patterns are variable and more complex than the regional geodetic and focal mechanism data would imply (see Figure 7.2).

Folding in the cover rocks is defined by the geometry of distinctive Oligocene-Miocene limestone horizons. The outcrop patterns are irregular and reflect basin and dome fold interference between approximately E-W and N-S trending folds. Secondary folds have developed oblique to the main fold sets, and composite conical fold surfaces, defined by numerous conical segments, are common.

The folding has developed in response to fault propagation and displacement within basement, together with shortening within the fault bounded blocks. The main fold sets are generally parallel to the major faults, and in the mid-Waipara region the folds are developed oblique to the azimuth of the principal regional compression. Fault-propagation folds with structural relief of 2-3 km. are commonly developed above contractional faults (see Figures 5.2 and 7.5). These folds tend to be asymmetric, with a steep (60^0 to overturned) limb on the footwall of the fault, and a relatively shallow ($10\text{-}30^0$) limb on the hanging wall. The folds verge in north, south, east and west directions, and both faults and folds appear to have been active simultaneously during the late Cenozoic. Faults and folds have accommodated finite strain at a ratio of 1:3. Their comparable kinematics implies that the patterns of both short and long term strain (as described by fault slickensides and fold shortening), are similar and have not changed markedly since deformation began.

The local predominance of compressional tectonics is in contrast to the major right-lateral faults of the Marlborough system. In this respect, the regional strain appears to be partitioned between inner and outer parts of the plate boundary, in a similar fashion to plate boundary deformation reported from the San Andreas Fault in

California (e.g. Zoback et al, 1987). In the mid-Waipara region the geometry and kinematics of active structures vary over short (< 2 km.) distances, accompanied by changes in the orientation of major faults and their cross cutting relationships, the main shortening directions, and the principal stress orientations and magnitudes. These conditions contrast with cratonic continental areas (e.g. Appalachian Mountains of the eastern U.S.A) where structural grains and styles persist over many kilometres. The complexity of deformation in North Canterbury may, in part, reflect the interference between reactivated faults of late Cretaceous age, and younger faults formed during the late Cenozoic. This may have contributed to the synchronous development of two orthogonal sets of structures.

7.2 PLATE BOUNDARY TECTONICS

7.2.1 EVOLUTION OF THE PLATE BOUNDARY IN NORTH CANTERBURY

Microtectonic structures in Oligocene limestones (Chapter 6) imply two periods of plate boundary deformation in North Canterbury. The first episode, involved weak deformation during the mid-late Oligocene, may relate to the development of the plate boundary transform system as a through-going structure (e.g. Molnar et al, 1975; Carter and Norris, 1976). This is the only indication of pre-Pliocene deformation in North Canterbury and may indicate that the plate boundary was laterally confined during the Oligocene and Miocene. The second period of deformation began locally during the late Pliocene and was marked by the sequential formation of joints, pressure solution seams and stylolites, macroscopic folds and faults. These structures record progressively increasing strain, and rapid

lateral spreading and widening of plate boundary deformation which began in Marlborough during the Pliocene (e.g. Lamb and Bibby, 1989) in response to increased plate convergence.

7.2.2 SOUTHERN LIMIT OF SUBDUCTION TECTONICS

The boundary between west directed subduction and New Zealand continental crust is marked by the Hikurangi Trough (see Figure 1.1). The trough terminates offshore south of Kaikoura (Figure 7.1), but the details of this termination, and the dimensions of the subducted slab beneath Marlborough and Canterbury remain unclear.

Between Marlborough and the mid-Waipara region, the styles and magnitude of deformation change significantly. Five main distinctions can be made:

(1) In contrast to the major right-lateral strike-slip faults that form the Marlborough Fault System, the main faults in North Canterbury are predominantly reverse dip-slip structures. This contrast is exemplified by the local predominance of left lateral minor faults over right lateral.

(2) The lateral extent, continuity and number of major faults decreases from Marlborough to North Canterbury.

(3) The rates of deformation implied by fault offsets (e.g. Cowan, 1990), rates of uplift (Wellman, 1979; Lamb and Bibby, 1989), geodetic shortening (Bibby, 1975, 1976 and 1981; Walcott, 1978) and seismicity (e.g. Reyners, 1989) decrease from Marlborough to North Canterbury.

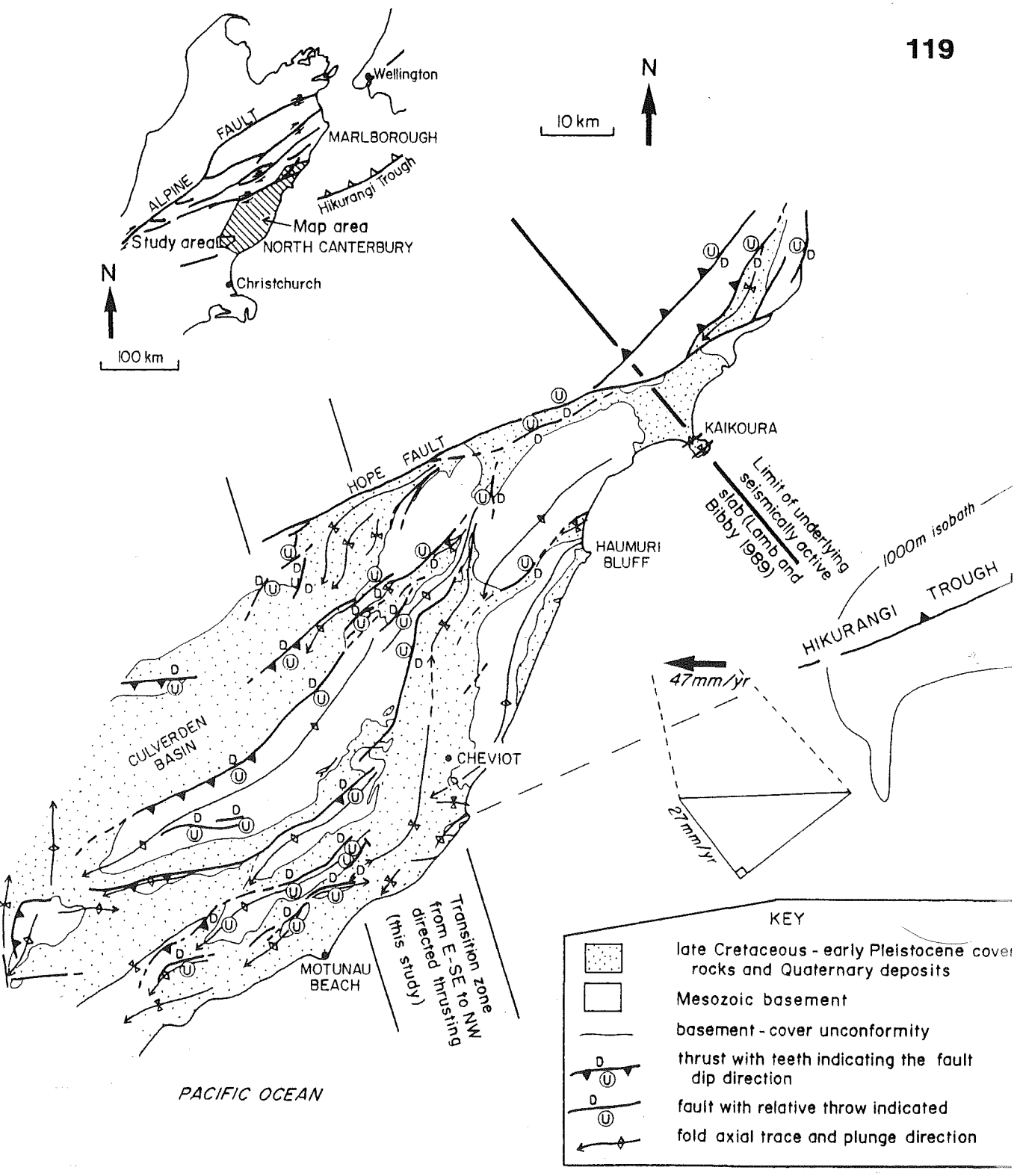

Figure 7.1. The structural geology of the North Canterbury and southern Marlborough drawn from Lensen (1962), Gregg (1964), Maxwell (1964), Yousif (1987), Dibble (unpublished) and this study. Note particularly the change in thrust vergence and the direction of fault upthrow across the transition zone south of Cheviot. The NW-SE plate boundary normal component of the plate motion vector (Chase, 1978), 27 +/- 7 mm a^{-1}, is indicated.

(4) Oblique dip-slip faulting and folding has locally promoted differential uplift and the development of valley and ridge topography in North Canterbury (Figure 7.1), while much of Marlborough is undergoing rapid regional uplift.

(5) Between the Culverden Basin and the coast basement, ridges are forming above a series of NW verging thrust and reverse faults (Gregg, 1963; Wilson, 1963; Maxwell, 1964; Dibble unpublished data and personal observations). The vergence direction of these thrusts is opposite to Pliocene and younger thrusts in Marlborough, which verge to the SE and E (Figure 7.1).

Although these variations in structural styles, magnitude and rates of deformation differentiate the Marlborough and North Canterbury structural domains, the boundary relationships are complex and no one single, simple boundary can be identified from the variations in deformation listed above. Lensen (1975) identified Marlborough as a region dominated by shear, whereas he inferred mainly compressional deformation in North Canterbury and placed a gradational boundary between the two domains south of the Hope Fault. Such a boundary must pass between the Hope Fault and the Culverden Basin with a ENE-NE orientation, and must also extend across the Fault NW of Kaikoura, defining a zone of thrusting related to subduction beneath the Kaikoura Mountains (Figure 7.1). The Hope Fault itself forms a major structural discontinuity and marks the northern limit of valley and ridge structures and topography. Wellman (1979) and Bull (pers. comm., 1991) infer uplift rates to decrease rapidly across the Hope Fault towards the south. However, neither rapid changes in the regional rates of shortening (Bibby, 1976; Walcott, 1978; Reilly, 1990), or changes in the azimuth of the principal horizontal compression and shortening directions (Figure 7.2) appear to have occurred across

the Hope Fault. The rates and magnitude of tectonic activity appear to decrease gradually to the SE away from the areas affected by subduction tectonics.

These changes in parameters and magnitudes of deformation crudely define a gradational boundary between outer plate boundary and subduction related tectonics. By contrast, the change in structural style marked by the reversal of fault throw and thrust vergence directions on the major faults can be located relatively accurately. Figure 7.1, compiled largely from Lensen (1962) and Gregg (1964), shows a distinct and relatively rapid reversal of the major fault upthrow and thrust vergence directions. The zone of transition is orientated SSE-NNW and separates predominately NW verging thrusts in North Canterbury from mainly E-SE verging thrusts in Marlborough. The transition zone passes through the NE end of the Culverden Basin, and extends offshore south of Cheviot at the point where the projection of the Hikurangi Trough strikes the coast (Figure 7.1). This zone, as broadly defined, shows a 20^0 divergence in trend from the southern limit of the seismically active slab, defined by Lamb and Bibby (1989). It is interpreted here as marking the boundary, at the surface, between the E-SE directed subduction related thrusting (Bibby, 1981; Lewis et al, 1985; Lamb and Bibby, 1989), and the NW directed thrusting characteristic of deformation further south. It may mark the surface expression of the SW limit of subduction related tectonics, but as the dip of this boundary is not well defined, it is not clear whether this represents the southern limit of the subducting slab beneath North Canterbury.

The transition zone in the upper crust where thrusts with opposing vergence pass one another is likely to be complex, as there is an inherent geometric incompatibility between the structures. Compatibility problems within the transition will be reduced

by the dying out of the respective thrust geometries and is likely to form an array of vertical and lateral wedge shaped bodies defined by the main faults. This zone may mark a significant crustal discontinuity.

7.2.3 STRESS TENSORS

Zoback and others (1987) recognised that compression is acting at much higher angles to the San Andreas Fault System than Mohr/Coulomb theory and typical coefficients of rock friction would predict. The question naturally arises as to the nature of stress orientation near other major transform fault zones.

Data from a number of sources provide an indication of present day shortening and stress in the northern South Island (Figure 7.2), but details of longer term stress orientations are largely unknown. This longer term view is important because the direction of plate convergence in Marlborough may have experienced significant clockwise rotation during the late Cenozoic (e.g. Walcott, 1979; Mumme and Walcott, 1985).

The stress tensors derived from this study date from the early stages of doming, probably between the late Pliocene and early Pleistocene through to Holocene fault activity (see Figure 2.4). On the northwest side of the Marlborough Fault System along the Waimea Fault, a stress tensor analysis of minor faults by Pettinga and Wise (in prep) yields essentially similar results (Figure 7.2). Further east, in the Marlborough Sounds, calcite twin lamellae and fault striation derived principal horizontal compression trend E to ESE (Nicol and Campbell, 1990). The results of these studies can be compared with indicators of modern principal horizontal

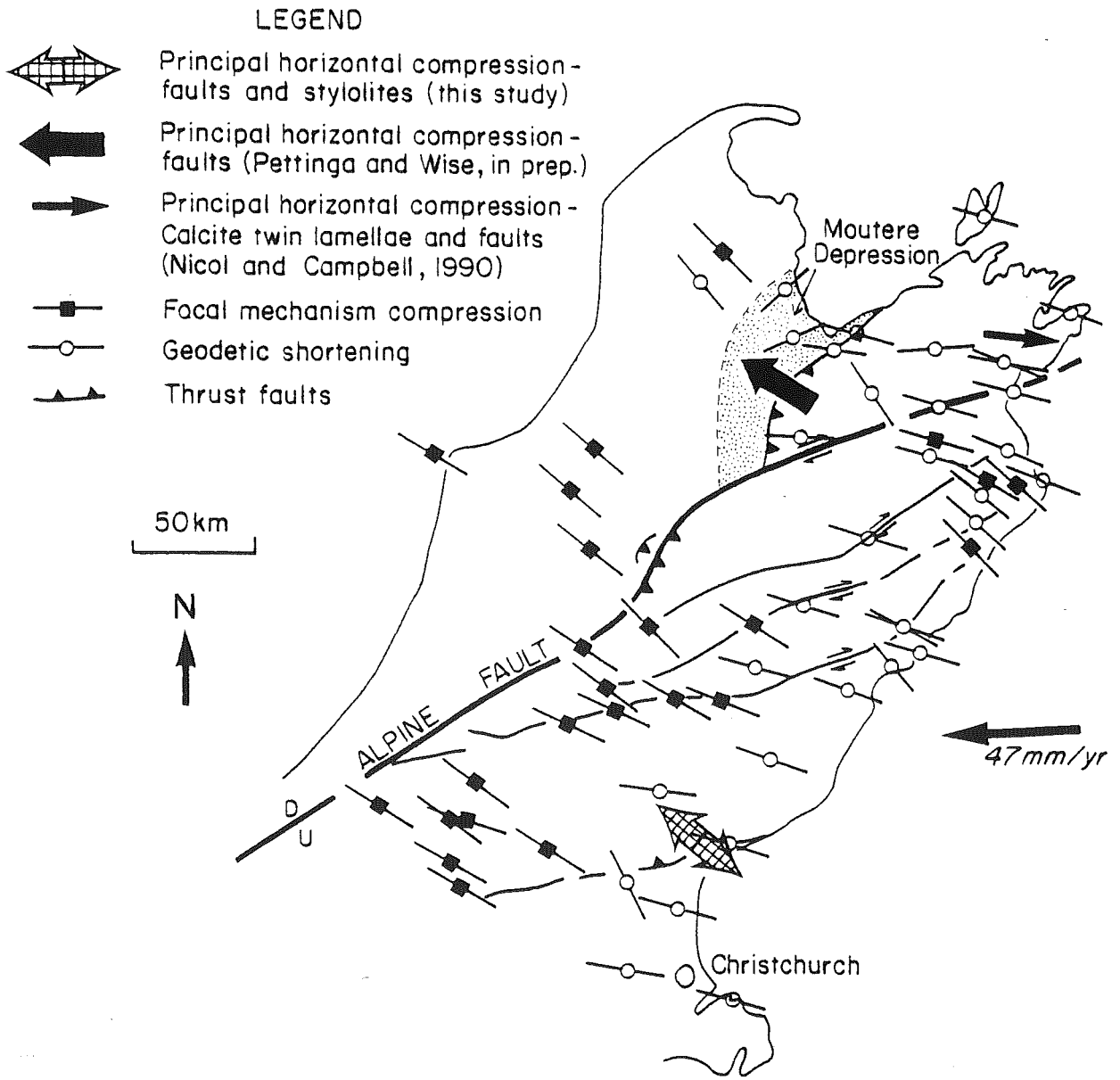

Figure 7.2. A compilation of the available focal mechanism (Arabasz and Robinson, 1976; Rynn and Scholz, 1978; Walcott, 1978) and geological (see figure) principal horizontal compression, and geodetic triangulation (Bibby, 1975, 1976 and 1981; Walcott, 1978) principal horizontal shortening data for the northern South Island. The orientation the principal horizontal compression and shortening is marked by the long axis of the symbols.

shortening and compression directions in the same area (Figure 7.2). The present day data are based on focal mechanism first motion studies (Arabasz and Robinson, 1976; Walcott, 1978; Rynn and Scholz, 1978) and on geodetic triangulation network measurements (Bibby, 1975, 1976 and 1981; Walcott, 1978; Reilly, 1990).

In the mid-Waipara region the orientation of geodetic and focal mechanism data is similar to the azimuth of the principal compressive stress direction derived from fault motion data and stylolites. These geological stress indicators represent a more long term view of plate boundary deformation and indicate that there has not been significant change in the orientation of the principal stress, or bodily rotation of the rock in this area since the early Pleistocene (the age of the stylolites see chapter 6). This is consistent with earlier observations of Walcott (1978). It must be pointed out that while the composite principal compressive stress (derived from 400 square kilometres) is compatible with the regional trend of the principal horizontal compression, the principal stresses derived from more restricted areas were much more variable. The orientations of the principal stresses vary locally according to changes in the style of macroscopic faulting in any one area, and the stress orientations appear to be partitioned in a similar way to the strain. The scale of observation selected for analysis of stress tensors derived from minor fault populations will markedly influence the orientation of the derived stress tensors.

Although there is local divergence in the data of up to 90^0 in the Moutere Depression (Figure 7.2), the preponderance of evidence indicates a relatively uniformly oriented, present day azimuth of 105 to 130^0 for compression and shortening across the plate boundary zone in the northern South Island. The fault tensor analyses yield essentially the same result and suggest that this pattern may

not have changed significantly since at least the late Pliocene or early Pleistocene in North Canterbury. The lack of change in the orientation of the stress and strain data in the block north of the Wairau and east of the Waimea faults is surprising given that the direction of relative plate convergence is thought to have been rotating in a clockwise direction in this area (Walcott, 1979).

This regional shortening direction is at a high angle to the strike of the Alpine Fault, and the faults of the Marlborough system. Zoback and others (1987), and Mount and Suppe (1987), note a similar relationship for the San Andreas Fault, a condition not predicted by classical wrench fault theory (Wilcox et al, 1973). Zoback and others suggest that plate motion is partitioned into strike-slip and dip-slip components which are taken up respectively in the soft gouge of the San Andreas and in the adjacent rocks.

Recent fault offsets along New Zealand's Alpine Fault suggest that this fault is also accommodating mainly strike-slip motion with horizontal to vertical displacement ratios commonly of between 5 and 10:1 (Berryman, 1975; Campbell, 1973; Berryman et al, 1986). Unlike the San Andreas System, the Alpine Fault is accommodating major plate convergence at a marked angle to its strike (Figure 7.2), and has accommodated a significant component of dip-slip movement which is largely responsible for the creation of the Southern Alps (e.g. Walcott, 1979). These factors suggest that to infer only simple partitioning along the fault traces may not fully account for the high angle between the principal shortening direction and the Alpine Fault. Instead, the shortening and compression are acting across the region, more or less normal to its strike. This shortening is at a 30-40^0 angle to the present direction of plate convergence (Figure 7.2), and for this reason, among

others, it has been proposed here (section 7.4) that much of Marlborough and North Canterbury is underlain by one or a number of sub-horizontal detachment faults.

The stress data from the mid-Waipara area provide a longer term view of the stress history of the region, a view which provides clues to its similarity and possible differences between the San Andreas System, and support the need for a new model to explain the relationships.

7.2.4 EVIDENCE FOR CRUSTAL DETACHMENT FAULTING IN THE NORTHERN SOUTH ISLAND

Any interpretation of the styles and intensity of deformation in rocks of the upper crust (< 2 km.) in North Canterbury is constrained by the structures exposed at the surface (e.g. Lensen, 1962; Gregg, 1964; Lamb and Bibby, 1989; this study). Many of the structures in North Canterbury appear to be of limited lateral and vertical extent, and may not extend below the upper crust. This raises the questions: (1) how is the mid to lower crust deforming and (2) what are the relationships between upper and mid to lower crustal structures?

Recent work based on exposed profiles of the middle crust (e.g. John and Musaka, 1990) and sub-surface seismic and drill hole data (e.g. Wentworth et al, 1983; Davis, 1983), suggests that in the western U.S.A the crust is being deformed by sub-horizontal detachment faults at depths of between 2 and 20 km. These faults may be normal (e.g. Davis and Lister, 1988), or reverse (e.g. Namson and Davis, 1988).

The presence of sub-horizontal zones of high strain within, and at the base of, the crust have been postulated for deformation beneath the southern portion of the Southern Alps. These have been invoked to account for the uplift of the Southern Alps (Wellman, 1979), the low heat flow and negative gravity anomaly associated with the Alps (Allis, 1981) and historical seismicity (Reyners, 1987) adjacent to the Alpine Fault. Norris et al (1990) also infer a mid to lower crustal decollement from their application of critical wedge mechanics, with erosional constraints, to the analysis of uplift across the Alps.

In North Canterbury and Marlborough crustal detachments may also provide a means of accounting for mid to lower crustal deformation, while conforming with the available geological and sub-surface geophysical data. On a regional scale, sub-horizontal detachments entirely within the rocks of the Pacific Plate may provide a means of accommodating deformation associated with the change from the east dipping Alpine Fault to the west dipping subduction of the Hikurangi margin. This could be achieved without substantially thickening the crust in the northern South Island, and so remain consistent with available gravity data (Reilly, 1965; Davy and Davey, 1985), which implies that the crust is not anomalously thick. Throughout North Canterbury active contractional deformation, dominated by thrusting and asymmetric folding (Figure 7.1, 7.3 and 7.5), is pervasively developed and indicative of thin-skinned tectonics. Boyer and Elliot (1982) suggested that it is common for thrusts and related structures to flatten and merge downwards into sub-horizontal sole thrust or decollement structures. The geometric relationships between the decollement and the overlying thrusts may vary, but changes in the orientation of the basal decollement in any one system are generally reflected as a variation in the characteristic style of thrust geometry. Such deep level controls may account for

Figure 7.3. A block diagram displaying the possible structure of the top 12 km. of the Pacific Plate continental crust in the Okuku to lower Waipara and Hanmer to Motunau areas. The geology of the upper crust, down to 3 km., is drawn to scale from cross-sections based on surface projections and gravity data, discussed and illustrated in the text (section 7.2.4). The projections below this level are speculative. The dots represent areas of Quaternary gravel deposition.

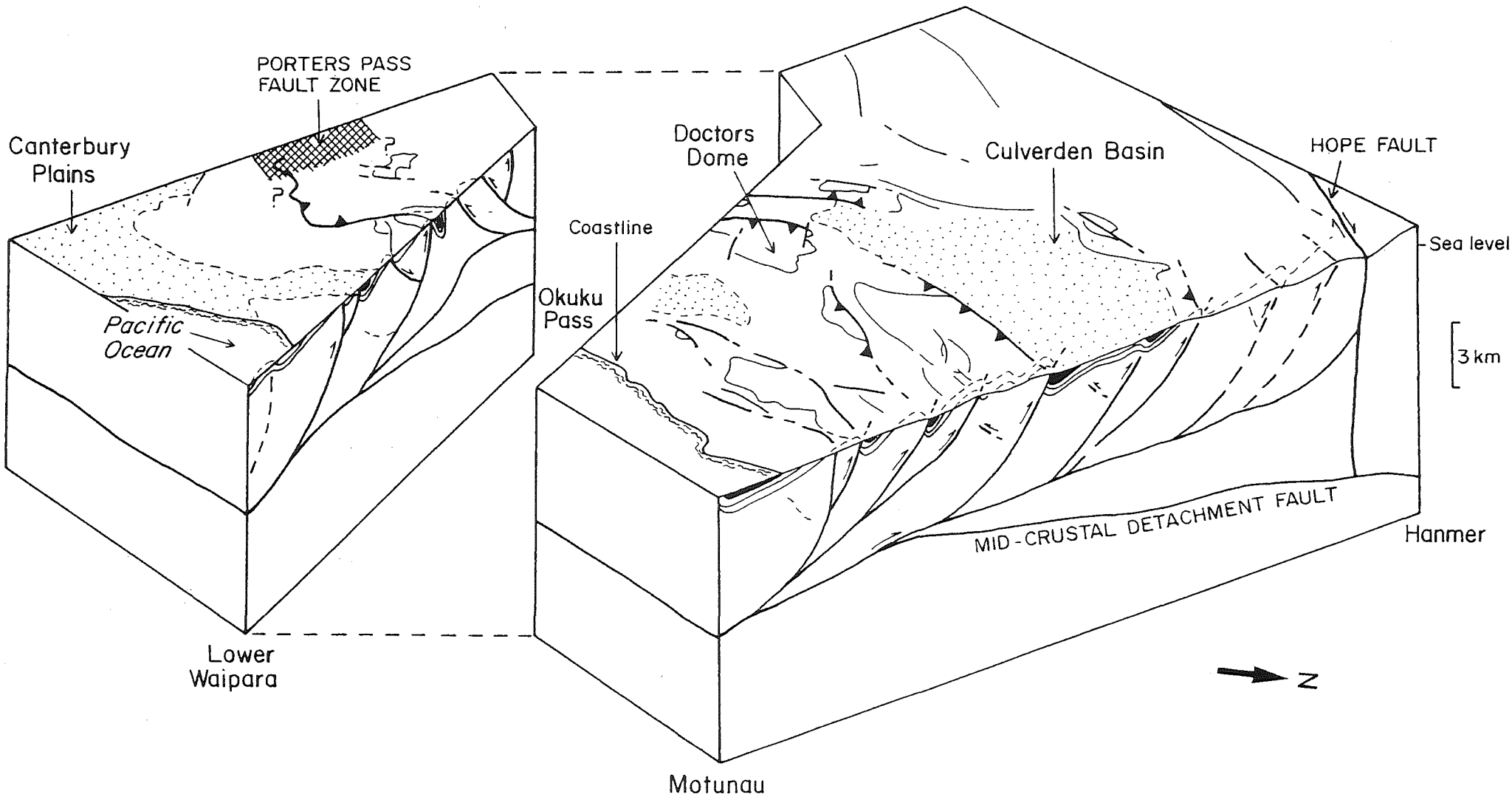
PORTERS PASS
FAULT ZONE
Canterbury
Plains
Pacific
Ocean
Lower
Waipara
Coastline
Okuku
Pass
Doctors
Dome
Culverden Basin
HOPE FAULT
Sea level
3 km
MID-CRUSTAL DETACHMENT FAULT
Hanmer
Motunau
N

the variation in thrust orientations throughout Canterbury. Crustal detachment structures may also account for the divergence between the regional principal horizontal compression (Figure 7.2) and the relative plate motion vector in the northern South Island, by allowing semi-independent behaviour of rocks of the upper crust with respect to plate kinematics. Detachment faulting is also consistent with the inferred rotation of discrete crustal blocks of varying size (< 5 to 100 km.) in Marlborough, implied by paleomagnetic data (Walcott, 1979; Mumme and Walcott, 1985; Lamb, 1988).

7.2.4.1 Crustal Detachment Model

The proposed detachment fault model for the northern South Island is one in which a series of sub-horizontal, high strain zones accommodate mid to lower crustal deformation (Figure 7.3). The continental crust in Canterbury appears to be approximately 25 km. thick (Reyners pers. comm. to Cowan, 1990) and initial analysis of microseismic data collected in Canterbury (Cowan pers comm, 1990) suggests the presence of an apparently aseismic zone between 12 to 15 km. depth and the base of the crust. This may place the brittle-ductile transition at about 12 to 15 km. If thrusts exposed at the surface are to merge with detachment faults at depth, then the short lateral extent of these surface structures (often < 10 km.) suggests that detachment structures are likely to be present well above the brittle-ductile transition (Figure 7.3).

Elsewhere, mylonites thought to have formed in conjunction with middle crustal detachments are commonly observed within greenschist and amphibolite facies

rocks, and are inferred to have formed at depths of 10-15 km. (e.g. John and Musaka, 1990). In New Zealand, mylonites exposed west of the Alpine Fault have been interpreted by Norris et al (1990) to have partially developed within sub-horizontal decollement zones. It may be that discrete detachment faults can exist both above and below the brittle-ductile transition and/or that a series of these structures are developed at different levels in the crust.

Implicit in Lamb's (1988) model for rotation of crustal blocks of varying size in Marlborough and along the Hikurangi Margin, are low angle detachments developed at numerous levels in the crust. If, away from the intensely deformed parts of the plate boundary the number of discrete 'rotating' crustal blocks is reduced, then the number of high strain zones required may decrease. A complex series of anastomosing sub-horizontal structures could exist (Figure 7.3). These might define lensoid shaped bodies of crust which respond to plate motions semi-independently. Under these conditions detachment structures could be simultaneously active at several structural levels in the crust, with changes in their relative and absolute rates of activity influenced by the magnitude of crustal deformation and the number of detachments.

The geometry of the detachment zone(s) in the northern South Island is likely to be controlled by interaction between the Pacific Plate continental crust, the Alpine Fault and the subducting oceanic crust of the Pacific Plate. On a regional scale, detachment structures possibly dip towards central Marlborough from the Alpine Fault and Hikurangi Trough, due oblique convergence forcing the edges of the continental crust upwards. The negative gravity anomaly in central Marlborough (Reilly, 1965; Davy and Davey, 1985) could mark the point at which detachment dips

are reversed. However, this geometry could vary on a local scale. Northwest verging thrusts in North Canterbury, SE of the Hope Fault (Figure 7.1), may imply that detachment structure(s) in this area dip at shallow angles to the SE. This might reflect local depression of the crust under the influence of subduction. Equally it might reflect the influence of buoyant continental crust of the Chatham Rise being forced up against the back edge of the deforming Pacific Plate. Geophysical data could better constrain these sub-horizontal surface(s), but John (1988) has emphasised the need for careful evaluation of seismic reflection profiles across complexly deformed crust, as several mid-crustal structures with complicated relationships may be developed.

Wise et al (in prep) have proposed that this region forms a vast surficial crustal slab of Pacific Plate rocks which rest on rocks of the Australian Plate across a detachment zone. This model implies that the Alpine Fault flattens and continues eastward for some distance under Marlborough and Canterbury. However, the absence of any significant negative gravity anomaly in this area (Reilly, 1965; Davy and Davey, 1985), suggests that the crust is not substantially thickened, which argues against Wise et al's model. In contrast to the expectations of the crustal slab model the magnetic anomaly associated with the Dun Mountain Ophiolite Belt does not appear to extend south of the Alpine (Wairau) Fault. For these reasons it is suggested here that the Alpine Fault possibly does not flatten beneath Marlborough and Canterbury, and that crustal detachment faults are likely to be contained solely within rocks of the Pacific Plate, in a similar way to that inferred by Norris et al (1990) for the Otago region.

7.3 LATE CENOZOIC DEFORMATION IN NORTH CANTERBURY

The style of deformation in the mid-Waipara region is in many respects similar to that which occurs in North Canterbury, on the eastern side of the Alps, between the Hope Fault and the Canterbury Plains. Data collected during this study has therefore been combined with previous work (Lensen, 1962; Wilson, 1963; Gregg, 1964; Maxwell, 1964; Bradshaw, 1975; Yousif, 1987; Barrel, 1989; Dibble unpublished gravity data; Nicol and Cowan unpublished data), to place some constraints on the kinematics of deformation throughout North Canterbury.

The region south of the Hope Fault is dominated by valley and ridge topography, which reflects the locations of the major faults and folds (see Figure 7.5). These appear to be mainly contractional structures developed in response to NW-SE compression (Maxwell, 1964; this study). Preliminary observations at Marble point (Syme, in prep), 4-5 km. south of the Hope Fault near Hanmer, indicate that contractional deformation extends at least this far to the NW. Strike slip deformation may therefore be restricted to the Hope Fault zone in a similar way to the San Andreas Fault (e.g. Zoback et al, 1987).

7.3.1 THE CULVERDEN BASIN: A COMPRESSIONAL STRUCTURE

The Culverden Basin is approximately 20 km. SE from the Hope Fault and is the largest of several basins in North Canterbury associated with Quaternary gravels. The basin is approximately 15 by 50 km., elongate in a NE-SW direction and crudely rhomb shaped (Figure 7.4). The shape of the basin and its proximity to the major

Figure 7.4. Geology of the Culverden Basin, North Canterbury (Gregg, 1964; Dibble, unpublished; this study). Cross sections are drawn normal to the basin at natural scale.

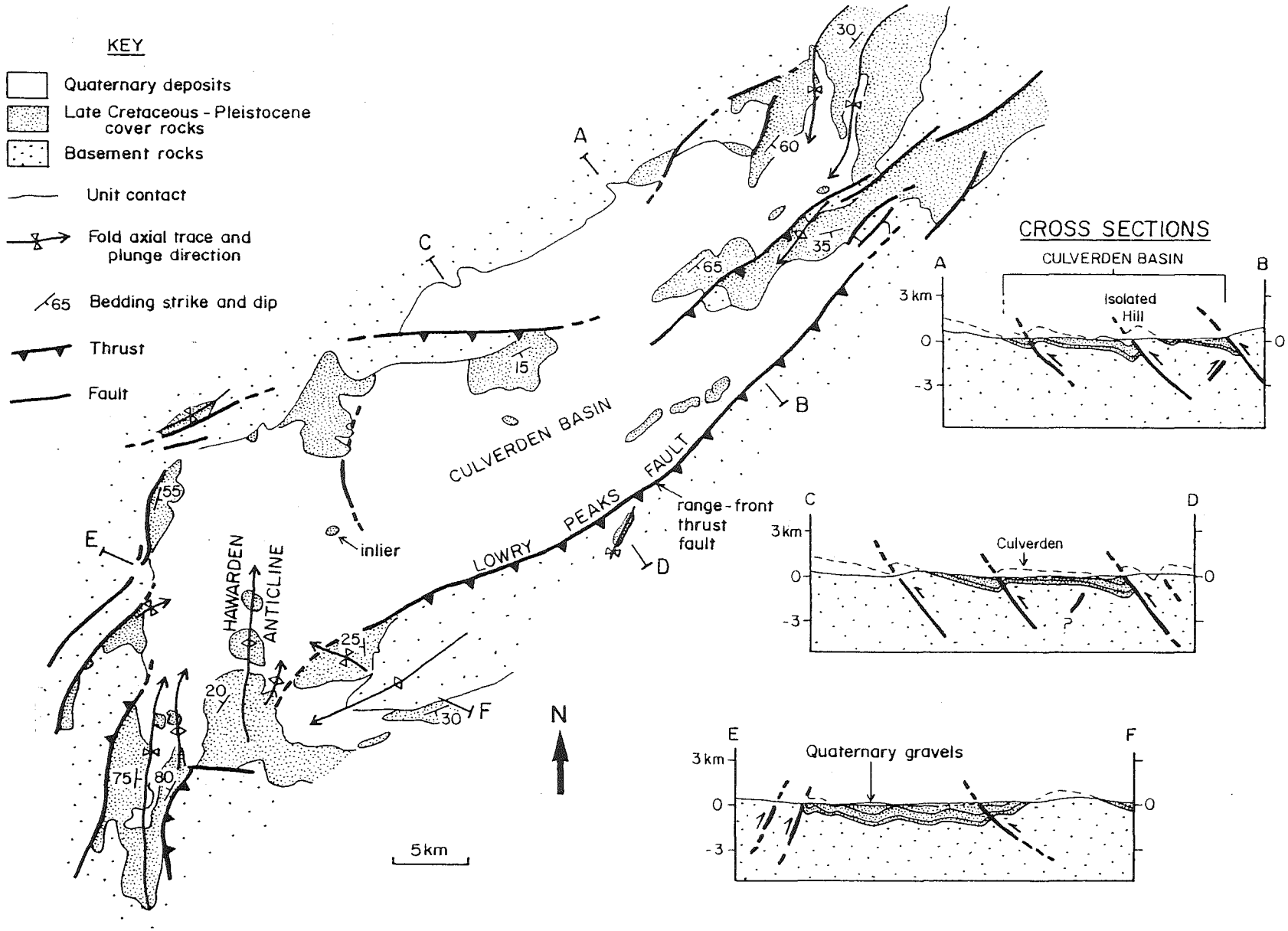

GEOLOGY OF THE CULVERDEN BASIN

lateral faults of the Marlborough system raise the question as to whether this is a pull-apart basin, formed at an extensional jog in a strike-slip fault system (Burchfiel and Stewart, 1966; Crowell, 1974). The results of work at the southern end of the basin (this study) and a gravity survey by Dibble (unpublished) suggest that at present the basin is bounded and penetrated by thrusts, but the question of a possible precursor origin under a different tectonic regime needs to be considered.

The margins of the Culverden Basin are partially controlled by faulting, with the Lowry Peaks Fault along the SE edge, and discontinuous faults to the W and NW (Figure 7.4). At the NE and SW ends of the basin subsidence is taken up by folding. The faulting along the SE edge and within the basin appears to be dominated by NE-SW striking thrusts (Dibble, unpublished), normal to the regional principal horizontal compression (see Figure 7.2). On the relatively straight western edge of the basin NNW-NNE striking reverse faults and thrusts are most common (this study). The crudely rhomb-shaped basin geometry is thus defined by a combination of thrust faulting and folding.

The estimated structural relief (Figure 7.4, cross sections) within the basin is also closely related to the pattern of faulting. The deepest parts of the basin appear to be along the SE edge adjacent to the Lowry Peaks Fault (Figure 7.4, cross section C-D). Here up to 3 km. elevation difference between the basement-cover unconformity within the basin and the surrounding peaks may be inferred from cross sections and the gravity data. However, despite this difference in height, the basin fill appears to comprise only a comparatively thin veneer (< 0.5 km.) of Quaternary gravel. This inference is drawn from the observation of a number of gently dipping inliers which poke up through the Quaternary deposits within the basin (Figure 7.4).

A new model is now proposed to account for the Culverden Basin; a relatively shallow basin developed within a contractional tectonic regime. A thrust-fold sedimentary basin, associated with Quaternary deposits, will only form in a structural low (a syncline on the downthrown side of a fault), when the upper surface of the depression passes below the base level of sedimentation. Thrust-fold basins are likely to have short depositional histories, because as compression and uplift (both local and regional) continues, peripheral parts of the basin will move above the base level of sedimentation, and the area of deposition will be reduced.

The estimated structural relief (Figure 7.4, cross sections) in the Culverden Basin represents a combination of faulting and fault-related folding, and is comparable to similar structures in North Canterbury (Figure 7.5). Basin development is controlled by thrusting and genetically related folding and basin width appears to be controlled by the strike-normal distance between the major faults and the rate of relative subsidence. In North Canterbury numerous elongate basins and valleys (see Figure 2.10), with a Quaternary gravel fill, probably have a similar origin to the Culverden Basin. The Culverden Basin is large relative to the other thrust-fold basins because the intervening thrust-fold structure (between the NW and SE sides of the basin), is mainly below the base level of sedimentation (Figure 7.4, cross section C-D). However, parts of the Culverden Basin are already being exhumed, for example the Hawarden Anticline is propagating into, and locally uplifting, the southern end of the basin (Figure 7.4). If this model is correct, then the basin cannot be older than the thrusting and folding, which at its SW end is post-early Pleistocene (i.e. post 2 ma). The predominance of Quaternary basin fill and the absence of syn-depositional thickening of the late Tertiary cover units towards the basin (see main map in map pocket) support this conclusion. The depositional phase of the Culverden Basin

development will probably be short lived, and is unlikely to be more than 2-3 ma in total.

7.3.2 LATE CENOZOIC FINITE STRAIN

Finite strain was calculated using deformed late Cretaceous-early Pleistocene marker horizons in the cover sequence. These data were derived from numerous local (map pocket) and regional (Figure 7.5) cross sections, drawn perpendicular to the strike of the main faults and folds. The estimates of shortening represent minimum values, as no account has been taken of strain accommodated by thickening and thinning of the cover beds in association with folding. The estimates of folding on the footwalls of the major faults are likely to be conservative, and measurement errors are inferred to be +/- 2% shortening.

The amount of shortening across the mid-Waipara region varies from <2% (NE-SW along The Deans) to approximately 70% in parts of the MacDonald Syncline. Over the entire study area shortening has occurred in N-S and E-W directions at 12-17% and 5-12%, respectively. These local values are comparable to the estimates of 14 to 15% regional (North Canterbury) shortening measured from regional E-W and NW-SE orientated cross sections respectively (Figure 7.5 A and B). Of the strain measured at the surface in North Canterbury approximately 25% of the shortening can be directly attributed to faulting. Given that these estimates of total shortening represent minimum values, they appear to be comparable with the 20% shortening predicted by Norris (1979) for coastal North Canterbury. Fifteen percent shortening across North Canterbury, between the Hope Fault and the coast, implies that this

Figure 7.5. Regional cross sections drawn approximately normal to the structural grain between Okuku Pass and Motunau (A), and Hanmer and Motunau (B). The late Cretaceous basement-cover unconformity forms the lower-most marker horizon, the mid-Oligocene unconformity the middle marker and the Mio-Pliocene boundary the upper marker. Vertical equals horizontal scale.

Regional cross sections – North Canterbury

A: Okuku–Motunau

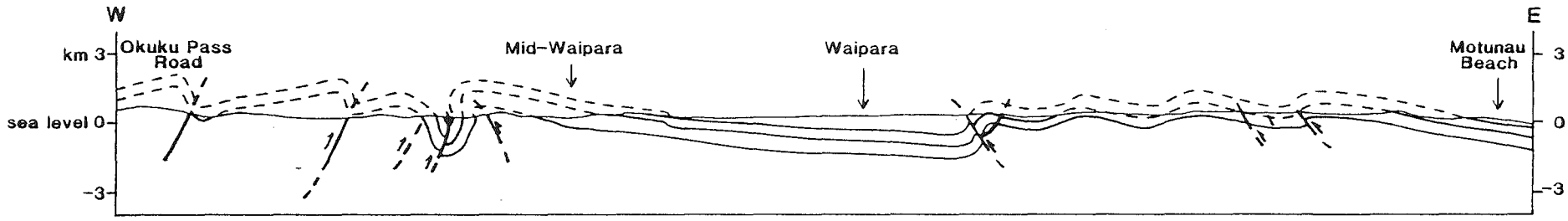

B: Hanmer–Motunau

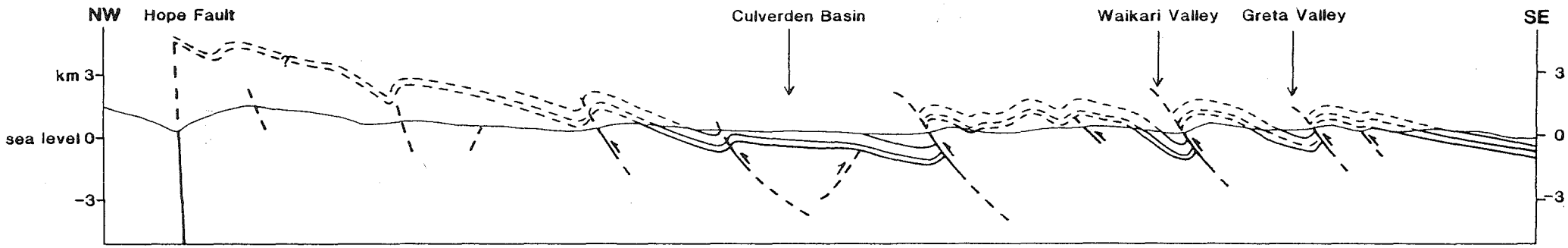

region has contracted by approximately 11 Km since the Pliocene in a NW-SE direction. The MacDonald Syncline, to the west of the Doctors Dome, has shortened by up to 2.5 km. over a distance of 2-3 km. In this case, where extreme shortening has taken place within the cover, paleogeographic reconstructions of the Cenozoic stratigraphy is of limited use, unless the post-depositional deformation is removed.

Most of the finite strain accommodated by the cover sequence has accumulated since the early Pleistocene. This is implied by the Pliocene to early Pleistocene age of the Kowai Formation (Wilson, 1963; Brown and Field, 1985). The Kowai Formation is the youngest unit in the sequence, and has been deformed conformably with the rest of the cover rocks. Given the inferred timing and amount of contraction, a minimum rate of shortening of 6 +/- 2 mm a^{-1} is calculated for the region between the Hope Fault and the coast, in a NW-SE direction, for the post-early Pleistocene period. This is comparable to the present strain rate inferred from geodetic triangulation networks in the same region (C. Pearson pers. comm., 1991).

The component of relative plate motion (Chase, 1978) normal to the plate boundary in North Canterbury is 27 +/- 7 mm a^{-1} (Figure 7.1). If the inferred minimum strain rate across North Canterbury since the Pleistocene is indicative of present strain rates in this region, then an additional 21 +/- 9 mm a^{-1} must be distributed across the Marlborough Fault System, Alpine Fault and areas to the NW. Similar values within the errors can also be derived using the deMets et al (1990) plate motion vector. These values serve to emphasise the significance of contractional deformation on the outer edge of the plate boundary zone in North Canterbury. Future plate boundary models for the northern South Island will need to consider the

style and magnitude of this deformation if they are to adequately account for North Canterbury geology.

ACKNOWLEDGMENTS

During the course of this thesis many people and several organisations have provided invaluable assistance. The project received funding from the University Grants Committee, while a field vehicle, purchased for the 'Neotectonics Programme', was funded by the Earthquake and War Damages Commission. I am grateful to my supervisors, Jocelyn Campbell and Jarg Pettinga for winning the funding necessary for this project and the establishment of the programme, suggesting a study area and initial topic, and smoothing the sometimes turbulent waters. In particular I wish to thank Jocelyn, both for her contribution to this project and to the authors geological education.

Don Wise, on sabbatical leave from the department of Geology and Geography at the University of Massachusetts, also contributed to my understanding of structural geology and in particular to the mapping and analysis of large numbers of small scale structures. Don provided computer programs to determine the orientations of the principal stress axes from minor faults, and to plot rose diagrams. Don and I have an ongoing cooperative project characterising basement deformation in the Doctors Dome.

Mapping and data collection were also undertaken with Hugh Cowan in the Mt Grey area. With the exception of limited fault and stress data this work is omitted here. Hugh is thanked for his involvement in many discussions on Canterbury and New Zealand geology, for reviewing (sometimes at short notice), parts of this thesis and providing the frontispiece photo. All technical staff from the University of Canterbury Geology Department are acknowledged for their assistance.

Fellow students, flatmates, friends and relatives have in many ways assisted during the course of this thesis, although neither they or I always realised it. Particular thanks to those friends who helped in the final stages, including Truus, Hugh, Ann, Todd, Kerri, Wendy and Lewis, and to those few people who managed to resist saying "have you finished yet?".

Lastly, and in many ways most importantly, I wish to thank Truus, my wife, for her continued support, encouragement and understanding throughout.

REFERENCES

Allis, R.G., 1981: Continental underthrusting beneath the Southern Alps of New Zealand. Geology 9, 303-307.

Andrews, P.B., 1963: Stratigraphic nomenclature of the Omihi and Waikari formations, North Canterbury. New Zealand Journal of Geology and Geophysics 6, 228-256.

Andrews, P.B., I.G. Speden and J.D. Bradshaw, 1976: Lithological and paleontological content of the Carboniferous-Jurassic Canterbury Suite, South Island, New Zealand. New Zealand Journal of Geology and Geophysics 19, 792-819.

Angelier, J., 1984: Tectonic analysis of fault data sets. Journal of Geophysical Research 89, 5835-5848.

Arabasz, W.J. and R. Robinson, 1976: Microseismicity and geological structure in the northern South Island, New Zealand. New Zealand Journal of Geology and Geophysics 19, 569-601.

Armijo, J.A., E. Carey and A. Cisternas, 1982: The inverse problem in microtectonics and the separation of tectonic phases. Tectonophysics 82, 145-160.

Arthaud, F., 1969: Methode de determination graphique des directions de raccourcissement d'allongement et intermediare d'une population de failles. Bull. Soc. geol. Fr. 11, 729-737.

Bahat, D., 1979: Theoretical considerations on mechanical parameters of joint surfaces based on studies on ceramics. Geological Magazine 116, 81-92.

Barrel, D., 1989: Geomorphic evolution and engineering geology studies at coastal Motunau, North Canterbury. Unpublished M.Sc. thesis, University of Canterbury, Christchurch, 221 p.

Berg, R.R., 1962: Mountain flank thrusting in the Rocky Mountain Foreland, Wyoming and Colorado. American Association of Petroleum Geologists Bulletin 46, 2019-2032.

Berryman, K.R., 1975: Earth Deformation Studies reconnaissance of the Alpine Fault.

New Zealand Geological Survey EDS Immediate Report 30a and 30b.

Berryman, K.R., H.N.C Cutten, D.L. Fellows and R.J. Sewell, 1986: Alpine Fault reconnaissance, Haast to Jerry River 12-20 March, 24-27 May 1986. New Zealand Geological Survey Report EDI 86/14.

Bibby, H.M., 1975: Crustal strain from triangulation in Marlborough, New Zealand. Tectonophysics 29, 529-540.

Bibby, H.M., 1976: Crustal strain across the Marlborough Faults, New Zealand. New Zealand Journal of Geology and Geophysics 19, 407-475.

Bibby, H.M., 1981: Geodetically determined strain across the southern end of the Tonga-Kermadec-Hikurangi Subduction Zone. Geophysical Journal of the Royal Astronomical Society 66, 513-533.

Bishop, D.G., J.D. Bradshaw and C.A. Landis, 1985: Provisional Terrane Map of South Island, New Zealand. In 'Tectonostratigraphic Terranes of the Circum-Pacific Region', edited by H.G. Howell. Circum-Pacific Council Energy Mineral Resources, Earth Science Service 1, 515-521.

Bott, M.H.P., 1959: The mechanics of oblique slip faulting. Geological Magazine 96, 109-117.

Boyer, S.E. and D. Elliott, 1982: Thrust Systems. American Association of Petroleum Geologists 66, 1196-1230.

Bradshaw, J.D., 1972: Stratigraphy and structure of the Torlesse Supergroup (Triassic-Jurassic) in the foothills of the Southern Alps near Hawarden (S60-61), Canterbury. New Zealand Journal of Geology and Geophysics 15, 71-87.

Bradshaw, J.D., 1973: Allochthonous fossil localities in melange within the Torlesse rocks of North Canterbury. Journal of the Royal Society of New Zealand 3, 161-167.

Bradshaw, J.D., 1975: The folds at Castle Hill (Canterbury) and their bearing on Kaikouran deformation style in the Canterbury Basin. Journal of the Royal Society of New Zealand 5, 209-217.

Browne, G.H. and B.D. Field, 1985: The lithostratigraphy of late Cretaceous to early Pleistocene rocks of North Canterbury, New Zealand. New Zealand Geological

Survey record 6.

Browne, G.H. and B.D. Field, 1988: A review of Cretaceous-Cenozoic sedimentation and tectonics, East Coast, South Island, New Zealand. In 'Sequences, stratigraphy sedimentology: surface and subsurface', edited by D.P James and D.A. Leckie. Canadian Society of Petroleum Geologists Memoir 15, 37-48.

Browne, G.H., 1987: In situ and intrusive sandstone in Amuri facies limestone at Te Kaukau Point, southeast Wairarapa, New Zealand. New Zealand Journal of Geology and Geophysics 30, 363-374.

Brown, W.G., 1988: Deformational style of Laramide uplifts in the Wyoming Foreland. In 'Interaction of the Rocky Mountain Foreland and the Cordilleran Thrust Belt', edited by C.J. Schmidt and W.J. Perry (Jr). Geological Society of America Memoir 171, 1-26.

Buchner, F., 1981: Rhinegraben: horizontal stylolites indicating stress regimes of earlier states of rifting. Tectonophysics 73, 113-118.

Burchfiel, B.C. and J.H. Stewart, 1966: 'Pull-apart' origin of the central segment of Death Valley, California. Bulletin of the Geological Society of America 77, 439-442.

Campbell, J.K., 1973: Displacement data from the Alpine Fault at Lake Rotoiti and its relevance to glacial chronology and the tempo of tectonism. Abstracts from the IXth INQUA Congress, Christchurch, 57-58.

Campbell, J.K. and H.M.k. Yousif, 1987: Tectonic Geomorphology of the Lower Waipara Gorge, North Canterbury. Geological Society of New Zealand Miscellaneous Publication 32b, 53-65.

Carter, R.M. and L. Carter, 1982: The Motunau Fault and other structures at the southern edge of the Australian/Pacific Plate Boundary, offshore Marlborough, New Zealand. Tectonophysics 88, 133-159.

Carter, R.M. and R.J. Norris, 1976: Cainozoic history of southern New Zealand; an accord between geological observations and plate tectonic predictions. Earth and Planetary Science Letters 31, 85-94.

Chase, C.G., 1978: Plate kinematics: the Americas, East Africa and the rest of the world. Earth and Planetary Science Letters 37, 353-368.

Chester, J.S., J.H. Spang and J.M. Logan, 1988: Comparison of thrust fault rock models to basement-cored folds in the Rocky Mountain Foreland. In 'Interaction of the Rocky Mountain Foreland and the Cordilleran Thrust Belt', edited by C.J. Schmidt and W.J. Perry (Jr). Geological Society of America Memoir 171, 1-26.

Choukroune, P., 1976: Strain patterns in the Pyrenean chain. Philosophical Transactions of the Royal Society A283, 271-280.

Cook, D.G., 1983: The northern Franklin Mountains, NW Territories Canada; a scale model of the Wyoming Province. In 'Rocky Mountain Foreland basins and uplifts', edited by J.D. lowell and R.R. Gries. Rocky Mountain Association of geologists, 315-338.

Cook, D.G., 1988: Balancing basement cored folds of the Rocky Mountain Foreland. In 'Interaction of the Rocky Mountain Foreland and the Cordilleran Thrust Belt', edited by C.J. Schmidt and W.J. Perry (Jr). Geological Society of America Memoir 171, 1-26.

Cooper, A.F., B.A. Barreiro, D.L. Kimborough and J.M. Mattinson, 1987: Lamprophyre dike intrusion and the age of the Alpine Fault, New Zealand. Geology 15, 941-944.

Cowan, H.A., 1990: Late Quaternary displacements on the Hope Fault at Glynn Wye, North Canterbury. New Zealand Journal of Geology and Geophysics 33, 285-293.

Coyle, S.A., 1988: The Porters Pass Fault. Unpublished M.Sc. thesis, University of Canterbury, Christchurch, 153 p.

Crowell, J.C., 1974: Origin of late Cenozoic basins in southern California. In 'Tectonics and Sedimentation', edited by W.R. Dickinson. Special Publication of the Society of Econ. Paleont. Miner, Tulsa, 22, 190-204.

Davis, G.A. and G.S. Lister, 1988: Detachment faulting in continental extension: perspectives from the southwestern U.S. Cordillera. Special paper of the Geological Society of America 218.

Davis, T.L., 1983: Late Cenozoic structure and tectonic history of the western "big bend" of the San Andreas fault and adjacent San Emigdio Mountains. Unpublished Ph.D dissertation, University of California, Santa Barbara, California, 579 p.

Davy, B.W. and F.J. Davey, 1985: Bounty Gravity Anomaly Map, Oceanic Series, 1:1

000 000 Wellington, New Zealand. Department of Scientific and Industrial Research.

deMets, C., R.G. Gordon, D.F. Argus and S. Stein, 1990: Current plate motions. Geophysical Journal International 101, 425-428.

Dibble, R.R., unpublished: Gravity data, with map and cross sections, from the Culverden Basin Area, North Canterbury, New Zealand.

Dunne, W.M. and C.P. North, 1990: Orthogonal fracture systems at the limits of thrusting: an example from southwestern Wales. Journal of Structural Geology 12, 207-215.

Engelder, T. and P. Geiser, 1980: On the use of regional joint sets as trajectories of paleostress fields during the development of the Appalachian Plateau, New York. Journal of Geophysical Research 85, 6319-6341.

Etchecopar, A., G. Vasseur and M. Daignieres, 1981: An inverse problem in microtectonics for the determination of stress tensors from striation analysis. Journal of Structural Geology 3, 51-65.

Fletcher, R.C. and D.D. Pollard, 1981: Anticrack model for pressure solution surfaces. Geology 9, 419-424.

Fleuty, M.J., 1964: The description of folds. Geological Association Proceedings 75, 461-489.

Freund, R., 1971: The Hope Fault: A strike-slip fault in New Zealand. New Zealand Geological Survey Bulletin 86.

Friedman, M., J. Handin, J.M. Logan, K.D. Min and D.W. Stearns, 1976: Experimental folding of rocks under confining pressure; Part III, faulted drape folds in multilithologic layered specimens. Bulletin of the Geological Society of America 87, 1049-1066.

Gephart, J.W. and D.W. Forsyth, 1984: An improved method for determining the regional stress tensor using earthquake focal mechanism data: application to the San Fernando earthquake sequence. Journal of Geophysical Research 89, 9305-9320.

Gregg, D.R., 1964: Sheet 18, Hurunui (1st edition). Geological map of New Zealand

1:250 000. Department of Scientific and Industrial Research, Wellington, New Zealand.

Haast, J. von, 1871: On the geology of the Waipara District, Canterbury, with geological map and sections. New Zealand Geological Survey reports of geological explorations during 1870-1871 6, 25-46.

Haman, P.J., 1961: Manual of the stereographic projection. West Canadian Research Publications, Calgary, series 1, No. 1.

Hancock, P.L., 1985: Brittle microtectonics: principles and practice. Journal of Structural Geology 7, 437-457.

Hancock, P.L., A. Alkadhi, A.A. Barka and T.G. Bevan, 1987: Aspects of analysing brittle structures. Annls Tectonicae 1, 5-19.

Hardcastle, K., 1989: Analysis of veins and faults along a cross section of the New England Appalachians: clues to the brittle history of an orogenic belt. Unpublished Ph.D dissertation, University of Massachusetts at Amherst, 242 p.

Harding, T.P., 1976: Tectonic significance and hydrocarbon consequences of sequential folding synchronous with San Andreas faulting Joaquin Valley, California. American Association of Petroleum Geologists Bulletin 60, 356-378.

Hector, J., 1887: (Weka Pass). New Zealand Geological Survey Report of Geological Explorations, 1886-87, xi-xiii.

Ivins, E.R., T.H. Dixon and M.P. Golombek, 1990: Extensional reactivation of an abandoned thrust: a bound on shallowing in the brittle regime. Journal of Structural Geology 12, 303-314.

Jaroszewski, W., 1972: Microscopic structural criteria of tectonics of non-orogenic areas: an example from the northeastern Mesozoic margin of the Swietokrzyski Mountains. Stud. Geol. Polon. 38, 1-215 (in Polish with English summary).

John, B.E., 1988: Structural reconstruction and zonation of a tilted mid-crustal magma chamber: the feldsic Chemehuevi Mountains plutonic suite. Geology 16, 613-617.

John, B.E. and S.B. Mukasa, 1990: Footwall rocks to the mid-Tertiary Chemehuevi

Detachment Fault: a window into the middle crust in the southern Cordillera. Journal of Geophysical Research 95, 463-485.

Kamp, P.J.J., 1986: The mid-Cenozoic Challenger Rift System of western New Zealand and its implications for the age of the Alpine Fault inception. Bulletin of the Geological Society of America 97, 255-281.

Laird, M.G., 1981: The Late Mesozoic fragmentation of the New Zealand segment of Gondwana. Fifth International Gondwana Symposium, Wellington, New Zealand, February, 1980, 311-318.

Lamb, S.H., 1988: Tectonic rotations about vertical axes during the last 4 ma in part of the New Zealand plate-boundary zone. Journal of Structural Geology 9, 877-891.

Lamb, S.H. and H.M. Bibby, 1989: The last 25 ma of rotational deformation in part of the New Zealand plate-boundary zone. Journal of Structural Geology 11, 473-492.

Lensen, G.J., 1962: Sheet 16, Kaikoura (1st edition). Geological Map of New Zealand 1:250 000. Department of Scientific and industrial Research, Wellington, New Zealand.

Lensen, G.J., 1975: Earth-deformation studies in New Zealand. In 'Recent crustal movements', edited by N. Pavroni and R. Green. Tectonophysics 29, 541-551.

Le Pichon, X, 1968: Sea-floor spreading and continental drift. Journal of Geophysical Research 73, 3661-3697.

Letouzey, J. and P. Tremolieres, 1980: Paleo-stress fields around the Mediterranean since the Mesozoic derived from microtectonics: comparison with plate tectonic data. Mem. Bur. Rech. Geol. Min. 115, 261-273.

Lewis, D.W., submitted: Tectonic implications of an unconformity: mid-Oligocene truncation of Amuri Limestone, Canterbury, New Zealand. Journal of Sedimentary Petrology.

Lewis, D.W., G.J. van der Lingen and D. Smale, 1979: A sandstone diapir cutting the Amuri Limestone, North Canterbury, New Zealand. New Zealand Journal of Geology and Geophysics 22, 295-305.

Lewis, D.W. and A.A. Ekdale, in prep: Composite Thalassinoides ichnofabric of a

mid-Tertiary unconformity Oligocene Amuri Limestone, Canterbury, New Zealand.

Lewis, K.B., D.J. Bennett, R.H. Herzer and C.C. von der Borch, 1985: Seismic stratigraphy and structure adjacent to an evolving plate boundary, Western Chatham Rise, New Zealand. Initial Reports of the Deep Sea Drilling Project XC, Washington.

Lisle, R.J., P. Styles and S.J. Freeth, 1990: Fold interference structures: the influence of layer competence contrast. Tectonophysics 172, 197-200.

Long, B.W. and V. Semeniuk, 1976: Dynamic metamorphism; processes and products in Devonian carbonate rocks, Canning Basin, Western Australia. Geological Society of Australia Special publication No. 6.

McCulloch, B.A., 1981: Geology of the Mount Brown beds. Unpublished M.Sc. thesis, University of Canterbury, Christchurch, 207 p.

McKay, A., 1887: On the Junction of the Amuri Limestone and Weka Pass Stone, Weka Pass, North Canterbury. Ibid. 1886-87, 18, 78-91.

Marshall, P., R. Speight and C.A. Cotton, 1911: The Younger Rock-series of New Zealand. Transactions of the New Zealand Institute 43, 378-407.

Maxwell, P.A., 1964: Structural geology and pre-Quaternary stratigraphy of the Kaiwara District. North Canterbury, New Zealand. Unpublished M.Sc. thesis, University of Canterbury, Christchurch, 223 p.

Molnar, P., T. Atwater, J. Mammerickx, and S.M. Smith, 1975: Magnetic anomalies, bathometry and the tectonic evolution of the South Pacific since the late Cretaceous. Geophysical Journal of the Royal Astronomical Society 40, 383-420.

Mount, V.S. and J. Suppe, 1987: State of stress near the San Andreas Fault: implications for wrench tectonics. Geology 15, 1143-1146.

Mumme, T.C., and R.I. Walcott, 1985: Paleomagnetic studies at Geophysics Division 1980-1983. Department of Scientific and Industrial Research, Geophysics Division Report 204.

Namson, J.S. and T.L. Davis, 1988: Seismically active fold and thrust belt in the San Joaquin Valley, central California. Bulletin of the Geological Society of America 100, 257-273.

New Zealand Geological Survey, 1972: South Island (1st edition) "Geological map of New Zealand 1:1 000 000". Department of Scientific and Industrial Research, Wellington, New Zealand.

Nicol, A. and J.K. Campbell, 1990: Late Cenozoic thrust tectonics, Picton, Marlborough Sounds, New Zealand. New Zealand Journal of Geology and Geophysics 33, 483-492.

Norris, R.J., 1979: A Geometric Study of finite strain and bending in the South Island. In 'Origin of the Southern Alps', edited by R.I. Walcott and M.M. Cresswell. Bulletin of the Royal Society of New Zealand 18, 21-28.

Norris, R.J., P.O. Koons and A.F. Cooper, 1990: The obliquely-convergent plate boundary in the South Island of New Zealand: implications for ancient collision zones. Journal of Structural Geology 12, 715-725.

Pettinga J.R. and D.U. Wise, in prep: Strain orientation adjacent to the Alpine Fault of New Zealand: fault analysis near Nelson, South Island.

Prebble, W.M., 1980: Late Cenozoic sedimentation and Tectonics of the east coast deformed belt in Marlborough, New Zealand. Special publication of the International Association of Sedimentologists 4, 217-228.

Price, N.J., 1966: Fault and Joint Development in Brittle and Semi-Brittle Rock. Pergamon Press, Oxford.

Ramsay, J.G., 1962: Interference patterns produced by the superposition of folds of "similar" type. Journal of Geology 60, 466-481.

Ramsay, J.G., 1967: Folding and Fracturing of Rocks. McGraw-Hill, New York.

Ramsay, J.G., 1974: Development of Chevron Folds. Bulletin of the Geological Society of America 85, 1741-1754.

Ramsay, J.G. and M.I. Huber, 1987: Techniques of Modern Structural Geology, Volume 2, Folds and Fractures. Academic Press, London.

Reches, Z., 1978: Development of monoclines: part I. Structure of the Palisades Creek branch of the East Kaibab monocline, Grand Canyon, Arizona. In 'Laramide

folding associated with basement block faulting in the Western United States', edited by V. Matthews (III). Geological Society of America Memoir 151, 235-273.

Reches, Z., 1987: Determination of the tectonic stress tensor from slip along faults that obey the coulomb yield condition. Tectonics 6, 849-861.

Reches, Z. and A.M. Johnson, 1978: Development of monoclines: part II. Theoretical analysis of monoclines. In 'Laramide folding associated with basement block faulting in the Western United States', edited by V. Matthews (III). Geological Society of America Memoir 151, 273-312.

Reilly, W.I., 1965: "Gravity map of New Zealand, 1:4 000 000, Bouguer Anomalies" (1st edition). Department of Scientific and industrial Research, Wellington, New Zealand.

Reilly, W.I., 1990: Horizontal crustal deformation on the Hikurangi Margin. New Zealand Journal of Geology and Geophysics 33, 393-400.

Reyners, M., 1987: Subcrustal earthquakes in the central South Island, New Zealand, and the root of the Southern Alps. Geology 15, 1168-1171.

Reyners, M., 1989: New Zealand Seismicity 1964-87: an interpretation. New Zealand Journal of Geology and Geophysics 32, 307-315.

Rynn, J.M.W. and C.H. Scholz, 1978: Seismotectonics of the Arthurs Pass Region, South Island, New Zealand. Bulletin of the Geological Society of America 89, 1373-1388.

Schofield, J.C., 1949: The Geology of the MacDonald Downs and Waikari Districts, North Canterbury. Unpublished M.Sc. thesis, University of Canterbury, Christchurch, 73 p.

Segall, P. and D.D. Pollard, 1983: Joint formation in granitic rock of the Sierra Nevada. Bulletin of the Geological Society of America 94, 563-575.

Sibson, R.H., 1985: A note on fault reactivation. Journal of Structural Geology 7, 751-754.

Sporli, K.B. and A.R. Lillie, 1974: Geology of the Torlesse Supergroup in the Northern Ben Ohau Range, Canterbury. New Zealand Journal of Geology and

Geophysics 17, 115-141.

Stauffer, M.R., 1964: The geometry of conical folds. New Zealand Journal of Geology and Geophysics 7, 340-347.

Stauffer, M.R., 1988: Fold interference structures and coaptation folds. Tectonophysics 149, 339-343.

Stearns, D.W., 1971: Mechanisms of drape folding in the Wyoming province. Wyoming Geol. Assoc. 23rd Annual Field Conference, Wyoming Tectonics Symposium Guidebook, 125-143.

Stearns, D.W., 1978: Faulting and forced folding in the Rocky Mountain Foreland. In 'Laramide folding associated with basement block faulting in the Western United States', edited by V. Matthews (III). Geological Society of America Memoir 151, 1-37.

Stein, R.S. and G.C.P. King, 1984: Seismic potential revealed by surface folding: 1983 Coalinga, California, Earthquake. Science 224, 869-872.

Stock, J. and P. Molnar, 1982: Uncertainties in the relative positions of Australia, Antarctica, Lord Howe and Pacific plates since the late Cretaceous. Journal of Geophysical Research 87, 4679-4714.

Suppe, J., 1983: Geometry and kinematics of fault-bending. American Journal of Science 283, 684-721.

Suppe, J., 1985: Principals of Structural Geology. Prentice-Hall, New Jersey. 537 p.

Sykes, L.R., 1978: Interplate seismicity, reactivation of pre-existing zones of weakness, alkaline magmatism, and other tectonism post-dating continental fragmentation. Rev. Geophys. & Space Phys. 16, 621-687.

Systra, YU.I., and N.I. Skornyakova, 1980: Conical folds in ancient complexly-folded metamorphic formations in northern Karelia. Geotectonics 14, 17-25.

Thiessen, R., 1986: Two-dimensional refold interference patterns. Journal of Structural Geology 8, 563-573.

Thiessen, R.L. and W.D. Means, 1980: Classification of fold interference patterns:

a reexamination. Journal of Structural Geology 2, 311-316.

Thomson, J.A., 1920: The Notocene geology of the middle Waipara and Weka Pass district, North Canterbury, New Zealand. Transactions of the New Zealand Institute 52, 322-415.

Turner, F.J. and L.E. Weiss, 1963: Structural Analysis of Metamorphic Tectonites. McGraw-Hill, New York.

van Dissen, R.J., 1987: Late Quaternary faulting in the Kaikoura region, southern Marlborough, New Zealand. Geological Society of New Zealand Miscellaneous Publication No. 32b.

Walcott, R.I., 1978: Present tectonics and late Cenozoic evolution of New Zealand. Geophysical Journal of the Royal Astronomical Society 52, 137-164.

Walcott, R.I., 1979: Plate motion and shear strain rates in the vicinity of the Southern Alps. In 'The origin of the Southern Alps', edited by R.I.Walcott and M.M.Cresswell. Royal Society of New Zealand Bulletin 18, 5-12.

Walcott, R.I., 1984: Reconstructions of the New Zealand region for the Neogene. Paleogeography Paleoclimatology Paleoecology 46, 217-231.

Walcott, R.I., 1987: Geodetic strain and the deformational history of the North Island during the late Cenozoic. Philosophical Transactions of the Royal Society of London A321, 163-181.

Webb, B.C. and D.J.D. Lawrence, 1986: Conical fold terminations in the Bannisdale Slates of the English Lake District. Journal of Structural Geology 8, 79-86.

Wellman, H.W., 1953: Data for the study of Recent and late Pleistocene faulting in the South Island of New Zealand. New Zealand Journal of Science and Technology B34, 270-288.

Wellman, H.W., 1979: An uplift map of the South Island of New Zealand, and a model for uplift of the Southern Alps. In 'Origin of the Southern Alps', edited by R.I. Walcott and M.M. Cresswell. Bulletin of the Royal Society of New Zealand 18, 13-20.

Wentworth, C.M., A.W. Walter, J.A. Bartow and M.D. Zoback, 1983: Evidence on the tectonic setting of the 1983 Coalinga earthquakes from deep reflection profiles

across the southeastern end of Kettleman Hills in the 1983 Coalinga, California, earthquake. In 'The 1983 Coalinga, California, earthquake', editors J.H. Bennett and R.W. Sherburne. California Division of Mines and Geology Special Publication 66, 293-306.

Wilcox, R.E., T.P.Harding and D.R. Seely, 1973: Basic wrench tectonics. American Association of Petroleum Geologists Bulletin 57, 74-96.

Wilson, D.D., 1963: The Geology of the Waipara Subdivision. New Zealand Geological Survey Bulletin 64.

Wilson, G., 1967: The geometry of cylindrical and conical folds. Proceedings of the Geological Association 78, 179-209.

Wilson, G.J., 1984: Two new dinoflagellates from the late Jurassic of North Canterbury, New Zealand. Journal of the Royal Society of New Zealand 14, 215-221.

Wise, D.U. in prep.: Rose plots: thorns among geology's weeds. Submitted to Geology 22.2.90.

Wise, D.U., J.R. Pettinga, J.K. Campbell and A. Nicol, in prep: A surface slab model for the Transfer Zone of New Zealand's Alpine Fault.

Yeats, R.S., 1987a: Active faults related to folding. In, 'Active Tectonics', National academic Press, 63-79.

Yeats, R.S., 1987b: Coseismic folding. In, 'Active Tectonics', National academic Press, 163-172.

Yeats, R.S. and K.R. Berryman, 1987: South Island, New Zealand, and Transverse Ranges, California: A seismotectonic comparison. Tectonics 6, 363-376.

Yousif, H.M.S., 1987: The applications of remote sensing to geomorphological neotectonic mapping in North Canterbury. Unpublished Ph.D thesis, University of Canterbury, 410p.

Zoback, M.D., M. Zoback, V.S. Mount, J. Suppe, J.P. Eaton, J.H. Healy, D. Oppenheimer, P.Reasenberg, L. Jones, C.B. Raleigh, I.G. Wong, O. Scotti and C. Wentworth, 1987: New Evidence on the state of stress of the San Andreas Fault System. Science 238, 1105-1110.

APPENDICES

APPENDIX 1A: LOCATION MAP.

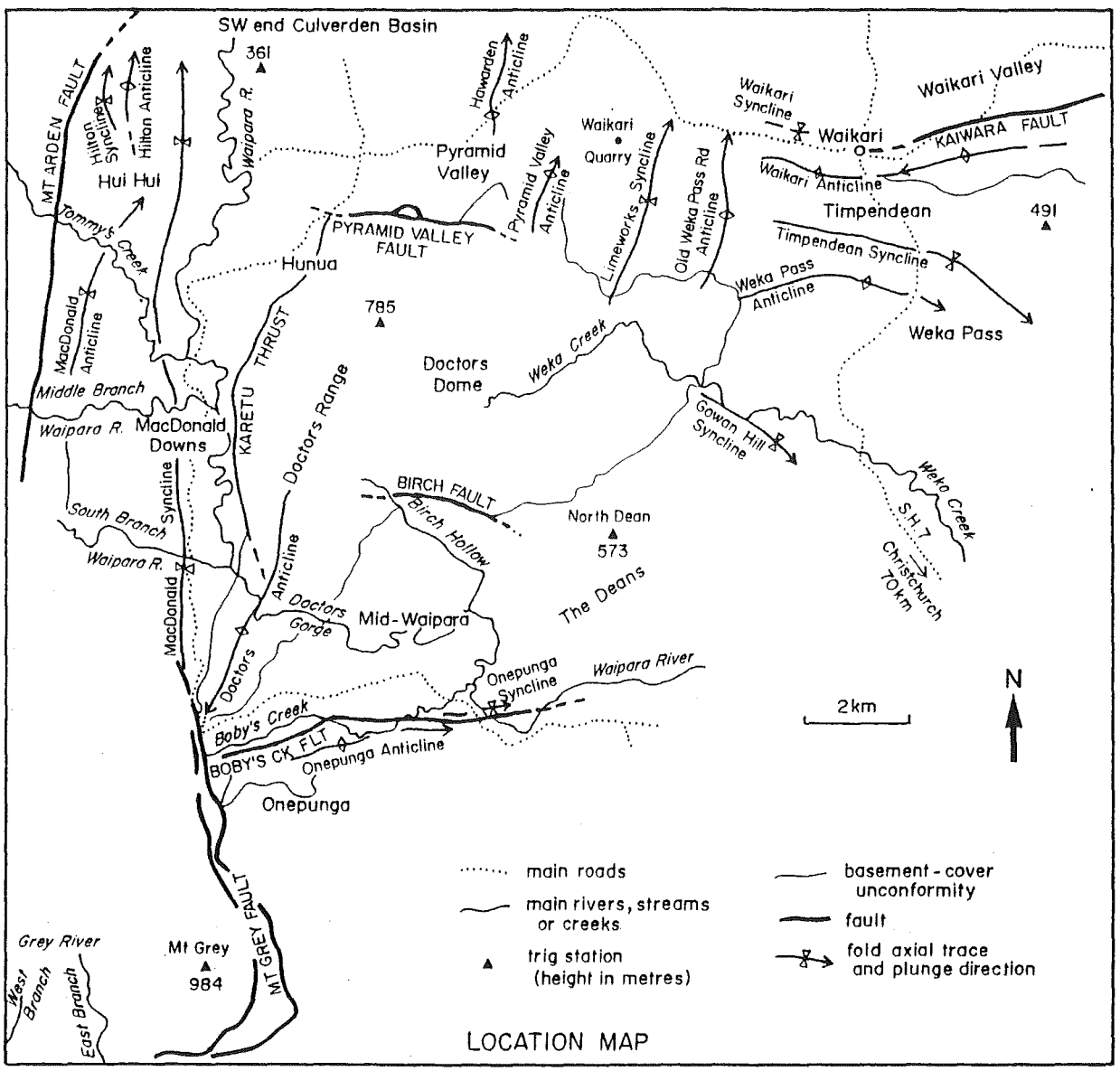

Figure 8.1. Locations of key geological, cultural and topographic features within the study area. Refer to main map (map pocket) for more topographic information.

APPENDIX 1B: LITHOLOGICAL UNIT DISTRIBUTIONS

This is a compilation of distribution data for the main lithological units in the area of study. The stratigraphic column (section 1.2) should be referred to for unit descriptions, ages and contact relationships. Data presented below were derived from field mapping. Unit thickness estimates are derived from the geological map (calculated by removing the effects of bedding dip) or directly from the cross sections (map pocket). Between 5 and 13 thickness estimates for each unit provide the data for the average and range values.

Unit: **Broken River Formation.**
Lateral Extent: lenses out N and E of Weka Pass.
Thickness: range; 0-240 m. average; 60 m.
Best Stratigraphic Sections: Boby's Creek, Birch Hollow.

Unit: **Conway Formation.**
Lateral Extent: thins east of Weka Pass.
Thickness: range; 0-500 m. average; 230 m.
Best Stratigraphic Sections: Birch Hollow, mid-Waipara.

Unit: **Loburn Formation.**
Lateral Extent: locally extensive.
Thickness: range; 30-80 m. average; 50 m.
Best Stratigraphic Sections: South Branch (Waipara), Mid-Waipara.

Unit: **Waipara Greensand Formation.**
Lateral Extent: locally extensive.
Thickness: range; 95-280 m. average; 185 m.
Best Stratigraphic Sections: South Branch, Mid-Waipara.

Unit: **Ashley Mudstone Formation.**
Lateral Extent: locally extensive.
Thickness: range; 30-190 m. average; 65 m.
Best Stratigraphic Section: Mid-Waipara.

Unit: **Homebush Sandstone Formation.**
Lateral Extent: thins to the N locally.
Thickness: range; 25-100 m. average; 70 m.
Best Stratigraphic Section: South Branch.

Unit: **Karetu Sandstone Formation.**
Lateral Extent: thins to the N and E of the South Branch.
Thickness: 25 m. (of limited extent).
Best Stratigraphic Sections: South Branch, Branches of the Grey River.

Unit: **Amuri Limestone Formation.**
Lateral Extent: regional; Waitaki River to East Coast North Island. Locally lenses out South of Mt. Grey.
Thickness: range; 0-30 m. average; 8 m.
Best Stratigraphic Sections: Weka Creek, Mid-Waipara.

Unit: **Weka Pass Stone Member (Omihi Formation).**
Lateral Extent: locally extensive thins to the N and S from study area.
Thickness: range; 10-110 m. average; 50 m.
Best Stratigraphic Sections: Weka Creek, Mid-Waipara.

Unit: **Waikari Formation.**
Lateral Extent: locally continuous and extensive.
Thickness: range; 140-270 m. average; 170 m.
Best Stratigraphic Sections: Mid-Waipara, Boby's Creek.

Unit: **Mt. Brown Formation.**
Lateral Extent: locally extensive, regionally thins to the NE.
Thickness: range; 30-220 m. average; 105 m.
Best Stratigraphic Section: Weka Creek.

Unit: **Kowai Formation.**
Lateral Extent: locally extensive, regionally thins to the NE and E.
Thickness:range; 20-730 m. (This is the uppermost unit is sequence and thickness estimates represent minimum values.)
Best Stratigraphic Section: Tommy's Creek.

APPENDIX 1C: COAL DATA

Ten coal samples, 6 from the late Cretaceous Broken River Formation and 4 from the Pliocene-early Pleistocene Kowai Formation (see Stratigraphic column) were analysed using proximate (performed by the Coal Research Association of New Zealand, CRA), and vitrinite reflectance analyses (carried out by Dr J. Newman). All proximate analyses have an air dried basis. The results are presented below.

BROKEN RIVER FORMATION COAL

Broken River Formation coal is preserved in seams ranging up to 0.5m thick. The coal is commonly weathered and often sheared, particularly within the MacDonald Syncline. These coals are mainly of sub-bituminous rank (using the ASTM classification), which is higher than the lignite ranks suggested by Browne and Field (1985). Intense shearing and subsequent weathering may have influenced these earlier rank estimates.

Table 8.1. Broken River Formation CRA Proximate Analyses.
Sample Numbers correspond to CRA References 45/195 - 45/198, 45/205 and 45/206.

SAMPLE NO	CN101	CN102	CN103	CN104	CN111	CN112
Moisture %	15.2	17.4	16.5	15.8	15.8	12.3
Ash %	12.1	15.4	19.6	15.6	8.0	22.7
VM %	36.1	32.6	30.8	33.4	41.1	35.8
FC %	36.6	34.6	33.1	35.2	35.1	29.2
CV MJ/kg	20.52	15.91	15.88	18.01	20.61	18.36
Btu/lb	8,820	6,840	6,830	7,740	8,860	7,890
Sulphur %	6.30	5.97	6.62	5.44	3.80	3.74

VM = Volatile Matter
FC = Fixed Carbon
CV = Calorific Value

Vitrinite reflectance analysis performed on 3 samples (CN102, 111 & 112) produced average Ro values of 0.37% (+/- 0.07%).

KOWAI FORMATION COAL

The Kowai Formation contains isolated horizons of carbonaceous material, mostly less than 10 cm. thick, and coalified logs. Vitrinite reflectance data implies that this material is mostly peat, while the proximate analyses (as applied to the ASTM classification) imply lignite ranks.

Table 8.2. Kowai Formation CRA Proximate Analyses.
Sample Numbers correspond to CRA References 45/199, 45/202, 45/203 and 45/204.

SAMPLE NO.	CN105	CN108	CN109	CN110
Moisture %	19.0	15.7	18.7	13.4
Ash %	13.1	6.3	7.4	31.0
VM %	40.4	45.4	43.9	33.1
FC %	27.5	32.6	30.0	22.5
CV MJ/kg	14.99	18.48	15.65	12.32
Btu/lb	6,440	7,940	6,730	5,300
Sulphur %	1.40	2.46	0.62	2.10

VM = Volatile Matter
FC = Fixed Carbon
CV = Calorific Value

Vitrinite reflectance analysis carried out on 2 samples (CN108 & CN109), produced Ro values of 0.23 and 0.28%.

APPENDIX 2A: DESCRIPTION OF THE MACROSCOPIC FAULTS

Data are from this study except where indicated. See figure 8.1 for locations.

Name: **Birch Fault** (Wilson, 1963).
Location: Mid-Waipara Area.
Best Exposure: Birch Hollow Stream.
Lateral Extent: 4 km.
Fault Zone: 10-20 m. of fracturing and shearing, with thin (< 5 cm. pug zone).
Orientation:90-110/75N-80S.
Type: normal Fault at lower structural levels, reverse at higher levels.
Movement: 150m.(+) upthrown on the north side.
Comments: reactivated late Cretaceous fault, with possible recent trace (Wilson, 1963).

Name: **Boby's Creek Fault** (Wilson, 1963).
Location: Mid-Waipara - Boby's Creek.
Best Exposure: Boby's Creek.
Lateral Extent: 8 km.(+).
Fault Zone: 0.5 m. brecciation bound on south side by 1-3 cm. pug zone.
Orientation: 65-95/70N-55S.
Type: oblique-normal fault.
Movement: 200 m. vertical displacement, upthrown to the S.
Comments: reactivated late Cretaceous fault.

Name: **Kaiwara Fault** (Gregg, 1964).
Location: Waikari (fault zone not exposed in study area).
Lateral Extent: 45 km.
Orientation: 20-95/40-80 (?)S.
Type: thrust (Dibble, unpublished; Maxwell, 1964).
Movement: estimated 500 m. vertical displacement (near Waikari), upthrown to the S.
Comments: a regional fault extending from waikari to Mt Ellen along the SE side of the Waikari Valley.

Name: **Karetu Thrust** (this study; Karetu Fault of Wilson, 1963)
Location: MacDonald Downs Area.
Best Exposure: creeks on western side of the Doctors Range near MacDonald Downs.
Lateral Extent: 13 km.
Fault Zone: 10-30 m. zone (in total) of intense fracturing and shearing in basement and cover units. Fault well defined by planar 1-3 cm. pug zone.
Orientation: 325-25/35-50E.
Type: thrust.
Movement: estimated 300 m., upthrown to the E.

Comments: range-front fault thrusts Torlesse over late Cretaceous to Miocene cover rocks.

Name: **Mt. Arden Fault** (this study).
Location: MacDonald Downs Area.
Best Exposure: Middle Branch Waipara River (poorly exposed).
Lateral Extent: 12 km.(+)
Orientation: 185-210/55-80W.
Type: reverse fault and thrust.
Movement: upthrown to the west.
Comments: range-front fault thrusts basement over cover rocks, particularly at northern end of trace.

Name: **Grey Fault** (Wilson 1963).
Location: Mt. Grey to Boby's Creek.
Best Exposures: Creeks on western side of Onepunga.
Lateral Extent: 9 km.(+).
Fault Zone: 10-30 m. brecciation, fracturing and shearing straddling 1-2 m. pug zone.
Orientation: 145-175/30-75W.
Type: reverse fault (with small left lateral component) to thrust.
Movement: upthrown to the W.
Comments: range-front fault with recent trace.

Name: **Pyramid Valley Fault** (this study).
Location: Pyramid Valley.
Best Exposure: poorly exposed.
Lateral Extent: 7 km.(+).
Fault Zone: fault zone not observed directly, although basement red cherts 10-30 m. above the fault are extensively fractured and faulted.
Orientation: 95/75-90N(?).
Type: normal right lateral (?) fault.
Movement: upthrown to the south.
Comments: range-front fault, reactivated (?) late Cretaceous fault.

APPENDIX 2B: STRESS TENSOR ANALYSIS

This appendix describes the technique used to determine local stress tensors from minor faults where the fault orientation, motion direction and sense could be determined. The stress tensor data are presented in figures 2.3 and 2.6 for several areas within basement and cover rocks respectively. Composite stress tensor nets representing most of the tensors derived from basement and all of the tensors derived from the cover faults are presented in figure 2.4.

During the last decade a number of methods for determining the stress tensor from inversion of fault data have been developed (Armijo et al, 1982; Angelier, 1984; Etchecopar et al, 1981; Reches, 1987). These techniques seek the best stress tensors for a given population of faults, in part by determining which are the "erratic" members of the main population and removing these for separate analysis. If several populations of approximately equal size are present in the data set, the attempt to find the main population by averaging or by least squares methods has obvious disadvantages.

An alternative method was developed for earthquake focal mechanisms by Gephart and Forsyth (1984) by using a grid search for all possible stress tensors. The search determines which faults would move under certain tensor orientations. The fault analysis presented here uses that philosophy in a computer program written by Hardcastle (1989) and M.S.Hills in conjunction with the Brittle Fracture Analysis Group at the University of Massachusetts.

The program performs a grid search of all possible stress combinations for each fault by moving the maximum compression axis (sigma 1) across an equal area net in approximately 10 degree increments. At each grid location, sigma 2 and sigma 3 is revolved about sigma 1 in 10 degree increments. In this way all possible stress orientations (approximately 5000) are considered for each fault in the data set. For each, a range of coefficients of friction and fluid pressure is examined using Bott's (1959) techniques to determine; (a) if a fault of that orientation would move under those conditions, and (b) what the motion vector would be. If this predicted motion vector lies within some given angle (here 25 degrees) of the slickenside striations orientations actually measured on that surface, the fault is recorded as having possible motion with that stress tensor. These selected faults are weighted for output of results by three levels of certainty recorded in the field from the reliability of motion sense indicators. Finally contours are drawn on each of three equal area nets (sigma 1,2 and 3, Figure 2.3, 2.4 and 2.6), surrounding those areas in which a stress axis could have been located for a given percentage of the total fault population to have moved. If "erratic" members of the population are present or several populations are included, these will appear either on the fringes of the plot or as separate clusters. Thus, the plots represent a weighted, separate treatment of each fault and its motion with minimal assumptions as to the distribution and nature of the total population.

APPENDIX 3A: DESCRIPTIONS OF THE MAIN MACROSCOPIC FOLDS.

Data derived from this study (see Figure 8.1 for locations).

Name: **Doctors Anticline.**
Axial Trace Length: 11 km.
Orientation: 163-210/5-18.
Shape: angular to sub-angular and open (interlimb = 80^0), with average limb dips of 22 and 75^0. An asymmetric fold with westward vergence.
Wavelength: 4-20 km.
Amplitude: 1 km.
Comments: forms the N-NNE component of the Doctors Dome fold interference structure. Closely associated with the Karetu Thrust.

Name: **Limeworks Syncline.**
Axial Trace Length: 4 km. (+).
Orientation: 025/15.
Shape: angular to sub-angular and gentle (interlimb = 140^0), with common limb dips of $10\text{-}20^0$.
Wavelength: 3.5 km.
Amplitude: 0.05-0.10 km.
Comments: contains several smaller scale folds, with wavelengths of 0.2-0.4 km.

Name: **MacDonald Anticline.**
Axial Trace Length: 7 km. (+).
Orientation: 348-10/5-45 (also plunges S).
Shape: angular to sub-angular, open to gentle (interlimbs = $110\text{-}13^0$), with limb dips of $20\text{-}55^0$.
Wavelength: 1.0-3.7 km.
Amplitude: 0.14-0.33 km.
Comments: immediately west of the MacDonald Syncline.

Name: **MacDonald Syncline.**
Axial Trace Length: 13.5 km. (+).
Orientation: 342-16/0-30 (also plunges S).
Shape: angular, mainly tight to close (interlimbs = $25\text{-}60^0$), with limb dips of $60\text{-}70^0$(overturned).
Wavelength: 2-6 km. (average 3.2 km.).
Amplitude: 0.21-1.61 km. (average 0.84 km.).
Comments: varies in morphology along the hinge line.

Name: **Old Weka Pass Road Anticline.**
Axial Trace Length: 3.5 Km. (+).
Orientation: 360/14

Shape: angular and gentle (interlimb = 130), with limb dips of 18-28^0.
Wavelength: 3.8 km.
Amplitude: 0.22 km.
Comments: terminates abruptly to the south.

Name: **Onepunga Anticline.**
Axial Trace Length: 5 km.
Orientation: 55-95/0-12.
Shape: angular and open (interlimb = 85^0), with limb dips of 8-70^0). Asymmetric with northward vergence.
Wavelength: 2-4 km.
Amplitude: 0.325 km.
Comments: closely associated with the Boby's Creek Fault.

Name: **Onepunga Syncline.**
Axial Trace Length: 4 km.
Orientation: 70-95/5-15 (also plunges W).
Shape: angular and gentle (interlimb = 125^0), with limb dips of 18-45^0.
Wavelength: 2-4 km.
Amplitude: 0.325 km.
Comments: closely associated with the Boby's Creek Fault.

Name: **Hawarden Anticline.**
Axial Trace Length: 12 km (+).
Orientation: 350-360/5-15.
Shape: sub-angular and gentle (interlimb = 125^0), with limb dips of 15-45^0.
Wavelength: 4.0-6.0 km.
Amplitude: 0.35 km.
Comments: plunges into the Culverden Basin (see also Figure 7.4).

Name: **Timpendean Syncline.**
Axial Trace Length: 7 km.
Orientation: 85-126/0-15 (also plunges W).
Shape: angular, open to gentle (interlimbs = 110-160^0), with limb dips of 12-28^0.
Wavelength: 0.5-3.2 km.
Amplitude: 0.1-0.18 km
Comments: varies in morphology along the hinge line.

Name: **Waikari Anticline.**
Axial Trace Length: 8 km.
Orientation: 255-285/0-13 (also plunges E).
Shape: sub-angular, open to gentle (interlimbs = 110-130^0), with limb dips of 10-40^0. Asymmetric with vergence to the north.
Wavelength: 2.2 km.
Amplitude: 0.12 km.
Comments: closely associated with the Kaiwara Fault.

Name: **Weka Pass Anticline.**
Axial Trace Length: 4 km.
Orientation: 65-107/10-18.
Shape: angular and gentle (interlimb = 125), with limb dips of 15-25^0.
Wavelength: 2.3-4.3 km.
Amplitude: 0.05-0.19 km.
Comments: axial trace difficult to locate east of State Highway 7.

APPENDIX 3B: STRUCTURE CONTOUR MAP OF THE HUI HUI AREA.

Structure contour maps have been constructed on the base or top of well defined lithological units for three areas (Figures 3.3, 3.4 and this figure (8.2), using a geological map, metric 1:25000 topoplots and an altimeter. The altimeter provided extra height information used to confirm the location of the topoplot topographic contours and give additional altitude control on the contoured surface.

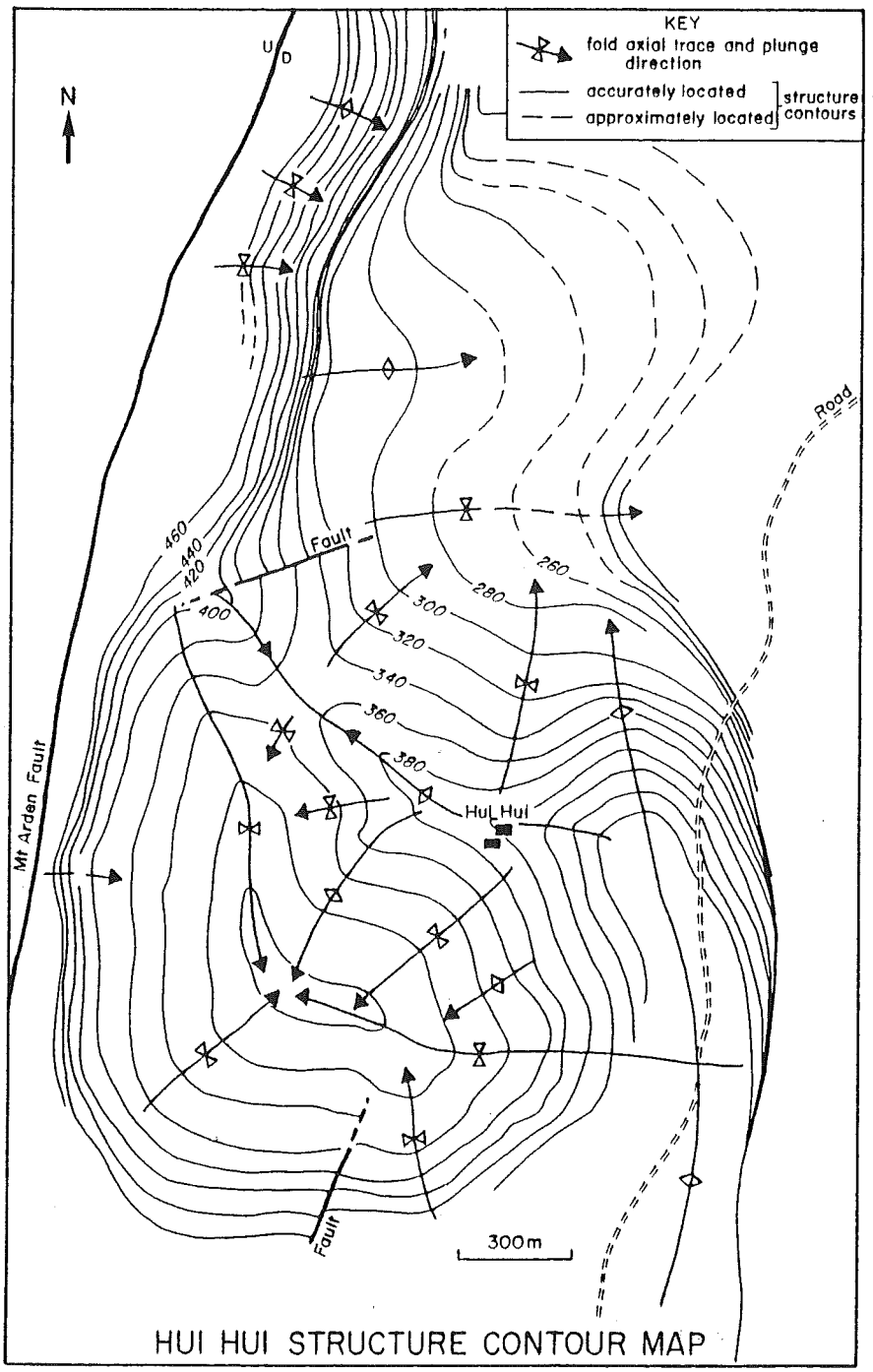

Figure 8.2. Structure contour map of the Hui Hui area. Contours are drawn on the base of the basal limestone within the Mt. Brown Formation. Supplementary to figures 3.3 and 3.4.

Figure 8.3. The 10 folds represented in this diagram represent macroscopic fold data not presented elsewhere in the main body of the text or in the appendices. These are lower hemisphere equal area plots of poles to bedding and are supplementary to chapter 4. These fold geometries are either not well defined (A,E,F,I and J) or too few data measurements were collected to be confident about the fold shape (B,C,G and H). These results reflect areas where the folds were not well enough exposed to define the fold geometries and data from the entire fold had to be lumped together to increase the size of the data set. In doing this local complexities in the fold surface geometry are not well defined and contribute to the spread of the data. Folds C,F,G,H,I and J may well be conical, while B,E and G appear to be approximately cylindrical.

APPENDIX 3C: FOLD SURFACE GEOMETRIES.

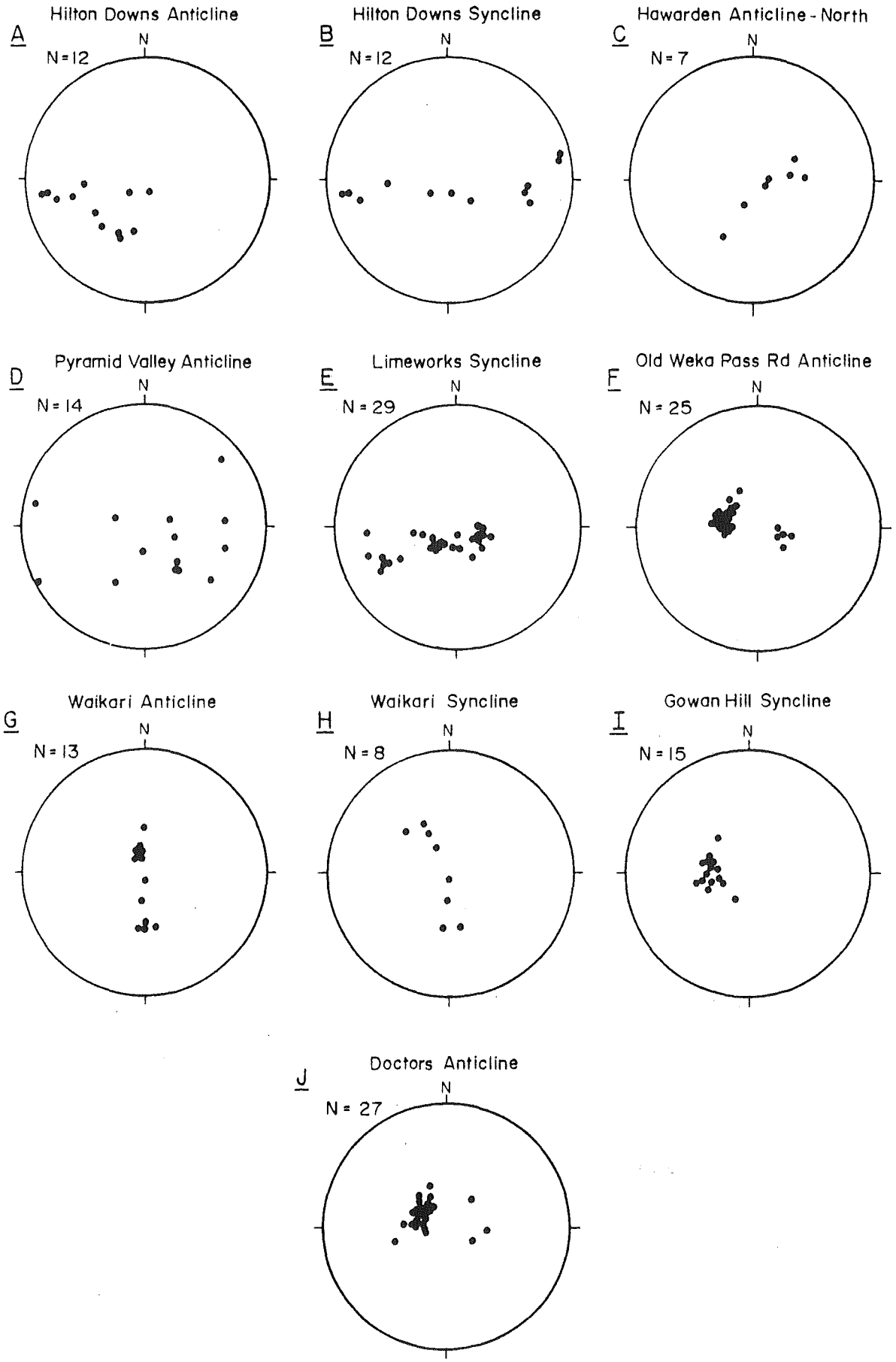

APPENDIX 3D: VARIATIONS IN FOLD CROSS SECTIONAL SHAPE.

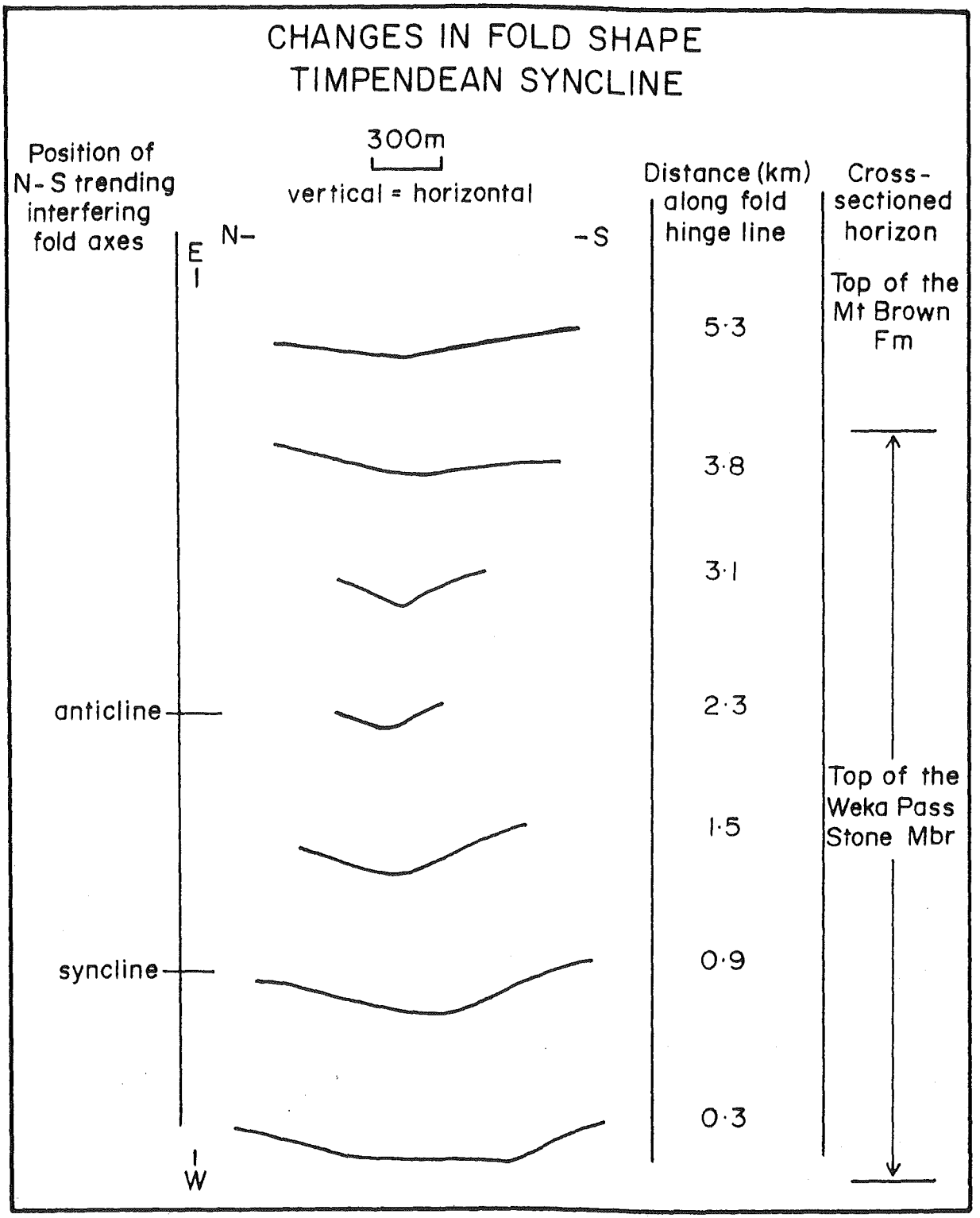

Figure 8.4. Variations in the cross sectional shape of the Timpendean Syncline along the fold hinge line. Supplementary to figure 3.8.

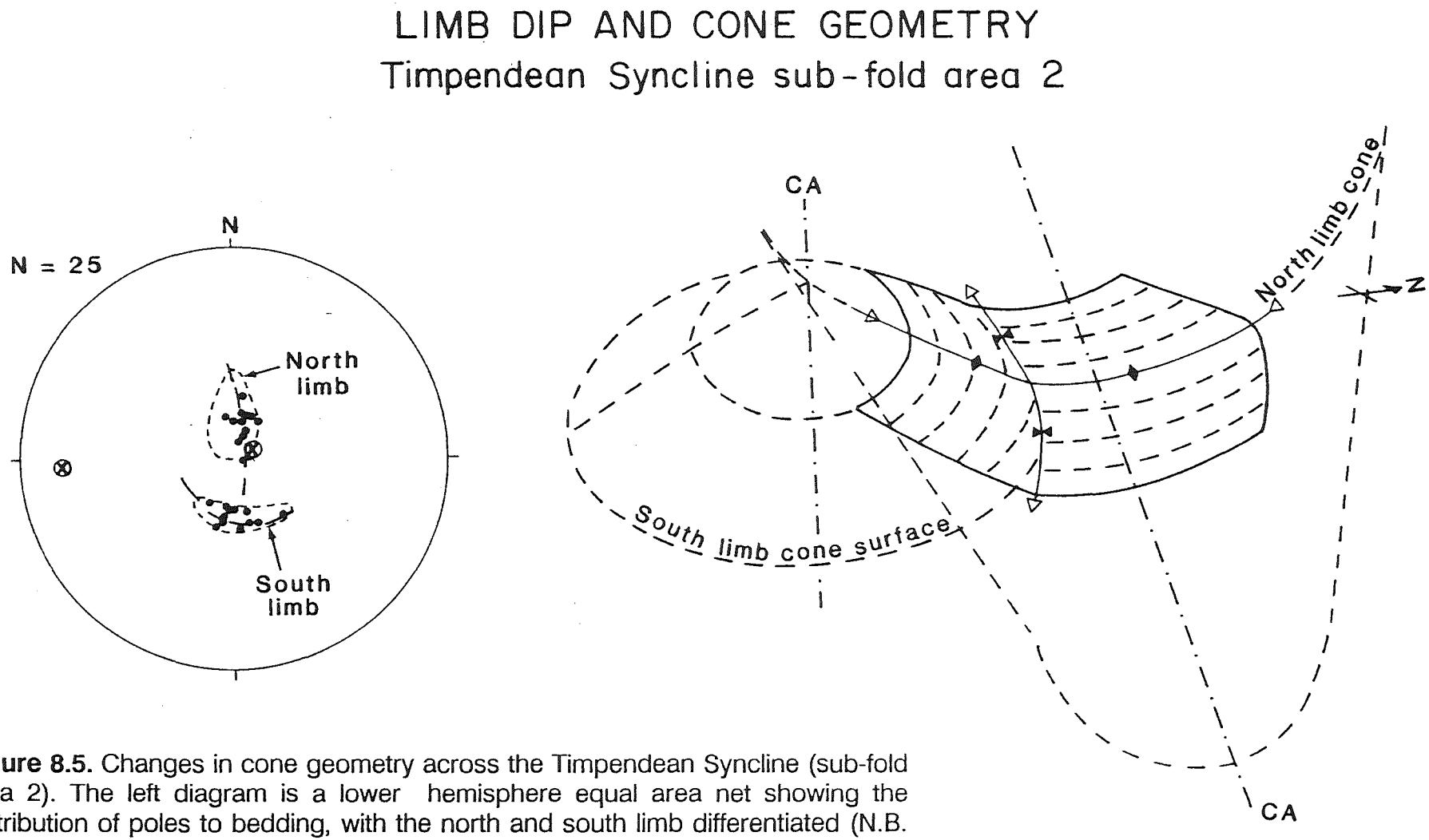

Figure 8.5. Changes in cone geometry across the Timpendean Syncline (sub-fold area 2). The left diagram is a lower hemisphere equal area net showing the distribution of poles to bedding, with the north and south limb differentiated (N.B. the cross enclosed by a circle symbol represents the position of the cone axis for each limb). The right diagram is three dimensional and shows the respective geometries and relationships of the cones on each limb. Supplementary to figure 4.4.

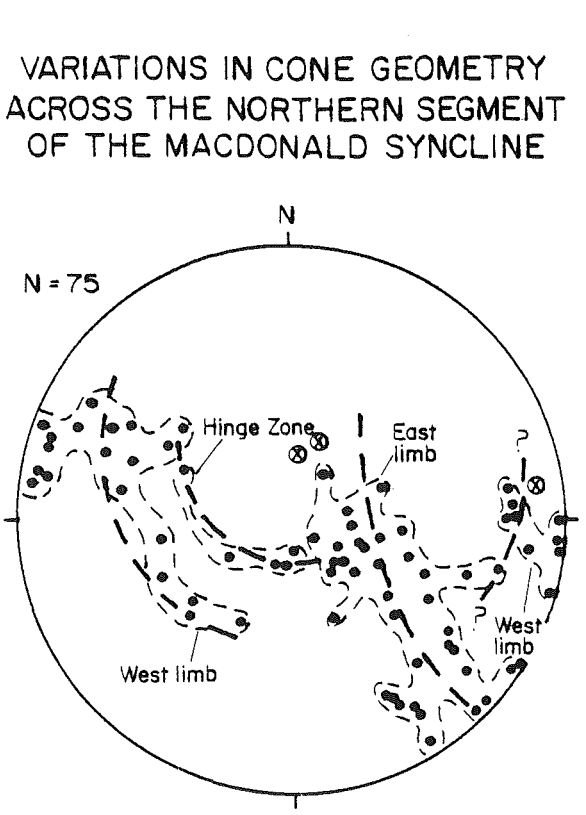

Figure 8.6. Changes in cone geometry across the northern end of the MacDonald Syncline. The changes in geometry across this fold may be more complicated than indicated. While the hinge zone and east limb fold geometries are reasonably well defined by their small circles, the near vertical dips on the west limb are not compatible with the small circle (cone) geometry for that limb. The geometry of the west limb is relatively complex and cannot be accurately defined by a single small circle. Supplementary to figure 4.4.

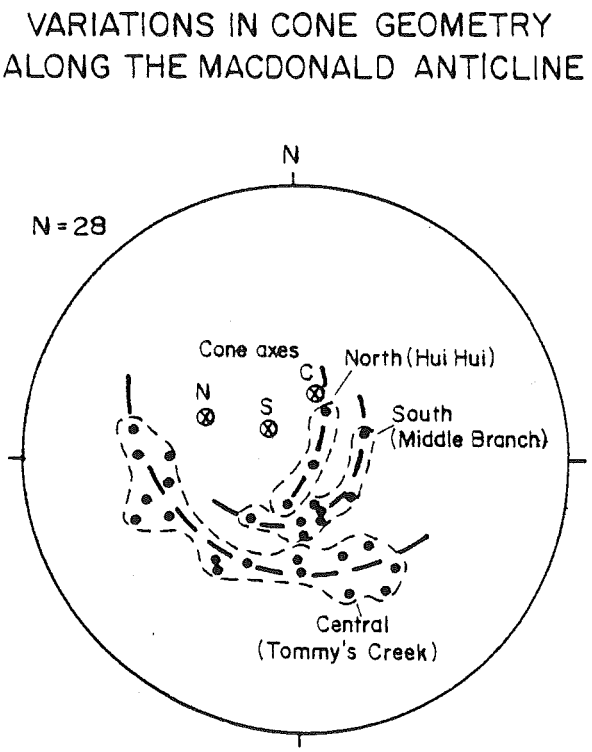

Figure 8.7. Variations in the conical fold geometry along the MacDonald Anticline. Supplementary to figure 4.5.

APPENDIX 4: PRESSURE SOLUTION STYLOLITES AND SLICKOLITE STRIATIONS; DEFINITION AND DESCRIPTION.

Pressure solution has taken place on numerous pre-existing joint surfaces. These surfaces are referred to as "pressure solution seams" (after Hancock, 1985), and contain stylolite columns indicative of the principal shortening direction. Two types of lineated pressure solution features have been identified according to their obliquity to the surface they are developed upon (Ramsay and Huber, 1987). Interlocking 'stylolite columns' are mainly orientated approximately normal to the surface (Figures 8.8 and 8.9a), while 'slickolite striations' (Figure 8.8), often preserved as striated grooves, are orientated at small angles to the surface. In the study area the development of orthogonal joint sets (parallel and normal to the principal shortening direction) has meant that both stylolites and slickolite striations are present. These pressure solution features are only found in the fine grained micritic horizons of the Amuri limestone.

The term slickolite combines the terms slickenside and stylolite, and implies a shearing and solution origin (Ramsay and Huber, 1987).

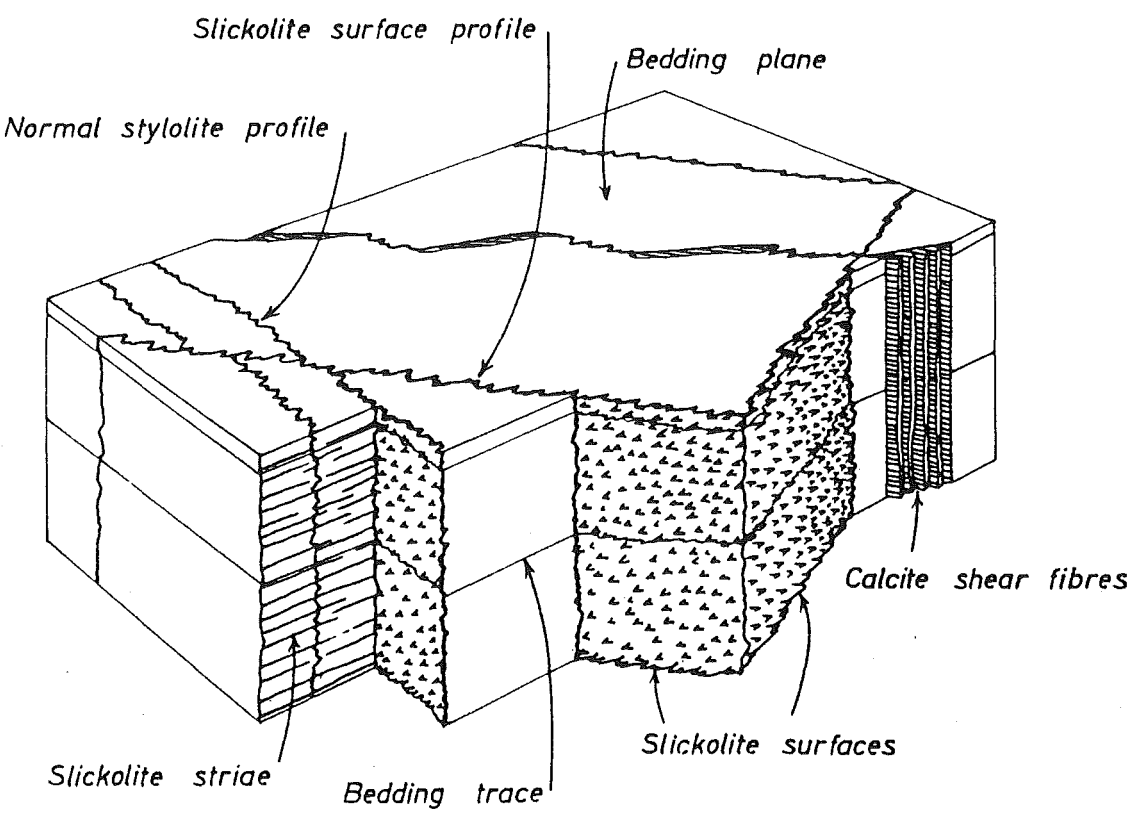

(from Ramsay and Huber, 1987)

Figure 8.8. Schematic block diagram showing the nomenclature and expected geometric relationships of stylolites (columns), slickolites and slickolite striations (from Ramsay and Huber, 1987).

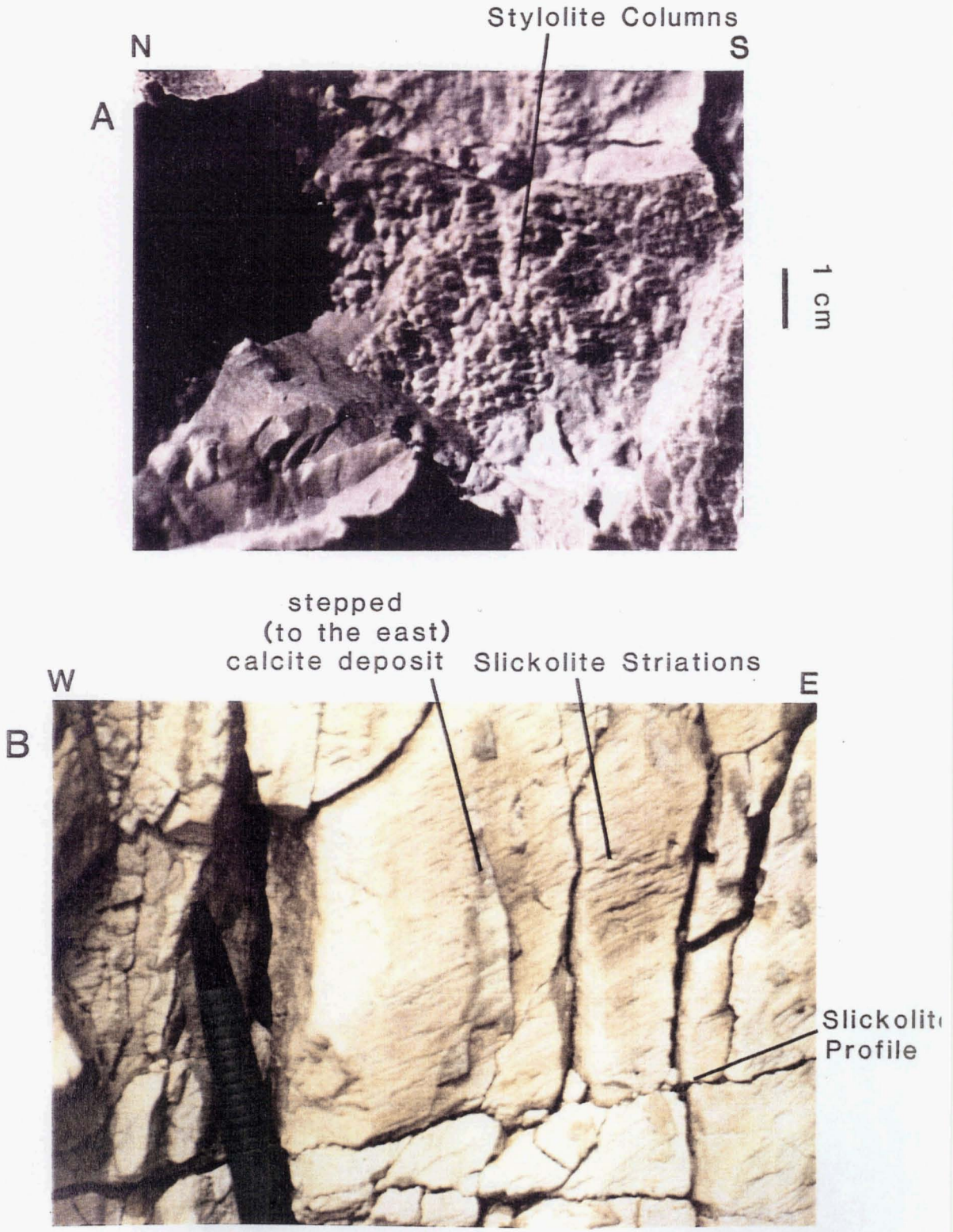

Figure 8.9. Stylolite columns (A) and slickolite striations (B) developed on pressure solution seam surfaces within the Amuri limestone at Tommy's Creek in the MacDonald Downs area (see Figure 8.1). Note that the stepping direction of calcite precipitated in a hollow in the striated surface (B), infers that slickolite striations are likely to have developed in association with oblique left lateral movement on this surface.